Hydrogeological Characterization of the Bakken Aquifer, Williston Basin (Canada-USA)

by

Daniel Skoreyko

A thesis submitted in partial fulfillment of the requirements for the degree of

Master of Science

Department of Earth and Atmospheric Sciences
University of Alberta

© Daniel Skoreyko, 2017

Abstract

The Bakken Formation is the most productive formation in the Williston Basin and one of the most important tight oil plays in North America. Oil in the Bakken Formation has been shown to migrate from the mature, central portion of the Williston Basin outwards towards the less mature portions of the basin, and north into Canada. A clear understanding of the hydrodynamics within the Bakken Formation is crucial for development; however, its regional hydrogeology, and the influences of regional groundwater flow on hydrocarbon migration in the Bakken Formation have been relatively poorly studied. A detailed hydrogeological and hydrochemical investigation of the Bakken Aquifer was conducted across the entire Williston Basin.

Hydrochemical results show that within the Bakken Aquifer, salinity and water composition are variable. Total dissolved solids concentrations range from less than 10,000 mg/L to over 300,000 mg/L. Salinities are highest in the central portion of the basin and decrease radially outward. Formation waters in the Bakken Aquifer are dominantly Na-Cl type waters, however, some Na-SO_4 waters are also present. Sodium-Chloride-Bromide systematics indicate that Bakken Aquifer brines originated from paleoseawater enrichment, halite dissolution, and the mixture between both. Results show a relation between waters with 250,000 mg/L TDS and the high resistivity anomaly found in the Bakken Formation.

Hydrogeological results show a large closed potentiometric high located in the center of the Bakken Aquifer with hydraulic heads greater than 1,400 m. Hydraulic

head values generally decreasing to less than 400 m in the northeast. Water driving force analysis reveals significant density dependent flow effects are present in northeast Montana and southeast Saskatchewan. Pressure depth analysis shows a large area with greater than hydrostatic formation pressures. Conditions return to near hydrostatic formation pressures outwards from the overpressured area.

Production data has been combined with hydrogeological interpretations to identify hydrodynamic effects on hydrocarbon migration and accumulation. Production behaviours from Middle Bakken oil wells were overlaid on UVZ maps. Results show that areas predicted by UVZ analysis as being migration pathways or hydrodynamic traps had favorable hydrocarbon production behaviours compared to elsewhere in the formation.

This study demonstrates that a complete understanding of the regional hydrogeology and hydrochemistry is imperative to determine the true flow direction of formation waters in deep saline aquifers. In addition, a sound understanding of the impacts of groundwater flow on hydrocarbon migration and accumulation can be used to further develop the economic potential of the Bakken Formation.

Dedication

To my family and my partner Alicia,

none of this would be possible without your love and encouragement.

Thank you.

Acknowledgements

The product of this work would not be possible without the patience, guidance, and support of my supervisor Dr. Ben Rostron. His undergraduate course introduced me to the field of petroleum hydrogeology, however, his passion and enthusiasm lead me to pursue the subject further. Thank you for all of the meetings, “quick questions”, and opportunities that you provided me.

I would like to thank Dr. Carl Mendoza for introducing me to the field of hydrogeology and who’s courses taught me the fundamental concepts of hydrogeology. I would also like to thank him for his availability, advice, and for providing extra motivation by constantly asking “are you done yet?”

Thank you to the other members of my defense committee: Dr. Daniel Alessi and Dr. Monireh Faramarzi. Your comments and suggestions have made for a superior final product and I am grateful for the time you have spent reviewing my thesis.

I would also like to thank my lab mates both past and present for the many laughs, and memories. Thank you to Chelsea and Gabby for keeping me company all the nights where we burnt the midnight oil. Thank you, Judit for always finding the time to answer a quick question, review an abstract, or sit through a practice presentation. To the many friends and colleagues I’ve met pursuing my graduate studies, you have all added to the experience, thank you.

I would like to thank my family for the support and encouragement they provided me throughout my academic career. Finally, thank you to my partner Alicia Pope for the mental and physical support. Thank you for putting up with all the long hours, late nights, and missed weekends. It took longer than expected but we made it! Thank you.

Table of Contents

List of Figures

List of Tables

1. Introduction

1.1. Motivation

The Mississippian-Devonian aged Bakken Formation is found within a large portion of the Williston Basin including parts of Saskatchewan, Manitoba, Montana, and North Dakota. It has been well documented as the most important petroleum source rock in the Williston Basin (e.g. Meissner, 1978; Schmoker and Hester, 1983; Dow, 1974; Leenheer, 1984; Webster, 1984; LeFever, 1991; Osadetz et al., 1992; Price and LeFever, 1994; Osadetz and Snowdon, 1995; Jarvie, 2001). The Bakken Formation is currently the most productive oil producing formation in the entire Williston Basin and, one of the most productive tight oil plays in North America (Sorensen et al., 2014).

Both the source of the petroleum, and its migration pathways and entrapment location are of ongoing interest to the petroleum industry. A clear understanding of how oil, gas, and, water migrate through sedimentary basins is essential for understanding the evolution of formation waters, and the exploration and development of natural resources such as hydrocarbons, mineral salts, and dissolved metals (Hubbert, 1953; Chebotarev, 1955; Clayton et al., 1966; Tóth, 1980; Davies, 1987; Hanor, 1994). The Bakken Formation is an excellent example of a system in which hydrocarbons are being generated in one part of the basin and migrating to another, because the southern portion is in the oil generating window, while the northern portion is thermally immature yet still produces significant hydrocarbons. It has long been proposed that there has been an outward migration of Bakken oil from the central, mature portion of the Williston Basin to the less mature, and immature portions of the basin (LeFever et al., 1991).

Despite the economic significance of the Bakken Formation, there have been few studies conducted on the fluid flow in the Bakken Formation. To this author's knowledge, there has never been a published basin-wide synthesis of the hydrogeology and hydrochemisty of the Bakken Formation.

Recently the Bakken Formation has undergone the most extensive exploration cycle in its history (Sonnenberg and Pramudito, 2009). As a result, operators have drilled Bakken Formation wells in previously unexplored areas, greatly expanding the spatial distribution of Bakken Formation data. In conjunction with the increase in drilling activity, the United States Geological Survey recently updated the Produced Waters Geochemical Database (USGSPWDB) adding nearly 100,000 new water analyses (Blondes et al., 2016). With a greater spatial distribution, and appreciably more data than previously available, a much more detailed investigation of the Bakken Formation is possible.

1.2. Research Objective

Many studies have previously examined the effects of moving groundwater on hydrocarbon migration (section 2.7). The hydrogeology of the Bakken Aquifer has previously been studied (section 3.4.1) however, the influence and implications of groundwater flow on oil migration in the Bakken Formation remain unclear. Thus, the purpose of this study is to determine the regional hydrogeology and hydrochemistry of the Bakken Aquifer across the entire Williston Basin.

With regards to hydrogeology the research objectives are:

1) Determine the Total Dissolved Solids (TDS) distribution in the Bakken Aquifer
2) Determine what water types are present in the Bakken Aquifer
3) Determine the origin of waters within the Bakken Aquifer

With regards to hydrogeology the research objectives are:

1) Determine the equivalent freshwater hydraulic head distribution within the Bakken Aquifer

2) Investigate for the presence of density dependent flow within the Bakken Aquifer and if present, determine the true flow direction of formation waters in the Bakken Aquifer
3) Determine the pressure distribution in the Bakken Aquifer
4) Investigate the effects and influences of groundwater on oil migration in the Middle Bakken reservoir.

By expanding our understanding of the Bakken Formation and the role that groundwater has played in the Bakken petroleum system, the economic potential of the Bakken Formation can be further maximized.

2. Theoretical Background

2.1. Fundamentals of Na-Cl-Br Systematics

Sodium-Chloride-Bromide (Na-Cl-Br) systematics have been used extensively to determine the origin and migratory history of saline formation waters in sedimentary basins (Rittenhouse, 1967; Carpenter, 1978; McCaffery et al., 1987; Engle and Rowan, 2012). Zherebtsova and Volkova (1966) showed that Br^- does not participate in diagenetic reactions making it an ideal tracer for the evolution of brines originating as seawater (Carpenter, 1978; Walter et al., 1990). During the progressive evaporation of seawater Na^+, Cl^-, and Br^- concentrations increase by the same factor prior to halite saturation (McCaffrey et al., 1987). Once a brine has reached halite saturation, Na^+ and Cl^- are removed from solution while Br^- is virtually excluded from the halite lattice. Further evaporation beyond halite saturation leads to a rapid increase in Br^- concentration relative to total dissolved solids (TDS) of the remaining solution (Rittenhouse, 1967). Thus, the behaviour of Br^- relative to Cl^-, Na^+, and TDS makes it useful for determining the origin of salinity in formation-waters. Brines resulting from the evaporation of seawater have lower Na^+/Br^- and Cl^-/Br^- ratios than seawater, while brines resulting from halite dissolution are depleted in Br^- and have Na^+/Br^- and Cl^-/Br^- ratios greater than those of seawater (Walter et al., 1990). Furthermore, in most waters the only appreciable source of Na^+, Cl^-, or Br^- is from halite dissolution or the evaporation of seawater, thus waters should evolve along a single linear trend called the seawater evaporation trajectory (SET) (Carpenter, 1978; McCaffery et al., 1987; Engle and Rowan, 2012).

Most previous studies plot raw concentrations of Cl^- versus Br^-, or the ratios of Na^+/Br^- versus Cl^-/Br^- in comparison to the SET to interpret the origin of saline fluids (Carpenter, 1978; McCaffery et al., 1978; Walter et al., 1990; Hannor, 1994; Iampen and Rostron, 2000; Gupta et al., 2011). The advantages of plotting raw concentration data are that it requires little data preparation, plots of this nature are intuitive to interpret, and Cl^- versus Br^- plots can also show mixing pathways between seawater, evaporated seawater, and freshwater (Engle and Rowan, 2012). While plots of Cl^-

versus Br^- are simple to construct, there is the potential for misrepresentation of the data. Cross plots of raw concentrations of Br^- versus Cl^- do not allow the components to vary independently and a change in one component results in the change of every other component. This causes the constituents in the brines to appear as if they were in a constrained system and generate results that may be misleading (Engle and Rowan, 2012).

Walter et al. (1990) improved the visual interpretation of Na-Cl-Br systematics by plotting the concentration ratios of Na^+/Br^- versus Cl^-/Br^-. Utilizing this method, concentration artifacts due to solute changes are avoided (Engle and Rowan, 2012). In this plot, dissolved Na^+ and Cl^- originating from halite dissolution plot on a linear trend with Na^+/Br^- and Cl^-/Br^- ratios greater than modern seawater. Sodium and Cl^- resulting from the evaporation of seawater have Na^+/Br^- and Cl^-/Br^- ratios less than modern seawater and plot along the same trend as modern seawater and halite dissolution waters.

While the Na^+/Br^- versus Cl^-/Br^- method is an improvement upon plotting raw concentrations, there are still disadvantages (Engle and Rowan, 2012). The disadvantage of the ratio plot is similar to plotting raw concentration data, the two ratios remain spuriously correlated due to Br^- being present in both denominators. Furthermore, this method cannot accurately estimate the amount of mixing or evaporation that has occurred, because both axes have Br^- in the denominator. Since Na^+/Br^- versus Cl^-/Br^- data plot on a linear trend, brines resulting from halite dissolution plot in the opposite direction of brines resulting from seawater evaporation. This makes mixtures between the two fluids difficult to recognize (Engle and Rowan, 2012).

To eliminate the drawbacks to these problems, Engle and Rowan (2012) created an isometric log-ratio coordinate transformation to better represent compositional data. This method removes spurious correlation between the data points.

Compositional data are transformed into two parameters:

$$Z_1 = \frac{1}{\sqrt{2}} ln \frac{[Na]}{[Cl]} \quad (1)$$

$$Z_2 = \frac{\sqrt{2}}{\sqrt{3}} ln \frac{\sqrt{[Na][Cl]}}{[Br]} \quad (2)$$

Using these equations, Z_1 relates Na^+ and Cl^-. Waters with a halite dissolution signature will move towards a Z_1 value of zero. This is because halite dissolution waters will have a Na^+/Cl^- ratio approaching one, and ln 1 is zero. The progressive evaporation of seawater leads to a depletion in Na^+ relative to Cl^- resulting in a Na^+/Cl^- ratio of less than one. This will lead to progressively smaller Z_1 values with increasing degrees of evaporation.

The Z_2 parameter relates Na^+ and Cl^- to Br^-. Once halite saturation is reached, the residual brine is enriched in Br^- relative to the initial seawater starting composition because Br^- is virtually excluded from the halite lattice during seawater evaporation. This results in decreasing values of Z_2 with progressive evaporation of seawater with further loss of Na^+ and Cl^- and further precipitation of halite. If the brines are the result of halite dissolution, the Br^- content will be low, and the corresponding Z_2 values will be large.

To illustrate this behaviour, the modeled pathway of seawater evaporation based on the findings of McCaffery et al. (1987) is plotted for reference (Figure 2.1). Starting at the composition of modern seawater, the SET is a curvilinear pathway down and away from the modern seawater composition. The Z_2 values (x-axis) decrease due to the relative gain in Br^- compared to Na^+ and Cl^-, and Z_1 (y- axis) values also decrease resulting from the relative loss of Na^+ to Cl^-.

The dissolution of Br-free halite with seawater produces a trend that extends up and away from modern seawater. Z_1 values increase with increasing halite dissolution

as the Na^+/Cl^- ratio approaches 1. Z_2 values also increase reaching a maximum value of 7.2 (Figure 2.1) (Engle and Rowan, 2012).

2.2. Fundamentals of Fluid Movement

Hubbert (1940) defined a fluid potential as the mechanical energy per unit mass of fluid in the flow system, given by:

$$\Phi = gz + \frac{P}{\rho} \tag{3}$$

Where: Φ is fluid potential; g is acceleration of gravity; z is elevation; P is fluid pressure; and ρ is fluid density.

Fluid potential is related to hydraulic head (h) by:

$$\Phi = gh \tag{4}$$

Substituting equation (4) into equation (3), and simplifying, yields the field form of hydraulic head:

$$h = z + \frac{P}{\rho g} \tag{5}$$

In equation 5, the term $\frac{P}{\rho g}$ represents pressure head (ψ) and z represents elevation head thus hydraulic head (h) is equal to elevation head (z), plus pressure head (ψ):

$$h = z + \psi \tag{6}$$

The dominant force affecting the movement of formation waters either vertically or horizontally is the gradient of fluid potential, which can be expressed by the gradient of hydraulic head. Fluid flows from high to low fluid potential regardless

of the orientation in space assuming there are no density variations within the domain (Hubbert, 1940; 1953).

2.3. Formation Pressure Extrapolation

A stabilized formation pressure is required to accurately calculate hydraulic head. However, if the formation pressure fails to stabilize, the Horner (1951) extrapolation method is employed:

$$p_w = p_f - 2148.8\frac{Q\mu}{kb}\log\left(\frac{t+\Delta t}{\Delta t}\right) \tag{7}$$

Where: P_w is shut-in pressure (kPa); P_f is stabilized formation pressure (kPa); t is total flow time (minutes); Δt is shut-in time (minutes); Q is volumetric flow rate (m^3/day); μ is viscosity (cP or mPa.s); k is intrinsic permeability (md); and b is reservoir thickness (m).

This method determines the stabilized formation pressure by plotting the shut-in pressure against the total flow time and shut-in time. As the length of the shut-in time increases, the ratio of $\frac{t+\Delta t}{\Delta t}$ approaches one, and the log value approaches zero. As the value approaches zero, the shut-in pressure approaches the formation pressure, therefore, the longer the test runs the closer the two pressures become.

2.4. Horizontal Movement of Groundwater

To visualize the movement of groundwater in the subsurface, hydraulic head values for an aquifer are posted on a map. Equipotential lines are then constructed. Flow is interpreted from high to low, perpendicular to the equipotential lines.

In unconfined aquifers, equipotentials of hydraulic head define the water table, with flow from high to low hydraulic head values. For confined aquifers, a potentiometric surface map is constructed by contouring hydraulic head values from a given aquifer.

A potentiometric surface is the imaginary surface to which water would rise in a well penetrating a fully confined aquifer (Dahlberg, 1995). As with hydraulic head, flow is orientated in the direction of decreasing values normal to the equipotential contours (Hubbert, 1940).

Inferring groundwater flow directions to be perpendicular to equipotential lines can be problematic in deep saline, dipping aquifers, as will be discussed in section 2.6.

2.5. Vertical Movement of Groundwater

As mentioned previously, potentiometric surface maps only show horizontal flow in an aquifer. To study vertical groundwater flow, pressure versus depth (P(d)) plots can be used to detect vertical variations in fluid potential. These variations can cause upward or downward movement of groundwater, even crossing aquitards provided there is sufficient time (Tóth, 1978; 1980).

Manifestations of cross-formational flow are indicated as convergences or divergences of equipotential contours on potentiometric surface maps. Divergences in the potentiometric surface represent an increase in energy, which can be attributed to the introduction of fluid flowing into an aquifer from either above or below. Convergences in the potentiometric surface represent energy sinks where flow is leaving the aquifer.

2.6. Density Effects on Groundwater Movement

Traditionally, groundwater flow is interpreted to be normal to equipotential lines. In deep saline aquifers, this has been shown to be problematic. Davies (1987) showed that even within shallow dipping aquifers, with low flow gradients, failure to consider density effects can produce significant errors in both predicted flow velocity, and direction.

To correct for density variations, Davies (1987) rewrote Darcy's law as:

$$q = -K\left[\nabla h_f + \frac{\rho - \rho_f}{\rho_f}\nabla E\right] \tag{8}$$

Where: q is groundwater flux [L/T]; K is hydraulic conductivity [L/T]; Δh_f is freshwater hydraulic head [L] calculated from the reference density ρ_f[M/L³]; $\rho - \rho_f$ is the difference in density between the formation water density and the freshwater density; and ∇E is the slope of the aquifer or corresponding formation top of interest.

The net water driving force at a point location can be represented by:

$$WDF = \nabla H_f + \frac{\Delta\rho}{\rho_f}\nabla E \tag{9}$$

Where: the water driving force (WDF) is the sum of the freshwater hydraulic head gradient (∇H_f) and the density related driving force ($\frac{\Delta\rho}{\rho_f}\nabla E$). This equation shows that it is not the absolute magnitude of one component of flow which dictates overall flow direction, rather the relative magnitudes each component has with the other (Figure 2.2) (Davies, 1987).

To quantify the potential importance of the density related error, Davies (1987) introduced the dimensionless driving force ratio (DFR) which is a measure of the relative importance of the gravity driven flow component to the fluid potential as a dimensionless ratio:

$$DFR = \frac{\Delta\rho|\nabla E|}{\rho_f|\nabla H_f|} \quad (10)$$

Where: $\Delta\rho$ is the difference between measured and freshwater density (ρ_f); ∇E is the magnitude of the elevation gradient; ∇H_f is the magnitude of the freshwater head gradient.

When the DFR value exceeds 0.5 significant errors in flow direction are predicted (Davies, 1987).

2.7. Effects of Moving Groundwater on Hydrocarbons

Munn (1909) first discussed the effects of moving groundwater on petroleum migration with the publication of the hydraulic theory of oil migration. The generalized hydraulic theory of petroleum migration (Tóth, 1980) built upon the works of Munn (1909) and Hubbert (1953). It provided a sound conceptual framework for the migration and accumulation of hydrocarbons in hydraulically continuous sedimentary basins. Tóth (1980) concluded that in mature geologic basins that are hydraulically continuous, groundwater flow is driven by elevation differences in the topographic surface. Water descends in areas of topographic highs, moves laterally through the subsurface and ascends in topographic lows resulting in different flow systems within the drainage basin. Within these flow systems, groundwater can mobilize, transport, and deposit hydrocarbons along its flow path as it moves from regions of high to low energy (Tóth, 1980).

2.8. Buoyancy Driving Force and Oil Driving Force Vectors

Hydrocarbons are thought to migrate as a separate phase (Palciauskas, 1991). In separate phase flow there is a second driving force, namely buoyancy (Tissot and Welte, 1978). Buoyancy impels hydrocarbons upwards displacing pore waters contained in the rocks. This buoyant force is proportional to the density contrast between the hydrocarbon and the formation water within the pore space. It acts inverse to the direction of the aquifer dip. The total buoyant force acting on a hydrocarbon molecule can expressed as:

$$F_{b\ oil} = -\frac{\rho_o - \rho_w}{\rho_f}\nabla E \tag{11}$$

Where: ρ_o is density of the hydrocarbon; ρ_w is density of the formation water; ρ_f is density of fresh water; ∇E is the slope of the aquifer.

In order to represent all forces acting on a hydrocarbon molecule in the subsurface three vector forces need to be accounted for: the oil buoyancy vector (equation 13), the density modified hydraulic head vector (equation 11), and capillary forces. Capillary forces were ignored in this thesis for two reasons:

1) It is not practical and beyond the scope of this work to quantify lateral capillary forces in large scale, regional studies (e.g. Alkalali, 2002).

2) Hubbert (1953) showed that in shales, the capillary pressure of oil is on the order of tens of atmospheres while in sand it is only tenths of atmospheres. The pressure gradient between the shale and the sand reservoir results in oil exiting shales and entering into sands. Once in the sand, the sand-shale interface becomes an impermeable boundary where oil cannot flow back into the shale unless a force greater than the capillary force is applied.

Therefore, the only capillary barrier to hydrocarbon migration assumed in this study is the Upper Bakken Formation shale which acts as the regional aquifer/reservoir seal.

The total oil driving force acting on a hydrocarbon molecule (Figure 2.2) can be expressed as:

$$ODFV = \left[\nabla H_f + \frac{\Delta\rho}{\rho_f}\nabla E\right] + \left[-\frac{\rho_o - \rho_w}{\rho_f}\nabla E\right] \quad (12)$$

Or more simply as:

$$ODFV = WDFV + BDFV \quad (13)$$

2.9. Hubbert's UVZ Method

Hubbert (1953) quantitatively investigated the movement of groundwater and its effects on hydrocarbon migration and accumulation. He formulated the UVZ method which is a graphical technique used to create equipotential lines for hydrocarbons in the subsurface.

In order to implement the UVZ method, knowledge of the freshwater hydraulic head (h_f) values within the aquifer, density of the formation water (ρ_w) and hydrocarbons (ρ_o) within the reservoir, and the elevation (Z) of the top of the reservoir are required.

Knowing these, the three surfaces (U, V, Z) can be constructed where:

$$U = \frac{\rho_o}{\rho_w - \rho_o}\, h_o \quad (14)$$

$$V = \frac{\rho_w}{\rho_w - \rho_o} h_f \quad (15)$$

$$\mathrm{Z} = \mathrm{Z} \tag{16}$$

Becoming Hubbert (1953):

$$U = V - \mathrm{Z} \tag{17}$$

In equation 15, V is a function of the hydraulic head of fresh water modified by the density of the formation water. Knowing the freshwater hydraulic head distribution, and the density of the formation water, V contours which are parallel to the potentiometric surface can be plotted. Subtracting the Z surface from the V surface results in the values of U which can then be contoured.

The U surface represents the potentiometric surface of the hydrocarbons. Hydrocarbon migration can be interpreted from the U surface map as fluids will migrate towards decreasing U values. In hydrodynamic conditions, entrapment of hydrocarbons occurs in areas of lowest fluid potential (Hubbert, 1953)

It is important to note that the migration pathways defined by the U surface map show the direction hydrocarbons would migrate (for hydrocarbons of the calculated density) if they were present in the reservoir and does not necessarily mean that hydrocarbons are actually present in all areas on the map.

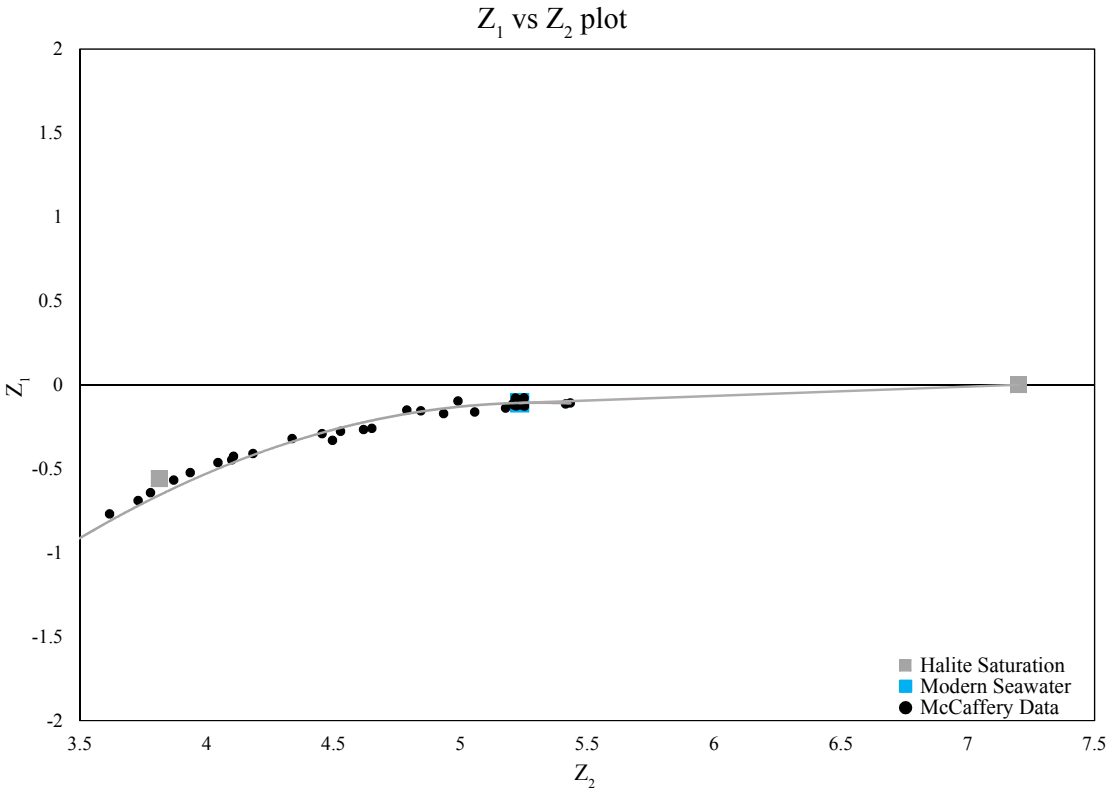

Figure 2.1: Isometric log-ratio transformation Z_1 versus Z_2 plot (after Engle and Rowan, 2012) showing the progressive evaporation of seawater to the point of halite saturation using the data from McCaffery et al. (1987).

Plan view

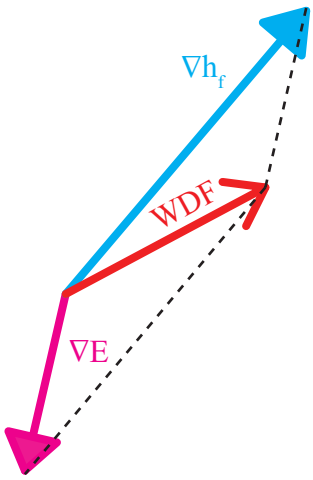

$$WDF = (\nabla h_f + [(\rho_w - \rho_f/\rho_f)]\nabla E)$$

Plan view

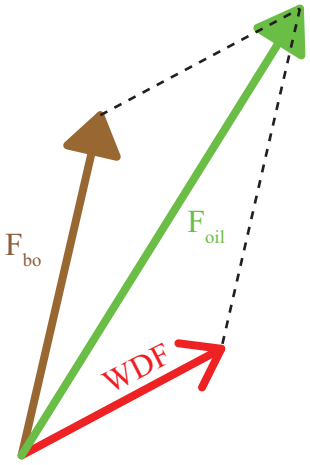

$$F_{bo} = -[(\rho_o - \rho_w)/\rho_f]\nabla E \qquad F_{oil} = WDF + F_{bo}$$

Figure 2.2: Graphical representation of fluid impelling forces in plan view.

3. Study Area, Geology, and Hydrogeology

3.1. Study Area

This study encompasses the Bakken Formation across the entire Williston Basin. The Williston Basin is a large intracratonic sedimentary basin spanning portions of Saskatchewan, Manitoba, North Dakota, South Dakota, and Montana (Figure 3.1) (Gerhard et al., 1982).

The Williston Basin was first named by Thom and Dobbin (1924). They considered the basin to exist in post Fox-Hills (late Cretaceous) time. However, they did not define a geological boundary to the basin because no definite boundary exists (Laird, 1956). Thus, the arbitrarily defined, widely accepted (i.e. Norford et al., 1994; Kent and Christopher, 1994) boundary of the Williston Basin is based on Laird (1956) as the zero elevation line of the Cretaceous Dakota Sandstone.

However, using a structural elevation of a Cretaceous unit to define a basin that spans the Phanerozoic era presents problems, as will be shown below. Subsidence of the Williston Basin began as early as the Ordovician (Gerhard et al., 1982). However, at various times the Williston and Alberta basins merged into one (e.g. during the Devonian and Mississippian when the Bakken-Exshaw formations were deposited) (Gerhard et al., 1982).

Thus, for the purpose of this study, the Williston Basin boundary was chosen based on the 40 m contour of the Silurian Interlake Formation (Figure 3.1). The Williston Basin covers 560,000 km², with the Bakken Formation covering 270,000 km² as defined by this boundary.

Using this boundary, the Bakken Formation is constrained to the north by the Punnichy Arch fronting the Saskatchewan monocline, the northeast by the Severn Arch of Central Manitoba, the southeast by the Transcontinental Arch of the Dakotas, the west by the Sweetgrass and Battleford arches (Figure 3.2) (Norford et al., 1994; Kent and Christopher, 1994).

3.2. General Geology of the Williston Basin

The comprehensive working geology of the Williston Basin has been studied previously by many authors including Gerhard et al. (1982), Peterson and MacCary (1987), and Kent and Christopher (1994), so only a brief summary of the geology of the basin is presented here.

The Williston Basin is a bowl shaped intracratonic sedimentary basin which straddles the northwestern United States and western Canada. It underlies a large portion of the northern Great Plains of the United States and of the Prairie region in Canada including parts of Montana, North Dakota, South Dakota, Manitoba, and Saskatchewan. Subsidence of the Williston Basin resulted from lithospheric thickening and cooling which initiated the depocenter in North Dakota (Ahern and Mrkvicka, 1984). The Williston Basin contains a near continuous sedimentary succession from the Middle Cambrian to the Tertiary age ranging in thickness from zero along the edges to a maximum thickness of approximately 4,800 m in the locality of 104°W and 47.7°N (Gerhard et al., 1982). The topographic high for the Williston Basin is located in Montana while the topographic low is located in Manitoba (Figure 3.3).

Sedimentation in the Williston Basin is characterized by six major depositional sequences; the Sauk, Tippecanoe, Kaskaskia, Absaroka, Zuni, and Tejas (Gerhard et al., 1982). These represent a series of major transgressive regressive cycles consisting of predominantly carbonate deposition during the Paleozoic, and clastic sedimentation during the Mesozoic and Cenozoic (LeFever et al., 1991). Only the Bakken Formation of the Kaskaskia sequence is of interest here and will be explained in detail below.

3.3. Geology of the Bakken Formation

The name Bakken Formation was informally introduced in 1953 by the Williston Basin Nomenclature Committee of the Saskatchewan Society of Petroleum Geologists and the Rocky Mountain Section of the American Association of Petroleum

Geologists (LeFever et al., 1991). This was done to eliminate confusion when referring to a sequence of persistent black shales and, gray siltstones at the base of the Mississippian aged Madison Group limestones which had previously been referred to by various other names. No formal definition of the formation was presented during this initial introduction (LeFever et al., 1991).

The first formal definition and description of the Bakken Formation were later defined by Nordquist (1953). He defined the Bakken Formation as the clastic strata occurring at depths of 2,930.6 m to 2,962.6 m (9,615' to 9,720') in the Amerada Petroleum Corporation- H.O. Bakken #1 deep test well, in CSWNW Section 12, Township 157N, Range 95W, in Williams County, North Dakota. As defined, the Bakken Formation consisted of two black organic rich shales separated by a light gray to grey-brown, very fine-grained calcareous sandstone. In the type section well, the Bakken Formation is 32 m (105'); 7.6 m (25') of lower Bakken shale overlain by 18.3 m (60') of middle Bakken sandstone capped by 6.1 m (20') of upper Bakken shale. (LeFever, 1991; LeFever et al., 1991).

Kume (1960; 1963) disagreed with the thickness of the lower and middle members in the H.O. Bakken #1 well as proposed by Nordquist (1953). Kume (1960) modified the thicknesses to of the lower, middle and upper members to 7.6 m, 18.3 m and 6.1 m (25', 60' and 20') respectively based on the cuttings and the log response. Kume (1960) selected the Socony Vacuum Oil Company – Dvorak #1 well located in SENE Section 6, Township 141N Range 94W as the standard reference well for the Bakken Formation. In this well, the Bakken Formation was located from 3,058.7 m (10,035') to 3,077 m (10,095'). This well was chosen because the gamma ray and lateral log traces of the formations are very characteristic and could be easily used to define the boundaries of the lithologic units.

Since the 1950's more than 23,000 wells have been drilled into the Bakken Formation, providing extensive data on the Bakken Formation. The Bakken Formation unconformably overlies the Devonian Big Valley, Torquay, and Three Forks formations, and is unconformably overlain by the Lodgepole Formation (Figure 3.4).

The Bakken Formation is most deeply buried in North Dakota (Figure 3.5). Generally, the Bakken Formation is relatively thin, reaching a maximum thickness of 47 m in the well defined depocenter in North Dakota. In Saskatchewan, salt dissolution into the underlying strata created lows filled by the Bakken Formation. Thus, in localized areas of underlying collapse, the Bakken Formation can reach thicknesses greater than 65 m (Figure 3.6) (Kreis et al., 2006).

The three members of the Bakken Formation exhibit an onlapping relationship with each other where each stratigraphically younger member covers a larger lateral extent of the basin (LeFever et al., 1991).

The sedimentology of the Bakken Formation will be briefly reviewed below.

3.3.1. Sedimentology of the Lower Bakken Member

The Lower Member of the Bakken Formation is a dark gray to dark brownish black to black fissile non-calcareous organic rich shale (LeFever et al., 1991; Kreis et al., 2006). The colour of the shale varies depending on the relative abundance of silt versus clay versus organic carbon present in the rock (LeFever et al., 1991). The shale can be hard or soft, and commonly has a “wax like” feel to it suggesting that it has a high organic content in it (LeFever et al., 1991; Kreis et al., 2006). The total organic carbon content in the Lower Bakken shale ranges from one percent to 20 percent (Aderoju and Bend, 2013).

Generally, the thickness of the Lower Member of the Bakken Formation ranges from zero to 17 m. In southeast Saskatchewan, the lower member can be anomalously thick (up to 26 m) in areas of known salt dissolution (e.g. 15-05-001-08W2) (Kreis et al., 2006). LeFever et al. (1991) state that in North Dakota, the maximum thickness of the Lower Member (17 m) is observed in the well-defined depocenter immediately east of the Nesson anticline (103°W, 47.7 - 48.8°N). In Manitoba, the lower member

reaches a maximum thickness of 7 m east of the Saskatchewan-Manitoba border just north of the Canadian United States border (Figure 3.7).

In the central portion of the Williston Basin the Lower Member of the Bakken Formation conformably overlays the Three Forks Formation, however, along the basin margins in North Dakota, an angular unconformity separates the Lower Member Bakken Formation from the Three Forks Formation (LeFever, 1991).

3.3.2. Sedimentology of the Middle Bakken Member

The Middle Member of the Bakken Formation is a light gray to medium dark gray interbedded siltstone and sandstone with a highly variable lithology. Lesser amounts of shales, dolostones, and limestones rich in silt, sand and oolites may be present within this member (LeFever et al., 1991). The silts and sands are generally well sorted, massive or coarsely bedded sequences with occasional trough or cross stratification. Minor evidence of soft sediment deformation such as microfaults, and flow structures are present and that bioturbation commonly disrupts bedding, especially in more argillaceous portions (LeFever et al., 1991).

As seen with the Lower Member of the Bakken Formation, the thickest succession coincides with the depocenter to the east of the Nesson Anticline in North Dakota (Figure 3.8). In this location, the Middle Member of the Bakken Formation reaches a maximum thickness of 27 m (LeFever et al., 1991). In Manitoba, the average thickness of the middle member of the Bakken Formation middle member is 4 m and reaches a maximum thickness of 16 m (LeFever et al., 1991). In southern Saskatchewan, the Middle Member of the Bakken Formation shows an obvious thickening towards the southern portion of the Williston Basin reaching a maximum of 25 m. As observed in the Lower Bakken shale, the Middle Bakken can be anomalously thick in areas of known salt dissolution (e.g. 15-05-001-08W2) reaching a maximum thickness of 37 m (Kreis et al., 2006).

The Middle Member of the Bakken Formation conformably overlies the Lower Member in the center of the basin while along the basin margins, it unconformably overlies the Three Forks Formation (Kreis et al., 2006).

3.3.3. Sedimentology of the Upper Member

Lithologically, the upper and lower members of the Bakken Formation are quite similar. The Upper Bakken Shale is a dark gray to brownish black to black fissile, non-calcareous, carbonaceous, and bituminous shale (LeFever et al., 1991). While lithologically similar, the upper Bakken shale is more fossiliferous (LeFever et al., 1991). The total organic carbon content of the Upper Bakken is higher than that of the lower Bakken Shale. Total organic carbon levels in the Upper Bakken shale ranges from two percent to 33% (Aderoju and Bend, 2013).

Overall the Upper Bakken member is thinner than the lower Bakken member (Figure 3.9). In North Dakota, the maximum thickness of the upper Bakken shale is 11 m while in Saskatchewan, the upper member of the Bakken Formation reaches a maximum thickness of 10 m and has an average thickness of 1.2 m. In the Waskada area of Manitoba (100.9°W, 49.1°N), the maximum thickness of the upper member of the Bakken Formation shale is 18 m, with a reported uniform average thickness of 2 m (Martiniuk, 1988; LeFever et al., 1991). Thickness anomalies are attributed to both differential erosion of the underlying Lyleton Formation as well as salt collapse features from the dissolution of Devonian salts during the Bakken sedimentation (Martiniuk, 1988)

The Upper Member of the Bakken Formation covers the largest lateral extent of all three members and conformably overlies the Middle Member of the Bakken Formation in the central portion of the basin while along the margins it unconformably overlies the Three Forks Formation. The Upper Member of the Bakken Formation is then unconformably overlain by the Lodgepole Formation (LeFever, 1991).

3.4. Hydrogeology of the Williston Basin.

The hydrogeology and hydrochemistry of the Williston Basin has been previously studied in both Canada and the United States. Political boundaries have often hampered regional studies due to the transboundary nature of the Williston Basin. In the Canadian portion of the Williston Basin regional scale hydrogeological studies include Hannon (1987), and Bachu and Hitchon (1996). On the United States side of the basin, previous studies include Downey (1982); (1984); Bredehoeft et al. (1983); Downey et al. (1987); Downey and Dinwiddie (1988); Berg et al. (1994); DeMis (1995); and LeFever (1998).

Regional groundwater flow within the Williston Basin is largely topographically controlled. Fresh meteoric waters are thought to recharge in the southwest in the topographic highs and flow down toward the basin center. Formation waters flow laterally through the aquifers towards the north and northeast (Downey et al., 1987; Bachu and Hitchon, 1996; LeFever, 1998). In Manitoba, brines discharging from Devonian carbonates have a distinct chemical composition from the lateral equivalents deeper in the basin. This composition is attributed to basinal brines mixing with Pleistocene-aged glacial meltwater (Grasby and Chen, 2005).

To overcome partial hydrogeology mapping studies based on political boundaries the University of Alberta Hydrogeology Group has conducted detailed hydrogeological and hydrochemical studies in various portions of the Williston Basin (Alkalali, 2002; Margitai, 2002; Iampen, 2003; Khan, 2006; Jensen, 2007; Palombi, 2008; Melnik, 2012). These studies have revealed a more complex hydrogeology on a basin scale than previous work. These studies significantly refined the understanding of the flow regime, as well as hydrochemical distributions within the Williston Basin.

These studies largely supported the previously interpreted flow directions in the Williston Basin. However, Alkalali (2002), Margitai (2002), Palombi (2008), and Melnik (2012) highlight the effects that density variations can have on regional groundwater flow. These studies showed areas within the Williston Basin where

regional groundwater flow is heavily modified by density variations; in instances to the point of stagnation or a flow reversal.

The chemical composition, and distribution of formation waters within the Williston basin have been the subject of multiple studies in the past (e.g. Downey, 1986; Downey and Dinwiddie, 1988; Bachu and Hitchon, 1996; Kreis et al., 1991; Hanor, 1994; Benn and Rostron, 1998; LeFever, 1998; Iampen and Rostron, 2000; Rostron and Holmden, 2003; Shouakar-Stash, 2008). One group of researchers attributed the observed salinity to be the result of water rock interactions and the dissolution of evaporite minerals (Downey, 1986; Downey and Dinwiddie, 1988; Bachu and Hitchon, 1996). Another group of researchers concluded that brines in the Williston Basin owe their salinity to a combination of the subareal evaporation of paleoseawaters, and evaporite dissolution (Kreis et al., 1991; LeFever, 1998; Iampen and Rostron, 2000).

Iampen (2003) investigated the hydrochemistry of saline brines in the Williston Basin. She concluded that there are at least three chemically distinct saline fluid end members in the Williston Basin, as well as mixtures between these end members, and fresh water. Iampen (2003) concluded that the saline fluids within the Williston Basin originated as paleoseawaters, halite dissolution brines, meteoric water, and mixing amongst these waters.

Jensen (2007) incorporated stable isotope data while investigating the hydrochemistry of the Mississippian Beds across the Williston Basin. This work supported the conclusions of Iampen (2003) showing that saline brines within the Williston Basin have multiple origins from multiple evolutionary events.

Shouakar-Stash (2008) supported the previous findings. He showed that formation waters of the Williston Basin originated from four end members: paleoseawater, residual paleoseawater which has undergone evaporation, waters (meteoric or seawater) which dissolved evaporate minerals, and meteoric water.

3.4.1. Hydrogeology of the Bakken Aquifer

The hydrogeology of the Bakken Formation has been poorly studied compared to other aquifers in the Williston Basin. Most studies have included the Bakken Aquifer in the larger Mississippian aquifer group (e.g. Bachu and Hitchon, 1996; Melnik, 2012) or include it in the confining unit above the Cambrian-Ordovician aquifer (e.g. Downey, 1982; Downey et al., 1987; Downey and Dinwiddie, 1988). Only more recently has the Bakken Aquifer been recognized and mapped as its own hydrostratigraphic unit. Previous studies which specifically investigated the Bakken Aquifer include Palombi (2008), Palombi and Rostron (2013) (covering eastern Saskatchewan and Manitoba), and Jensen et al. (2015) (covering Saskatchewan).

The Bakken Aquifer is the upper aquifer in the Devonian Aquifer system based on the hydrostratigraphy of Palombi (2008) (Figure 3.4). This aquifer is defined here as the permeable Middle Member of the Bakken Formation which is encased by the Upper and Lower Bakken Formation shales. These shales create a confining layer, restricting lateral flow to within the Middle Bakken Member. Flow in the Canadian portion of the Bakken Aquifer is from southwest to northeast (Palombi, 2008; Palombi and Rostron, 2013; Jensen et al., 2015).

These recent studies examined the Bakken Aquifer in greater detail than previous studies however, they were limited to the Canadian portion of the Williston Basin and did not extend into the United States. To the author's knowledge, there is no detailed hydrogeological characterization of the Bakken Aquifer publicly available.

3.5. Williston Basin Petroleum System

The Williston Basin has been producing hydrocarbons since 1892 with the discovery of non-commercial gas in a Dakota Sandstone water well in the southeastern part of North Dakota (Anderson and Eastwood, 1968). Commercial gas production from the Gammon shale and Judith River Formations began in 1913 in the Cedar Creek

anticline. By 1932 more than 12 billion cubic feet of gas was produced (Anna et al., 2013). The first commercially produced oil well in the Williston Basin was completed in the Silurian aged Interlake Formation on the Nesson Anticline in 1951.

The Williston Basin contains ten total petroleum systems (TPS): Winnipeg-Deadwood; Red River; Winnipegosis; Duperow; Bakken-Lodgepole; Madison; Cedar Creek Paleozoic composite; Tyler; Shallow Biogenic Gas; and Coalbed Gas total petroleum system. Combined the ten TPS have produced over 3.2 billion barrels of oil (Anna, 2013).

This study focuses on only one of those systems, as described below.

3.5.1. Bakken Petroleum System

The Bakken Formation is currently the most productive oil producing formation in the Williston Basin producing more than 2.7 billion barrels to date. Development of the Bakken Formation can be divided into four cycles.

3.5.1.1. Cycle 1:

Production from the Bakken Formation began in 1953 in the Antelope Field of McKenzie County, North Dakota (LeFever, 1991). Development was focused on a tightly folded structure that had fracture enhanced permeability (Sonnenberg and Pramudito, 2009). Wells were drilled vertically and stimulated using a sand and oil fracture treatment in the Antelope field (LeFever, 1991). All three members of the Bakken Formation, as well as the upper Three Forks Formation (Sanish Member) were perforated, establishing them as petroleum reservoirs in the Williston Basin (Sonnenberg and Pramudito, 2009).

3.5.1.2. Cycle 2:

The next notable discovery in the Bakken Formation occurred in 1961 when Shell discovered the Elkhorn Ranch field in the Billings Nose area. This well was

significant in that it showed that significant reserves could be produced out of the Upper Bakken shale. The Billings Nose area is located near the depositional limit of the Bakken Formation. As the formation thins, the fracture density increases. Previous drilling had shown natural fractures necessary for successful vertical production in the Upper Bakken Shale (LeFever, 1991; 2005; Sonnenberg and Pramudito, 2009). However, due to the remoteness of this area (which would become known as the "Bakken Fairway"), and a slump in commodities prices, further development did not occur until 1977 (LeFever, 1991; Sonnenberg and Pramudito, 2009).

3.5.1.3. Cycle 3:

The first horizontal well in the "Bakken Fairway" was drilled in 1987. In principle, horizontal wells intersected more natural fractures and produce more oil. Horizontal drilling of the upper Bakken Formation shale in the Bakken Fairview area continued into the 1990s. However poor prices and mixed production results lead to the Bakken Formation becoming a secondary exploration target by the late 1990s (Sonnenberg and Pramudito, 2009).

3.5.1.4. Cycle 4:

The fourth and current cycle of development commenced at the Elm Coulee Field in 2000. This field was discovered using horizontal drilling and hydraulic fracture stimulation (Sonnenberg and Pramudito, 2009).

The Elm Coulee Field was conceived in 1996 with the completion of a vertical well in the middle Bakken Formation (typically the Upper Bakken shale would also have been perforated). This well underwent a water-sand fracture stimulation treatment producing very encouraging results. Thus, the concept that a large field existed in an area previously drilled through (targeting deeper formations) was developed. Well logs from previously drilled vertical wells in the area were re-examined and it was determined that in this area there was sufficient porosity in the Middle Member and the pore space was filled with oil (Sonnenberg and Pradmudito, 2009).

The first horizontal well targeting the middle member in the Elm Coulee Field was drilled in 2000. Middle Bakken wells in this area were subjected to hydraulic fracture stimulations and initially produced 200-1200 barrels of oil per day (BOPD) (Sonnenberg and Pradmudito, 2009). The technological breakthrough of horizontal drilling and hydraulic fracturing was the catalyst driving this exploration cycle.

Using the Elm Coulee Field as a model, operators begin searching for the equivalent field in North Dakota. In July 2004 an Elm Coulee equivalent of North Dakota was located. In April 2006, EOG Resources spudded what would become the discovery well for the Parshall Field; a field over 2.7 million acres with recoverable oil reserves estimated over three billion barrels of oil and that would require 4,200 wells to fully develop (Johnson, 2011).

The Bakken Formation requires a fracture network in order to produce significant hydrocarbons. In the past, a naturally occurring fracture network was required however thanks to advances in horizontal drilling and hydraulic fracture stimulation the Bakken Formation is currently the most productive oil producing formation in the Williston Basin and one of the most productive tight oil plays in North America (Sorensen et al., 2014).

Figure 3.1: Study area location map. The outline of the Williston Basin shown by the black dashed line is defined by the 40 m contour of the Silurian Interlake Formation. Shaded in blue, the Williston Basin covers portions of Saskatchewan, Manitoba, Montana, North Dakota and, South Dakota. The Bakken Formation outlined in red, shaded yellow is the subject of this study.

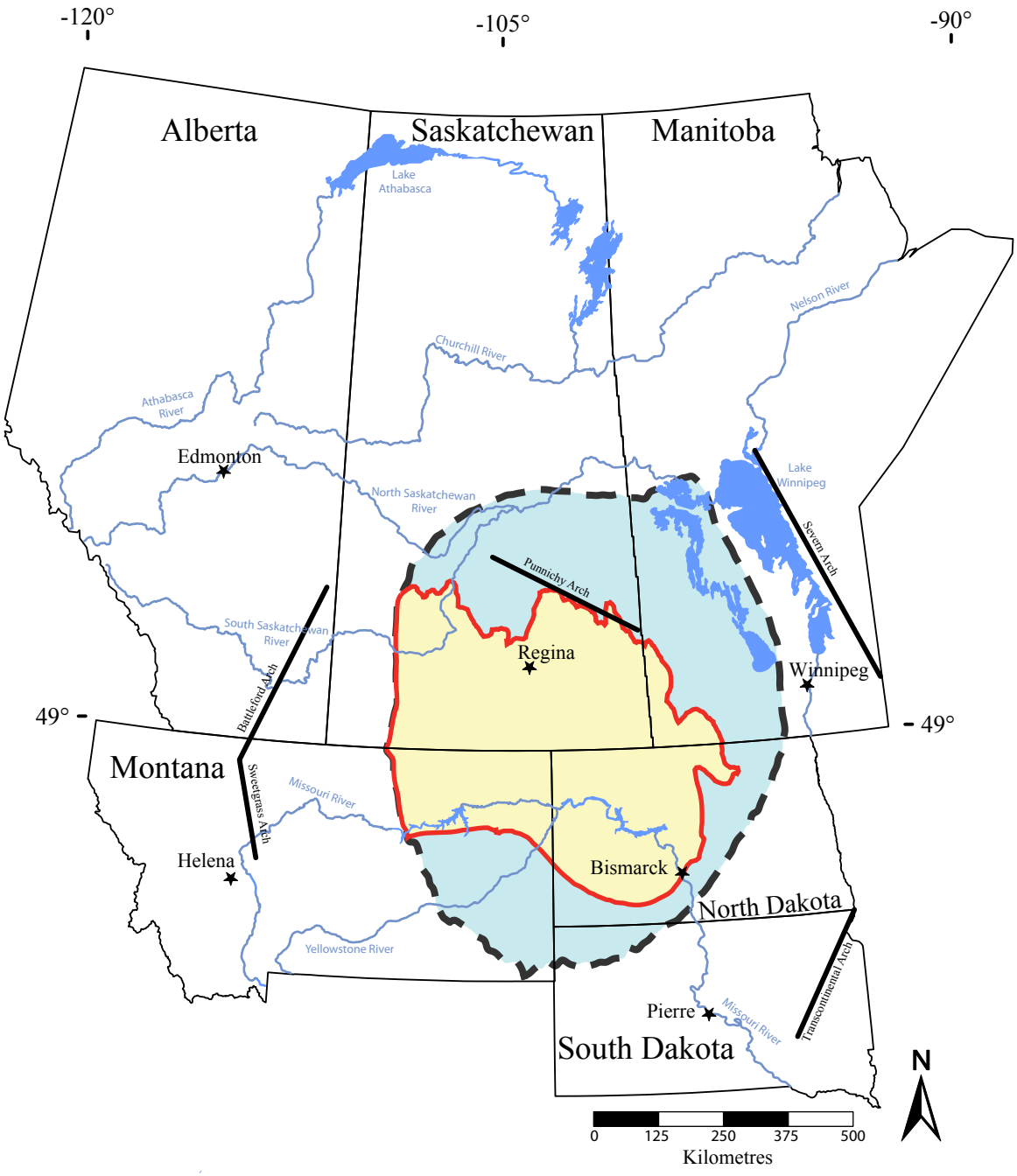

Figure 3.2: Map showing select major structural features in the Western Canadian Sedimentary Basin and their relation to the study area.

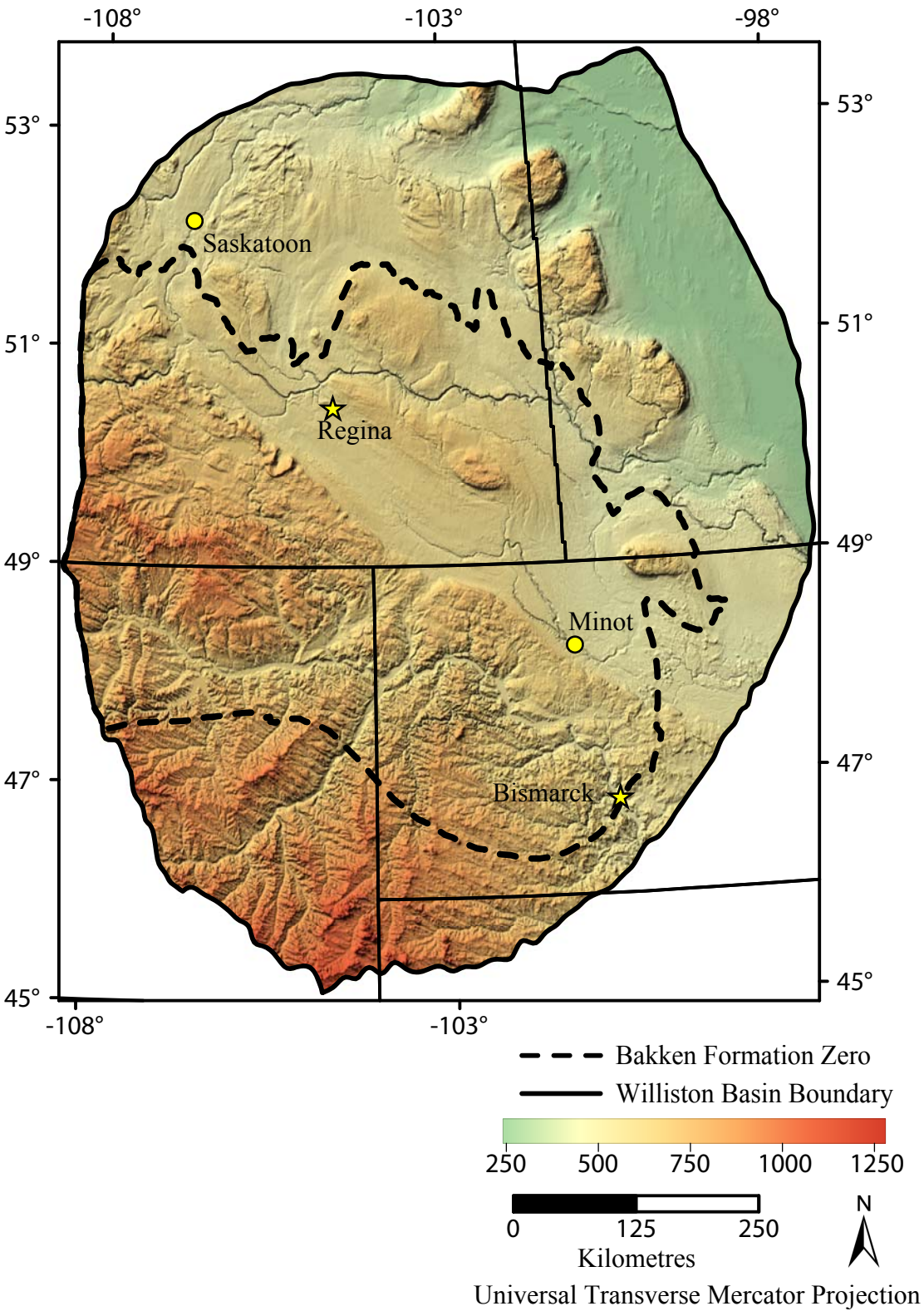

Figure 3.3: Topographic map of the Williston Basin (DEM compiled from USGS).

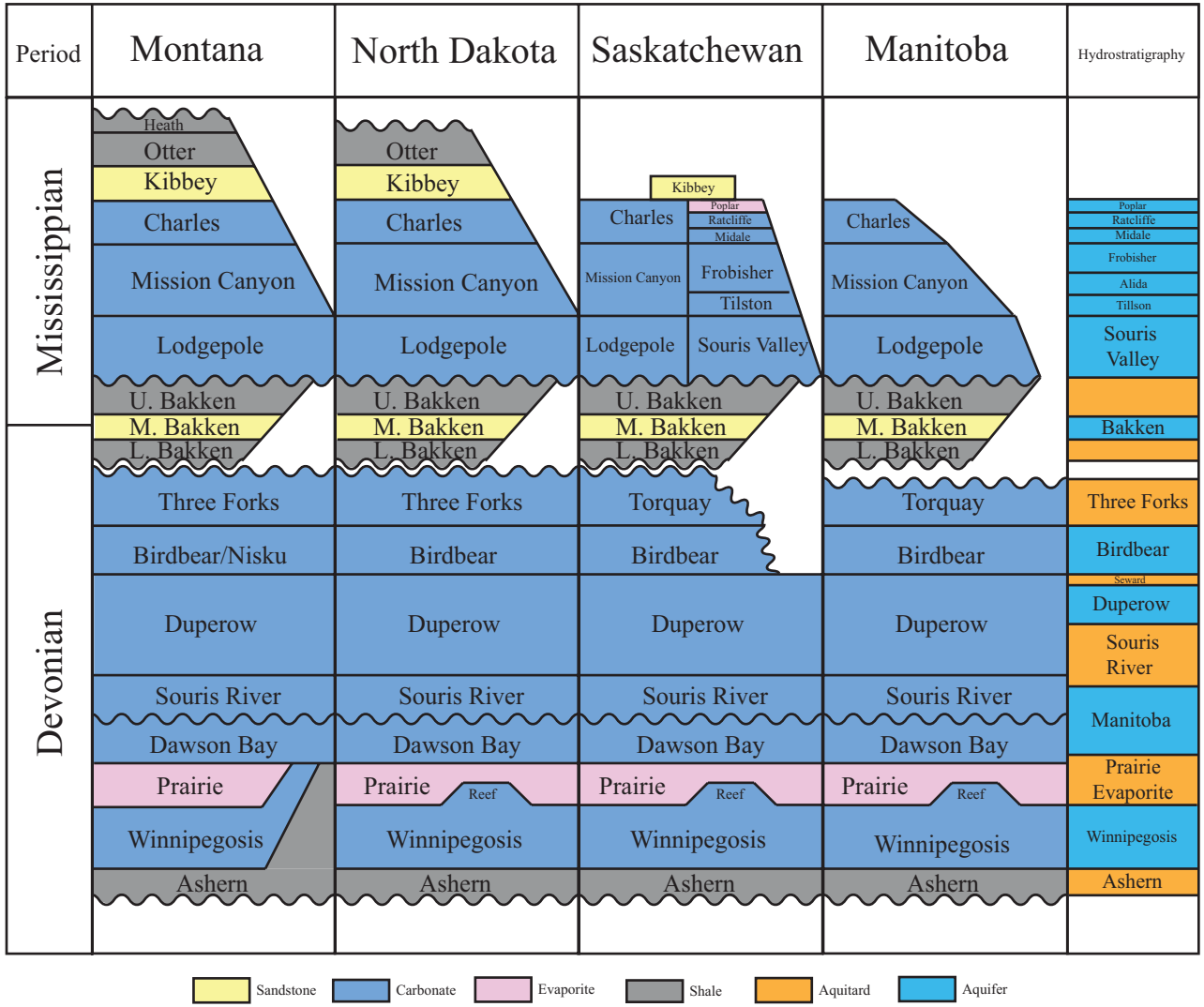

Figure 3.4: Stratigraphy (after Core Laboratories) and hydrostratigraphy (after Palombi, 2008) of the Devonian and Mississippian formations in the Williston Basin .

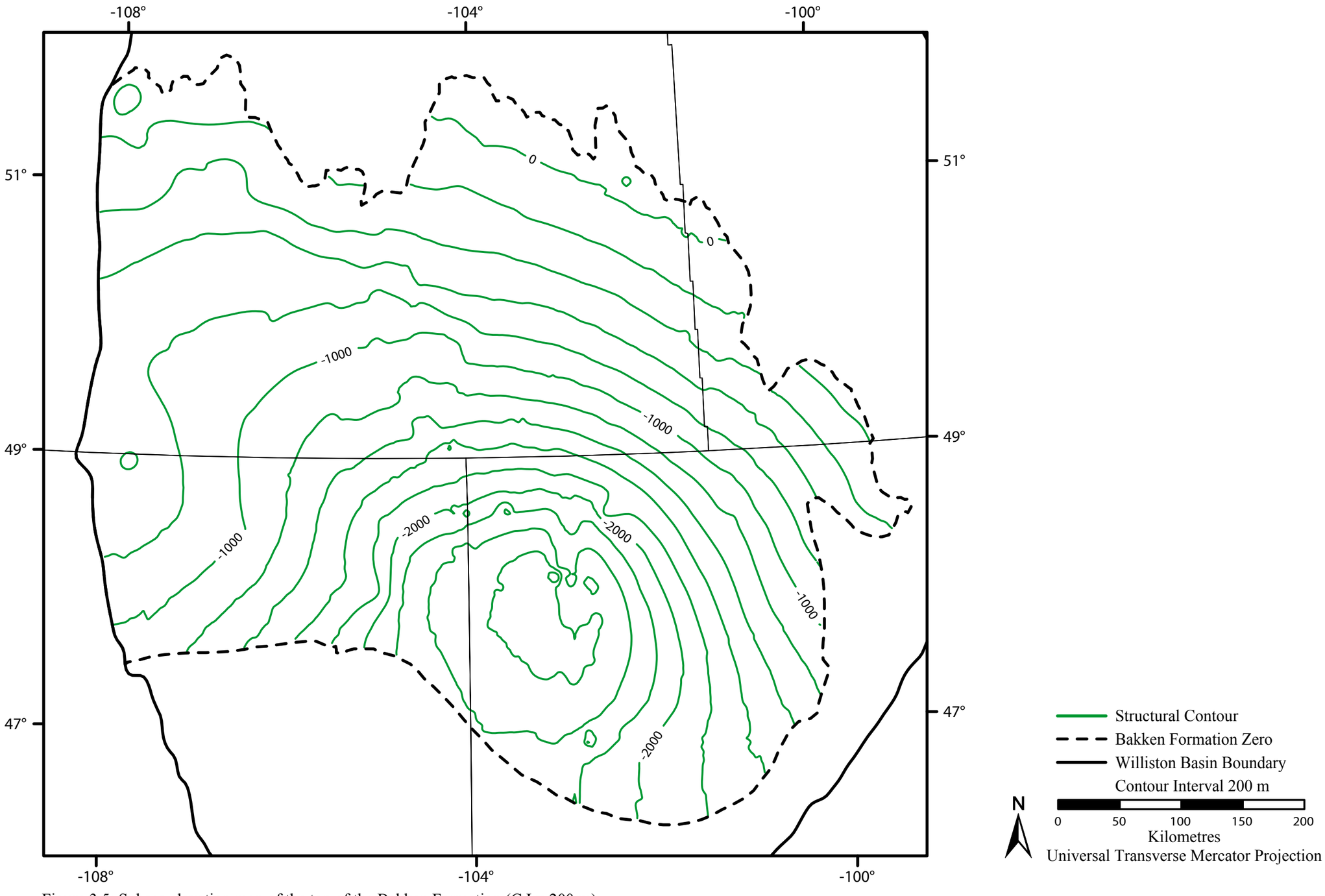

Figure 3.5: Subsea elevation map of the top of the Bakken Formation (C.I.= 200 m).

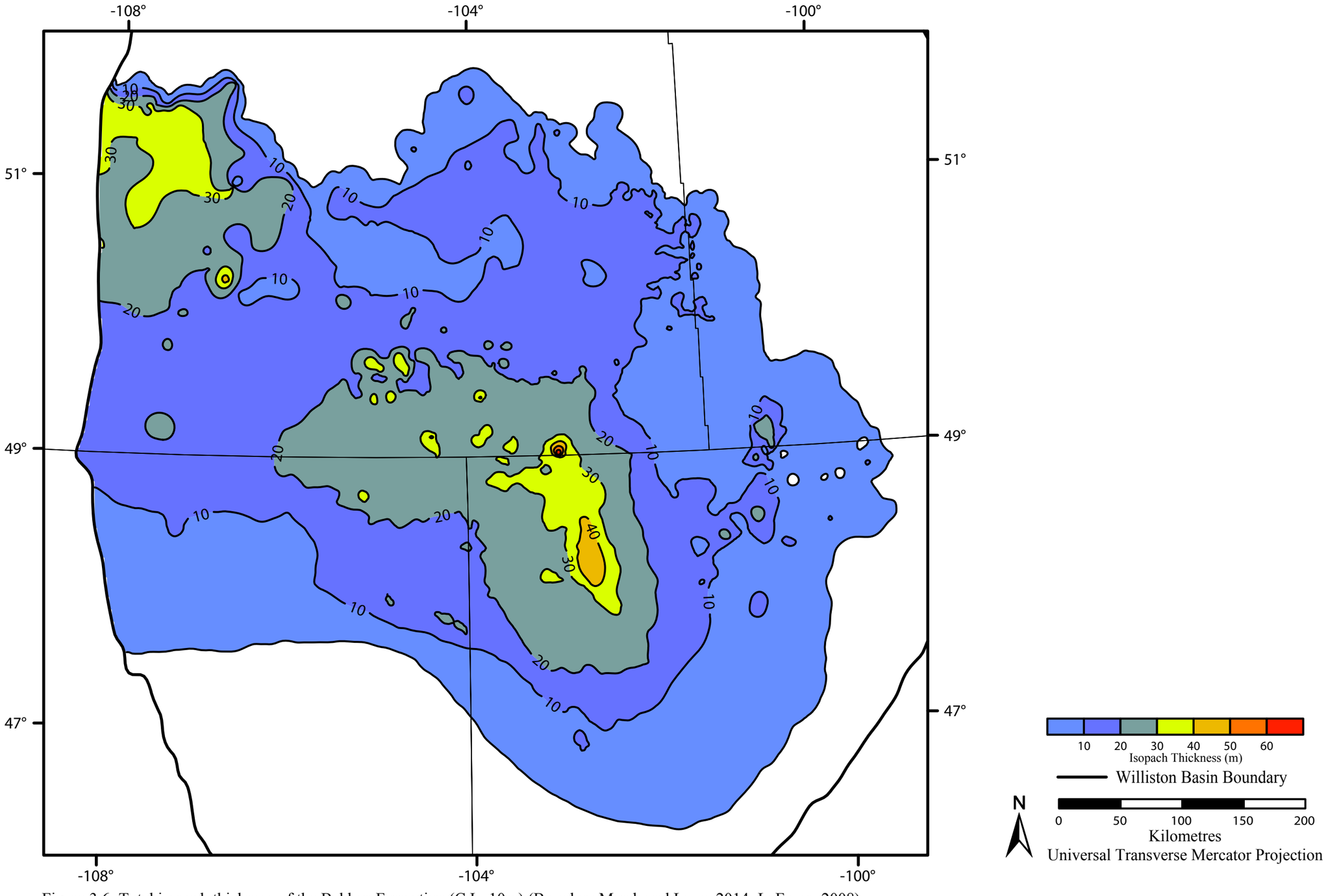

Figure 3.6: Total isopach thickness of the Bakken Formation (C.I.=10m) (Based on Marsh and Love, 2014; LeFever, 2008).

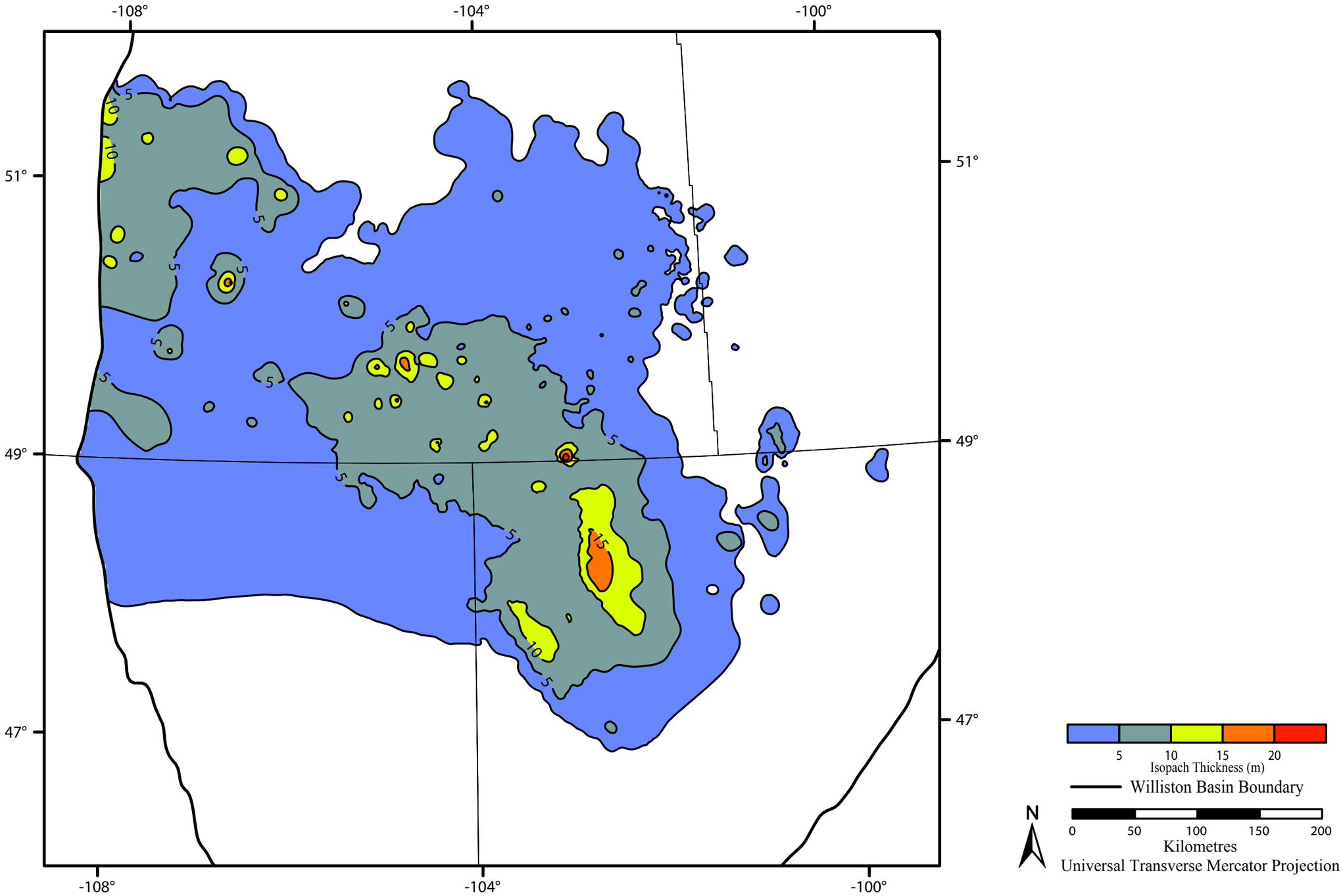

Figure 3.7: Isopach thickness of the Lower Bakken Member (C.I.= 5 m) (Based on Marsh and Love, 2014; LeFever, 2008).

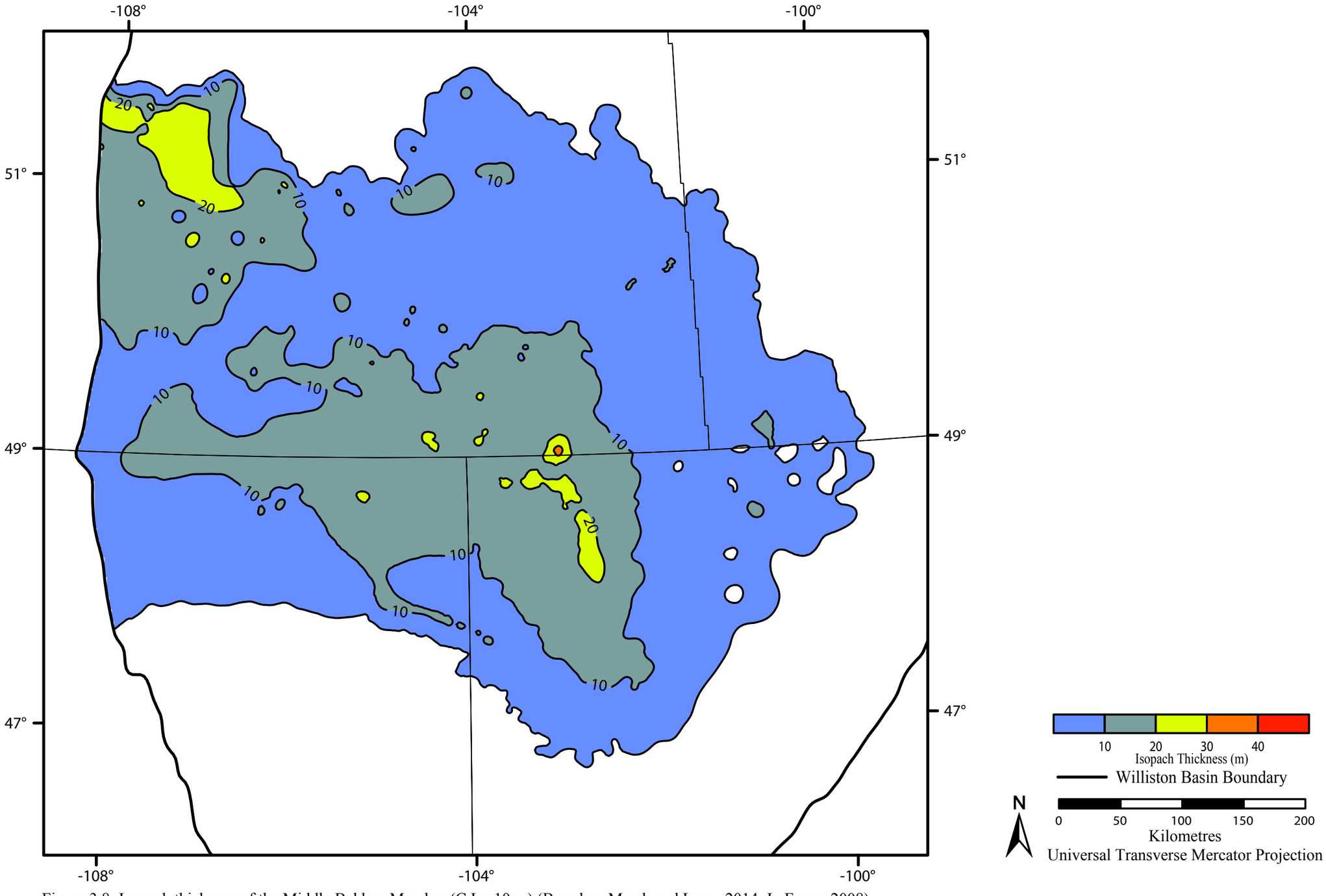

Figure 3.8: Isopach thickness of the Middle Bakken Member (C.I.= 10 m) (Based on Marsh and Love, 2014; LeFever, 2008).

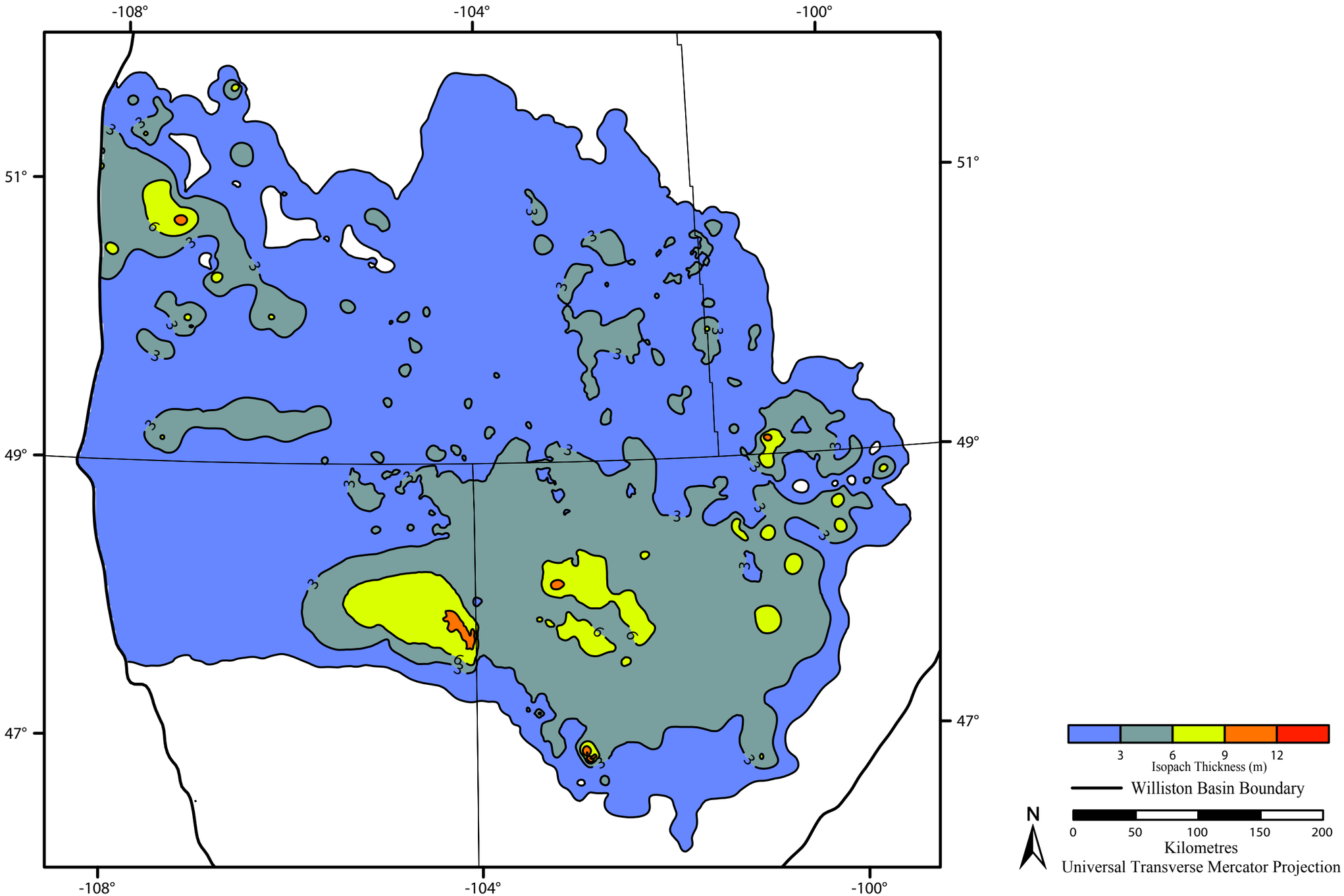

Figure 3.9: Isopach thickness of the Upper Bakken Member (C.I.= 3 m) (Based on Marsh and Love, 2014; LeFever, 2008).

4. Data and Data Processing

4.1. Data Sources

Multiple forms of data were collected all from publicly available sources. Sources included: The American Institute of Formation Evaluation, AccuMap, the Canadian Institute of Formation Evaluation, geoSCOUT, Montana Board of Oil and Gas, North Dakota Board of Oil and Gas, United States Geological Survey, peer reviewed scientific literature, government reports, and unpublished theses projects. Once the data collection was complete it was compiled into Microsoft Excel databases. A summary of the collected data types is shown in Table 1.

4.1.1. Structural Data

The geological framework for this study was constructed using stratigraphic formation tops from over 10,400 oil and gas wells across the Williston Basin. Marsh and Love (2014) provided formation tops on the Canadian side of the basin. LeFever (2008) provided Bakken Formation data for North Dakota. In Montana, formation tops in the Elm Coulee Field were provided from the Montana Bureau of Mines and Geology (Jay Gunderson, personal communication, 2017). Elsewhere in Montana, formation tops from the geoSCOUT database were used in conjunction and supplemented by my own investigation of wells. All formation tops were combined to generate a regional surface map across the entire Williston Basin (Figure 3.5).

4.1.2. Pressure Data

Pressure data were obtained from drill stem tests (DSTs) conducted by the oil and gas industry over the past 60 years. Drill stem tests are temporary completions of wells where an interval of interest is open to atmospheric pressure and therefore fluids are allowed to flow into the test tool (Dahlberg, 1995). From a successful DST, reservoir properties such as the formation temperature, pressure, and flowrate, are measured, and formation fluids are collected.

In the Canadian portion of the Bakken Formation, DST data was obtained from the American Association of Formation Evaluation, the Canadian Association of Formation Evaluation, geoSCOUT (Hydrofax database) and AccuMap (Canadian Hydrodynamics database) current to March 2016.

Drill stem test pressure data in the United States portion of the basin were not included in the AccuMap or geoSCOUT databases. Pressure data for these wells were obtained from digital wellfiles available on the Montana Board of Oil and Gas website and the North Dakota Department of Mineral Resources data subscription website. Drill stem test reports for these wells were qualitatively investigated to determine if a reliable formation pressure could be extrapolated. When possible, a Horner (1951) extrapolation was conducted and the well added to the pressure database.

Combined a total of 1,392 formation pressures were obtained from all available data sources.

4.1.3. Chemistry Data

Publically available data from the AccuMap and Geofluids databases were obtained for the Canadian portion of the basin. Water chemistry data for the United States portion of the basin were obtained from the recently published United States Geologic Survey Nationals Produced Waters Geochemical Database (USGS PWGDB) (Blondes et al., 2016). Water analyses from the AccuMap, Geofluids and USGS

PWGDB databases were supplemented with key unpublished confidential data (Rostron, 2017, personal communication) creating a database spanning the entire Williston Basin.

This database contained 1,982 water samples collected at depths between 500 m and 3,400 m.

4.1.4. Production Data

Production data for this study were obtained from geoSCOUT, the North Dakota Department of Mineral Resources, and the Montana Board of Oil and Gas. Monthly production data by producing formation was obtained and compiled into one composite database with monthly production volumes current to December, 2015.

4.2. Data processing

4.2.1. Interval Testing

To ensure that measured pressures correlated to the correct formation, a process of "interval testing" of all the data was undertaken. If a DST were to straddle multiple formations, it would not accurately represent the pressure in the formation of interest, instead, it would be an average of all the formations sampled.

Interval testing was enabled by the high resolution structural surfaces of the top and bottom of the Bakken Aquifer (top of middle member and top of the lower member).

Drill stem test intervals were compared to formation tops in the database. Tests were categorized as being conducted within; straddling; or outside the Bakken Formation. Tests identified as straddling or outside the Bakken Formation were flagged

and manually examined. Any DSTs confirmed to be outside the Bakken Aquifer were removed from the database.

Drill stem tests straddling the Bakken Formation were treated differently. Tests straddling the Bakken Formation by less than ten metres had their pressure values compared to pressure maps constructed from non-straddle data. Tests which did not agree with the regional trend were removed from the database due to an interpreted cross-formational pressure interaction. Straddle tests which matched the regional values underwent a further geochemical examination to ensure the formation water collected during the DST matched the formation water fingerprint of the Bakken Formation. Tests which showed an out of zone fingerprint were removed from the database.

4.2.2. Water Chemistry Culling

Given the source of the water chemistry samples, i.e. from DSTs and well completions, there is a high potential for contamination from drilling and completion fluids (Hitchon, 1996). The removal of such non-representative water analyses is required to ensure that only representative formation waters are used for further analysis.

The University of Alberta Hydrogeology Research group has previously developed an iterative culling procedure that has been used on Williston Basin Formation waters (i.e. Khan, 2006; Palombi, 2008; Melnik, 2012). Rather than the single knockout approach of other studies (e.g. Hitchon and Brulotte, 1994; Bachu and Hitchon, 1996; Hitchon, 1996; Grasby and Chen, 2005) each analysis is tested against multiple criteria indicating the potential for sample contamination from: drilling; well completions; sample handling; or lab analysis. Using a series of "IF" statements in Microsoft Excel, each time a sample shows signs of contamination it is assigned a value of 1 while clean samples receive a zero. Samples are then ranked by how many criteria indicate non-representative parameters. Samples with the highest cumulative

indications of contamination are removed from the dataset first. By using this technique, a single problematic criterion does not always remove an otherwise good sample.

Previous studies conducted by the University of Alberta Hydrogeology Research Group have shown that up to 75% of raw water samples collected in the Williston Basin show signs of contamination. The following is a summary of the methods used to flag samples showing signs of contamination.

4.2.2.1. Incomplete Analysis

Many water analyses are incomplete and missing vital information such as the sample depth/interval, pH, test type/sampling method. Some samples were also missing major ion species (Chloride, Bicarbonate, Sulphate, Sodium, Calcium, and Magnesium) and were flagged as potentially erroneous. Samples missing a major ion were not immediately removed because if the missing element was below detection limit, or sufficiently low in concentration, it would not influence the overall water chemistry. Samples flagged as incomplete were later manually investigated to determine their suitability for use in the study.

4.2.2.2. Charge Balance Error

A cation-anion balance is the most fundamental item in quality control of a chemical analysis (Davis, 1988). The presence of a large ion imbalance may be the result of an unusual constituent in the sample and can be used as an indicator of a poor quality sample due to the fact that dissolved chemical species are in equilibrium with one another. The percent charge balance was calculated from the following equation (Freeze and Cherry, 1979):

$$\%CBE = \left[\frac{\sum Z * m_c - \sum Z * m_a}{\sum Z * m_c + \sum Z * m_a}\right] * 100\% \qquad (18)$$

Where:

Z is absolute value of the ion's charge, m_c is molality of the cations and m_a is molality of the anions

Water samples with a charge balance error of greater than 10% were flagged and further investigated before removal from the database.

4.2.2.3. Contaminated Samples

The following list represents the culling criteria applied to all water analysis based on similar studies conducted by Alkalali (2002), Khan (2006), Palombi (2008), and Melnik (2012).

4.2.2.4. General Culling Criteria

- A pH of <5 or >8: Formation water typically has a pH between 5 and 8, samples with a low pH could be indicative of a completion fluid while samples with a pH greater than 8 could be contaminated with corrosion inhibitor.
- OH^- present: Samples containing hydroxide may be contaminated with a large amount of drilling mud.
- Carbonate (CO_3^{2-}) reported: Carbonate can not exist in large quantities in pH environments below 8.1 (Langmuir, 1997). Samples containing CO_3^{2-} could be contaminated with drilling mud.
- Density <1000 kg/m³: Fluids with a density of less than 1000 kg/m³ may indicate the presence of alcohol based drilling mud.
- Recovery <100 m: DSTs with small recoveries were avoided when ever possible due to their susceptibility to contamination from drilling fluid. However, due to the tight nature of the Bakken Formation, this was not always possible. Low recovery samples (<100 m) were flagged and underwent further manual investigation to determine their representativeness compared to the regional trend.

4.2.2.5. Evidence of Acid Water/Completion Fluid

- pH <4.5
- Ca/Cl ratio <0.3 combined with pH >5.7
- Na/Ca ratio <1.2
- Na/Ca <5 and Na/Mg <10, combined with pH <6
- Na/Cl <0.4 and pH <6.8

4.2.2.6. Corrosion Inhibitor

- pH >9
- Na/Cl >3.5 and SO_4/Cl >1.5
- SO_4/Cl >10

4.2.2.7. Mud Filtrate/ GelChem

- Na/Cl >5
- Na/Cl >3.5 and SO_4/Cl >1.5

4.2.2.8. KCl Mud Filtrate ("Kill Fluid")

- Na/K <20

In conjunction with these chemical criteria, a number of other parameters were examined to determine the quality of the water analysis.

First, the sampling point location was considered when evaluating ion ratios. Samples can be collected from various locations including different positions in the drill pipe (top, middle, bottom), a given height above the downhole sampler, and within the downhole sampler. The most representative samples are generally found at the bottom of the fluid column, or in the down-hole sampler. The further from the bottom, or the further up from the sampling tool, the more likely the sample is contaminated (Palombi, 2008). This is due to the fact that during drilling, high-density drilling fluid displaces the lower density formation water, therefore, contaminating the formation

near the well annulus. When a formation is sampled in a DST, the initial fluids produced into the wellbore are drilling fluids. As the DST recovery proceeds formation fluids are produced into the wellbore making the lower samples reflect the formation water composition.

The second operation of concern is the use of a water cushion in DSTs. A water cushion is often used in DSTs conducted at great depths to help mitigate damage to the formation which could result from the extreme pressure differential between the formation and open atmosphere. Water cushions are installed in the drill pipe prior to testing by adding a volume of fluid to the drill pipe. This extra volume of fluid can dilute the recovered formation water, therefore; care must be taken when using DSTs which used a water cushion.

The third practice that can cause non-representative samples are samples collected after hydraulic fracture stimulations. This is especially true in the Bakken Formation where hydraulic fracturing has become a common practice. These hydraulic fracture stimulations inject large volumes of anthropogenic water into the formation. That injected water must be produced back before a sample can be considered representative. In some cases, flowback can take months or more rendering samples collected from the well immediately following treatments non-representative.

To mitigate this, records of the well stimulations were obtained from AccuMap, geoSCOUT, and the North Dakota Board of Oil and Gas that included the stimulation date and volume of fluid injected. The sampling date and the stimulation date were compared using an "IF" statement in the Excel database. If the sample was collected from a well with no stimulation treatment, or prior to the stimulation a zero flag was assigned. If sampling occurred following the stimulation a value of one was assigned.

Wells sampled after stimulation underwent additional investigation. The volume of water produced at the time of sampling was compared to the volume of water injected during stimulation using monthly production data. If the sample was collected post stimulation, and prior to the date where the total injected volume could be produced, the sample was again assigned a value of one indicating the potential for

contamination/dilution. Flagged wells were finally investigated in greater detail and compared to the regional chemical pattern obtained from representative samples in the area to determine the extent of influence from the stimulation. Samples which did not agree with the regional trend were removed from the database.

Finally, the high pressure and high volume of water used in stimulations treatments, have the potential to influence surrounding wells as well. Thus, water samples collected from wells near stimulated wells were also investigated for signs of contamination or dilution from nearby operations. Samples showing signs of contamination from a neighbouring stimulation were removed from the database.

Overall, the culling procedure ended up being mostly manual due to the variability of formation waters on a regional scale. This culling procedure combined with multiple successive mapping iterations produces the best representation of the hydrochemical distribution within the Bakken Aquifer. After culling, 92% of the data were removed from the database (Figure 4.1; Table 1).

4.2.3. Drill Stem Test Culling

Formation pressures obtained from DSTs can provide valuable hydrogeological parameters such as aquifer pressures, flow rates, temperatures, and fluid samples (Dahlberg, 1995). All pressure data were screened using both automated and manual techniques to remove any non-representative formation pressures.

Each DST was interval tested (section 4.2.1) to ensure the interval tested was in the Bakken Aquifer. Drill stem test quality codes (Table 2) were evaluated. Ideally, the best quality (A-B) tests were utilized, however, due to the limited data available for the Bakken Formation, all tests with a stabilized formation pressure were retained for

further mapping. The DST chart(s) for each well were qualitatively investigated. Tests with a qualitative permeability of low, and virtually none were removed from the database. Test fluid recoveries were examined and compared to the Bakken Aquifer chemical fingerprint. When possible tests with large water recoveries were used however all tests which stabilized were plotted.

4.2.4. Cumulative Interference Index

A stabilized formation pressure is required for the calculation of hydraulic head among other things. However, in mature sedimentary basins with extensive hydrocarbon development, production, and injection wells have modified the natural pressure distribution in the subsurface. As fluids are produced from a well, the fluid potential in the aquifer near the well is reduced conically around the wellbore and as time increases the cone of depression extends radially outwards into the basin (Tóth and Corbet, 1986). For injection wells, the pressure disturbance is reversed but the creation of disturbed conditions still exists.

Pressure from a DST conducted near a producing field can be stabilized, however, the pressure obtained may be influenced by nearby production and/or injection wells. To accurately represent the natural pressure distribution, wells that have been influenced by production or injection must be identified and removed from the database.

To account for the potential influence from nearby wells, the Cumulative interference index (CII) was employed (Barson, 1993; Rostron, 1994; Alkalali, 2002). The CII method was developed as a series of iterative improvements to the pressure culling algorithms starting with Tóth and Corbet, (1986). They proposed an "interference index" (I), as a method of assessing the influence of a single production

wells on a nearby DST. The interference index was based on the Theis equation where the drawdown in an aquifer as a result of pumping can be calculated:

$$s = \frac{QW(u)}{4\pi T} \tag{19}$$

Where Q is specific discharge, T is aquifer transmissivity, $W(u)$ is well function

$$W(u) = \int_{u}^{\infty} \frac{e^{-u}du}{u} \tag{20}$$

Where:

$$u = \frac{r^2 S}{4Tt} \tag{21}$$

Where: r is distance between the production well and the DST well, S is aquifer storativity, T is aquifer transmissivity, and t is pumping time.

It is clear from equation (19) and (21) that drawdowns are dominated by $\frac{1}{r^2}$ and t. On a regional scale storativity and transmissivity are difficult to estimate but the value of u can be controlled by t and r^2 if the well has been produced for an extended period of time, or if the distance between wells is large (Alkalali, 2002).

Tóth and Corbet (1986) showed that the effects of production are directly proportional to the interference index:

$$I = \log \frac{t}{r^2} \tag{22}$$

Where: t is the pre DST production time (in days) and r is the distance between the production wells and the DST well (in km).

By using the interference index, a threshold value could be determined at which effects of nearby production become significant and therefore pressure measurements are no longer representative of the virgin formation pressure and should be removed.

Barson (1993) included the principle of superposition in the calculation to account for multiple wells and created the cumulative interference index:

$$CII = \log \Sigma \frac{t}{r^2} \tag{23}$$

Alkalali (2002) developed a computer program to calculate CIIs for every DST in the interval of interest. Drill stem tests with a CII of greater than 0.2 were removed from the dataset and the remaining DSTs were manually investigated. A sensitivity analysis of the CII value and search radius was undertaken. The search radius was varied from 1 to 200 km and the CII value cut off was incrementally varied from -2 to 0.2. This revealed that using a search radius of 20 km and a CII of - 1.5 produced the best results highlighting wells which showed significant production effects. More recently Sing et al, (2017) developed a C-language program to calculate the CII. After culling, 90% of the initial pressure data was removed (Figure 4.2; Table 1).

4.2.5. Water Driving Force Calculation

From Davies (1987) the net driving force of water at a point location can be represented by the equation:

$$WDF = \nabla H_f + \frac{\Delta \rho}{\rho_f} \nabla E \tag{24}$$

Where: the water driving force (WDF) is the sum of the freshwater hydraulic head gradient (∇H_f) and the density related driving force ($\frac{\Delta \rho}{\rho_f} \nabla E$) This equation shows that it is not the absolute magnitude of one component of flow which dictates overall flow direction, rather than relative magnitudes each component has with the other (Figure 2.2) (Davies, 1987).

Following the methods of Khan (2006), formation water density was determined from Chierici's (1994) equation of state:

$$\begin{aligned}\rho_w = {} & 730.6 + 2.025T - 3.8 * 10^{-3}T^2 \\ & + [2.362 + 1.197 * 10^{-2}T + 1.835 * 10^{-5}T^2] \\ & + [2.374 - 1.024 * 10^{-2}T + 1.49 * 10^{-5}T^2 \\ & - 5.1 * 10^{-4}P]C\end{aligned} \quad (25)$$

Where: ρ_w is formation water density; P is pressure (in MPa); T is temperature (in kelvin); and C is TDS (in g/L).

This equation was chosen because it estimates densities above 1050 kg/m³ better than other methods (Khan, 2006).

Formation water temperatures used in Chierici's (1994) equation were calculated from the predicted temperature at depth based on an average geothermal gradient of 25°C/km. A sensitivity analysis of the geothermal gradient was conducted and changes of ± 5°C/km. It had little effect on the calculated formation water density.

Vector addition of the WDF equation was used to determine flow directions using discretized grids of the formation water density and the hydraulic gradients calculated from the freshwater hydraulic heads. Vectors were calculated in an excel spreadsheet and plotted using Golden Software Surfer following the methods of Melnik (2012).

4.2.6. Production Data Manipulation

The influence of regional groundwater flow in the Bakken Aquifer on hydrocarbon production and accumulation is unclear. Production behaviours of Bakken Formation oil wells were characterized based on a series of regularly spaced north to south transects (Figure 4.3). Wells in the transects were selected based on the following criteria:

1) The orientation of the well: Vertical wells were preferentially selected when ever possible.
2) The initial production date: The oldest wells were preferentially selected because they were the least likely to be influenced by external fluids introduced by other production wells.
3) The production duration: Wells with the longest production history were preferentially selected to show the production behaviour over the longest interval possible.
4) The relative proximity to other production and/or injection wells: Care was taken to avoid wells near other production or injection wells to limit the effects of external fluids that could be produced from nearby hydraulic fracture stimulation operations.

A detailed culling procedure was employed ensuring only wells completed and producing from the Middle Bakken Member were included in this investigation rather than wells producing from the entire Bakken petroleum system. Production intervals were verified by cross examining the production interval listed in the geoSCOUT well ticket against the formation tops (verified by investigating wireline logs and drillings reports), and the production interval as listed in the drilling and completion reports available from the North Dakota Department of Mineral Resources wellfile database, and Montana Board of Oil and Gas websites. Care was taken to ensure that all perforations, and hydraulic fracture stimulation operations were conducted solely within the Middle Member of the Bakken Formation. Wells completed in multiple formations, or that had the wellbore contacted a shale member in the horizontal section of the well were removed from the database.

The distribution of production behaviours was then combined with hydrogeological interpretations to identify any influences from regional groundwater flow.

Data Type	Raw Data	Mapped Data	Percent Removed
Pressure Data	1392	137	90%
Chemistry Data	1982	167	92%
Structural Data	25926	10449	60%

Table 1: Summary of data types collected and mapped in this study.

Quality Code	Description
A	Best Quality
B	Nearing Stabilization
C	Caution (DST tool plugging)
D	Questionable (or misrun)
E	Low permeability; Low pressure
F	Low permeability, High pressure
G	Misrun

Table 2: Description of DST quality codes.

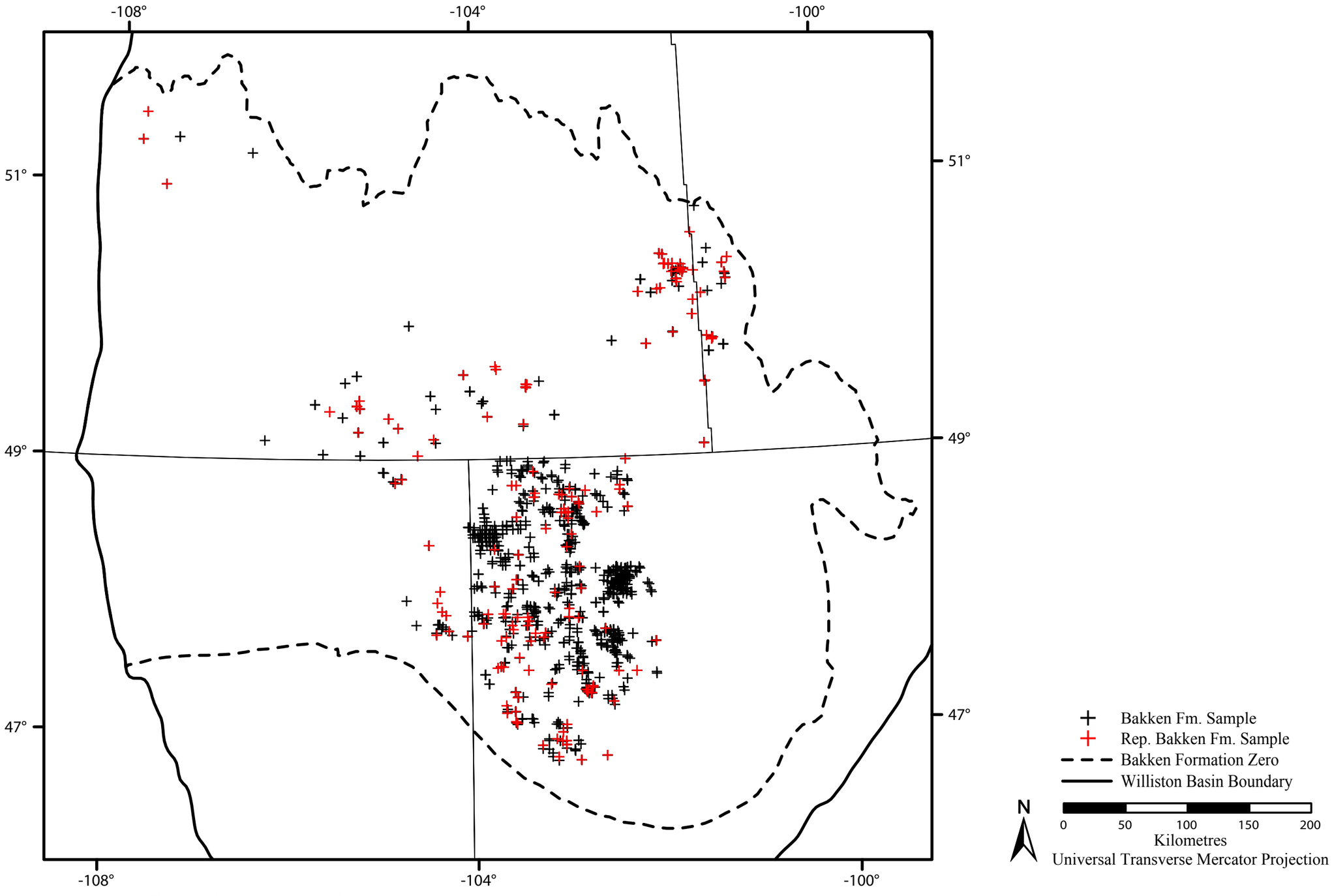

Figure 4.1: Distribution of representative Bakken Water samples.

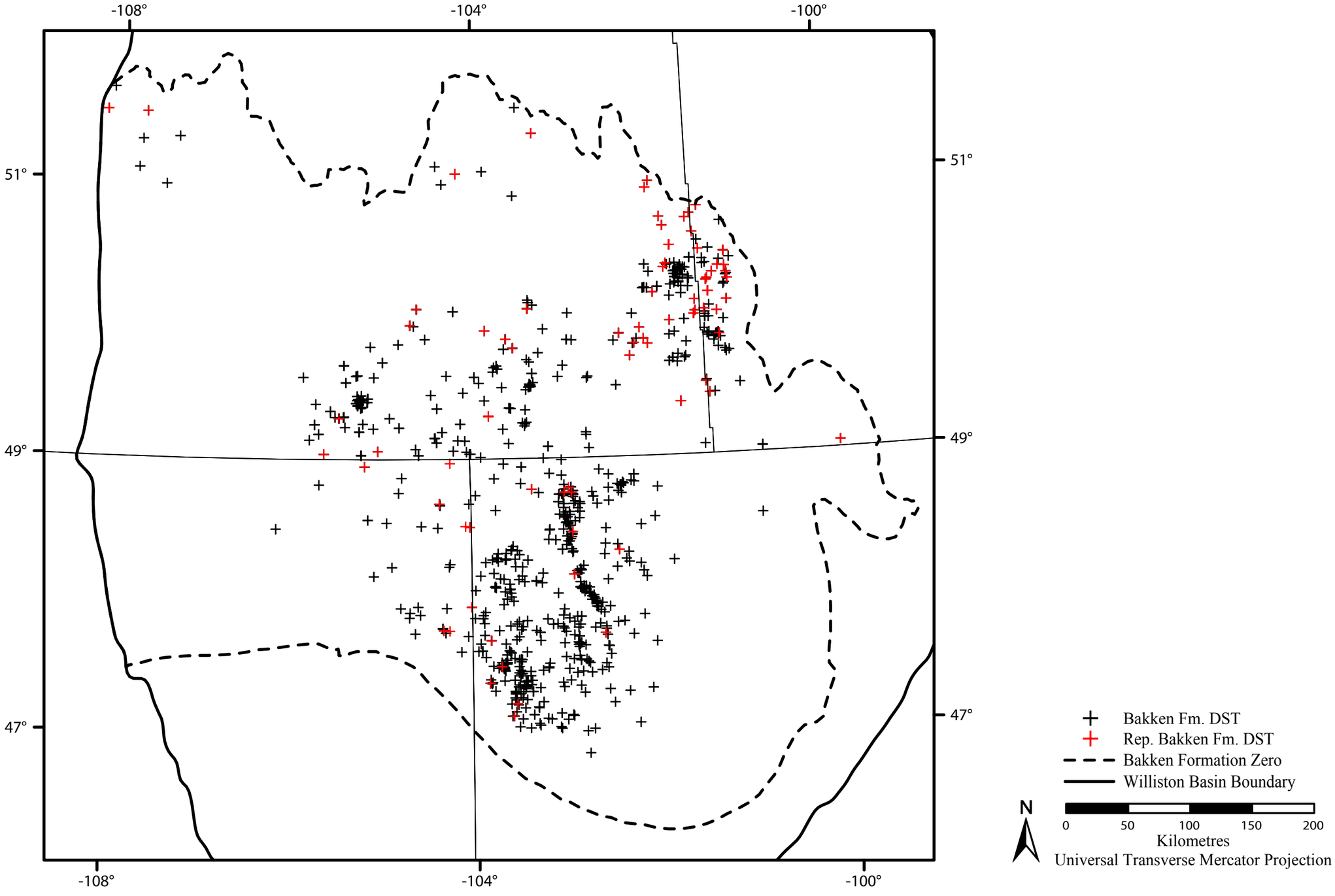

Figure 4.2: Distribution of representative Bakken DSTs.

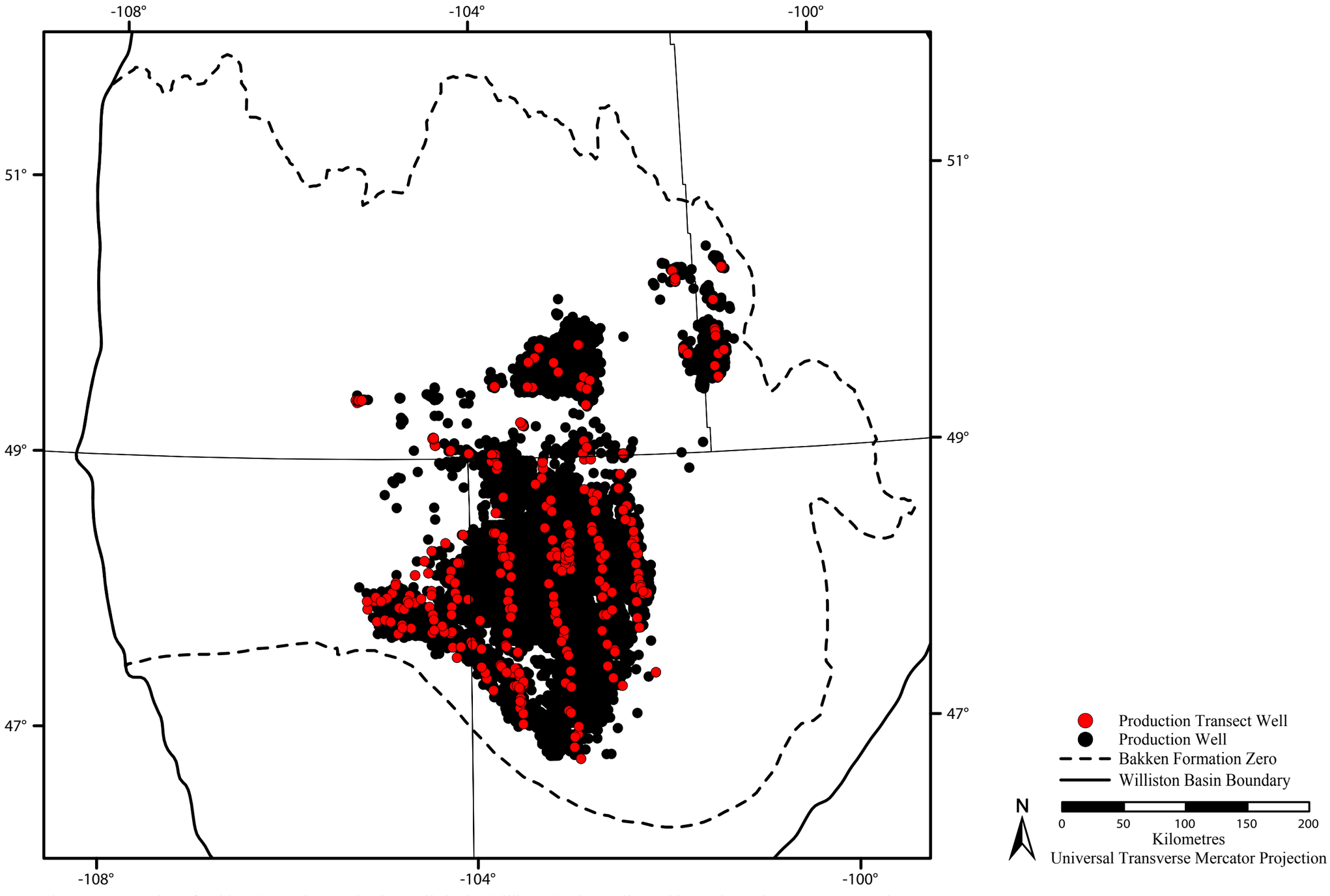

Figure 4.3: Location of Bakken Formation production wells in the Williston Basin. Wells used in north-south transects across the productive area of the Bakken are shown in red.

5. Results

5.1. Hydrochemical Results

5.1.1. TDS Distribution

The regional distribution of total dissolved solids (TDS) in the Bakken Aquifer is shown in Figure 5.1. The TDS concentration values of Bakken Aquifer water range from <5,000 mg/L to >300,000 mg/L. Dissolved solids in the Bakken Aquifer are highest in the central portion of the basin and decrease radially outward with decreasing depth. The lowest salinities within the Bakken Aquifer are found in central Montana extending in a circular arch north into Saskatchewan towards the Bakken Formation subcrop. The interpreted salinity gradient within the Bakken Aquifer is steeper in the west than the north or south. Little is known about the salinities and salinity gradients near the margins due to data limits.

5.1.2. Major Ion Chemistry

Bakken Aquifer waters are dominantly Na-Cl type waters with the exception of three Na-SO_4 waters (Figure 5.2). Water types are spatially correlated (Figure 5.3) with Na-SO_4 formation waters found in the northwest corner of the Bakken Formation and Na-Cl waters are everywhere else.

The chemical composition of Bakken Aquifer waters as a function of TDS is highly variable (Figure 5.4, Figure 5.5).

Sodium (Na^+) exhibits a strong linear relationship with TDS up to 200,000 mg/L. Beyond 200,000 mg/L, the linear relationship deteriorates (Figure 5.4a) with more variable Na^+ content with less Na^+ as TDS increases. There appears to be a group of linear Na^+ versus TDS waters and a group with less Na^+ between 200,000 and 300,000 mg/L.

Calcium (Ca^{2+}) concentrations in the Bakken Aquifer are highly variable. Calcium accounts for up to 28% of the total cations in waters with 50,000 mg/L TDS. Waters with a TDS between 50,000 and 200,000 mg/L contain the lowest Ca^{2+} percentage (between 1% and 8%), while brines with salinities over 200,000 mg/L consist of up to 25% Ca^{2+}. As the salinity increases, the abundance of calcium in Bakken Aquifer water increases resulting in a "U" shape in the $\%Ca^{2+}$ versus TDS plot (Figure 5.4b).

Potassium (K^{+}) concentrations are highly variable exhibiting an exponential increase with increasing TDS (Figure 5.4c). Bakken Aquifer waters with TDS values of <200,000 mg/L contain roughly the same K^{+} concentration regardless of salinity. K^{+} concentrations over this range are between approximately 110 mg/L to approximately 600 mg/L. At salinities >200,000 mg/L, K^{+} concentrations become highly variable increasing up to 9,000 mg/L K^{+}.

Magnesium (Mg^{2+}) concentration in the Bakken Aquifer generally increase with TDS but are highly variable. For waters with <50,000 mg/L TDS Mg^{2+} account for up to 5.5% of the total cations. Waters with TDS between 50,000 and 350,000 mg/L generally contain 0.5% to 2% Mg^{2+}. Two high TDS waters contain approximately 4% Mg^{2+} (Figure 5.4d).

Chloride (Cl^{-}) concentration in the Bakken Aquifer is strongly correlated to TDS. As TDS increases, Cl^{-} increases (Figure 5.5b) Chloride is the dominant anion in the Bakken Aquifer with most samples >75% Cl^{-} (Figure 5.2).

Sulphate (SO_4^{2-}) exhibits an opposite correlation with TDS (Figure 5.5c). For waters with TDS <50,000 mg/L, SO_4^{2-} accounts for up to 85% of the total anions in Bakken Aquifer waters. As TDS increases, SO_4^{2-} decreases exponentially. Waters with 100,000 mg/L TDS contain approximately 10% SO_4^{2-}; at 200,000 mg/L SO_4^{2-} concentrations do not exceed exceeds 2.5%; and by 300,000 mg/L TDS and above, SO_4^{2-} accounts for only a fraction of a percent. With the exception of three samples, SO_4^{2-} accounts for <20% of the total ions (Figure 5.5c).

Bicarbonate (HCO_3^-) also exhibits a strong negative correlation versus TDS (Figure 5.5d). Waters with <50,000 mg/L contain up to 8.5% HCO_3^- however as TDS increases HCO_3^- decreases exponentially. With the exception of a handful of samples, HCO_3^- accounts for <1% of the total anions in waters with TDS >100,000 mg/L.

5.1.3. Bakken Aquifer Water Types

Examination of the ion concentrations and TDS allows the recognition of four chemically distinct waters in the Bakken Aquifer. This is recognizing three subdivisions of the Na-Cl type water along with the Na-SO_4 type water (Figure 5.6, Figure 5.7, Figure 5.8). This follows previous research in the Williston Basin showing three distinct water types as well as mixes amongst themselves (Iampen, 2003; Palombi, 2008; Melnik 2012). The four water types are discussed in detail below (Table 3).

Type 1 formation waters (Na-SO_4) are the freshest waters in the Bakken Aquifer. Type 1 Bakken Aquifer waters have TDS <10,000 mg/L, and have >50% SO_4^{2-} (Figure 5.7, Figure 5.8).

Type 2 (a,b,c) waters are all Na-Cl type waters (Figure 5.6) but can be subdivided accordingly. Type 2a Bakken Aquifer waters have a TDS between 10,000 and 280,000 mg/L, and contain <400 meq/L Ca^{2+} (Figure 5.8a). Type 2b waters are highly saline with TDS >300,000 mg/L, and contain >400 meq/L Ca^{2+} (Figure 5.8a). Type 2c waters are similar to Type 2b waters with >400 meq/L Ca^{2+} however; these waters are comparatively fresher with TDS between 200,000 and 235,000 mg/L (Figure 5.8a).

Figure 5.7 and Figure 5.8 shows the relationship between ion concentration and TDS for Type 1, Type 2a, Type 2b and, Type 2c formation waters. Type 1 and Type 2a waters plot along a well-defined linear trend on the Na^+ versus TDS plot (Figure 5.7a). Type 2b and Type 2c formation waters plot in a second more scattered field. Type 1

waters contain a lower Na^+ and TDS content than Type 2a waters. Type 2b and Type 2c waters plot along a separate linear trend with significantly more scatter. Type 2c waters contain less Na^+ than type 2b waters.

Calcium abundance in the Bakken Aquifer are variable as shown by the U shaped curve in Figure 5.7b. Type 1, Type 2b and, Type 2c waters generally contain >10% Ca^{2+} while Type 2a waters generally contain <10% Ca^{2+}. Type 2a waters with TDS <50,000 mg/L can contain up to 13% Ca^{2+} however, Type 2a waters with salinities over 150,000 mg/L contain <6% Ca^{2+}. Type 2a and Type 2c waters both have a TDS range between 200,000 and 235,000 mg/L however, the percentage Ca^{2+} is different. Based on the Ca^{2+} content, it is apparent that these waters have experienced different evolutionary histories. Calcium abundance at a given salinity are variable within each water type especially at the salinity endmembers in the Bakken Aquifer. In any case there are high Ca^{2+} brines within the Bakken Aquifer.

Potassium concentrations in Type 2a, Type 2b and, Type 2c waters increases with increasing TDS (Figure 5.7c). Potassium concentration in Type 2a waters in relatively similar between 30,000 and 200,000 mg/L (30-600 mg/L). Type 2b and Type 2c waters experience significantly more variability in K^+ concentration at a given salinity. Between 200,000 and 350,000 mg/L TDS, K^+ concentrations are between 1,000 and 8,000 mg/L.

Magnesium abundances in the Bakken Aquifer are variable (Figure 5.7d). Types 1 waters contain between 5 and 6% Mg^{2+}. Type 2a waters experience a decrease in Mg^{2+} abundance from 4.5% to <1% as TDS increases from 25,000 to 250,000 mg/L. Type 2b and 2c waters contain between 0.1 and 4.2% Mg^{2+} regardless of the salinity.

Chloride concentrations increase linearly with respect to Type 1, Type 2a, and Type 2b waters all plotting along a well defined linear trend with a slope of 1:2 (Figure 5.8b). Type 2c waters have a lower Cl^- and TDS content than Type 2b waters plotting between the Type 2a and 2c waters on the Cl^- versus TDS trend.

The SO_4^{2-} abundance in Type 1, Type 2a and, Type 2b waters decreases with increasing TDS (Figure 5.8c). Type 1 waters contain up to 85% SO_4^{2-}. Type 2a waters with low salinity contain up to 27% SO_4^{2-} however at salinities of 150,000 mg/L and higher SO_4^{2-} accounts for <5% of the anion fraction of the waters. Type 2b and Type 3c waters contain little to no SO_4^{2-}.

Bicarbonate abundance generally decreases with increasing TDS (Figure 5.8d). Type 1 waters have between 3.7% and 6.2% HCO_3^-. Type 2a waters with <50,000 mg/L TDS may contain up to 8.5% HCO_3^-, however as TDS increases HOC_3^- concentrations decrease. Type 2b and Type 2c waters have <6% HCO_3^- with the exception of one sample.

5.1.4. Spatial Distribution of Water Types

Spatially the four water types plot in distinct locations within the Bakken Aquifer (Figure 5.9). Type 1 formation waters are found in the northwest corner of the study area near the transition from the Bakken Formation in the Williston Basin to the Exshaw Formation of the Alberta Basin. Type 2a waters are generally located outside the central area of the Bakken Aquifer. Type 2b waters are located in Montana and North Dakota and only within the area of extremely limited permeability (Figure 5.10). Type 2c waters are located in southern North Dakota, outside of the area with extremely limited permeability (Figure 5.10).

5.1.5. Na-Cl-Br Systematics

Thirty Type 2 waters had been analyzed for Br^- of the 167 Bakken Aquifer waters (Figure 5.11). While the number of samples analyzed for Br^- is small, the spatial distribution of these samples is sufficient to allow for a representative investigation of the formation waters within the entire Bakken Aquifer (Figure 5.11).

Figure 5.12 shows the raw concentration plot of Cl^- versus Br^- compared to the seawater evaporation trajectory (SET) from McCaffery et al. (1987). Bakken Formation waters can be grouped into three distinct groups on the raw concentration plot (Table 4).

Group 1 formation waters have Br^- concentrations between 15 and 25 mg/L, Cl^- concentrations between 15,000 and 24,000 mg/L and a TDS range between 30,000 and 40,000 mg/L. Group 1 waters do not plot along the SET. Group 1 formation waters contain similar Cl^- concentration found in modern seawater however they are heavily depleted in Br^- (Figure 5.12).

Group 2 formation waters have Br^- concentrations between 420 and 1,080 mg/L, Cl^- concentrations between 150,000 and 210,000 mg/L, and a TDS range between 250,000 and 350,000 mg/L. Group 2 waters plot along the SET and in some cases reaching the point of halite saturation (Figure 5.12).

Group 3 formation waters have Br^- concentrations between 115 and 265 mg/L, Cl^- concentration between 80,000 and 155,000 mg/L and a TDS range between 135,000 and 255,000 mg/L. Group 3 waters plot above the SET and like Group 1 waters, are depleted in Br^- relative to Cl^- compared to modern seawater (Figure 5.12).

Cl^-/Br^- versus Na^+/Br^- ratios are also useful, having been used previously to infer the origins of dissolved salts in the Williston Basin (Iampen, 2003). Cl^-/Br^- versus Na^+/Br^- concentration ratios of Bakken Aquifer waters (Figure 5.13) revealed three distinct groups as found in the Cl^- versus Br^- plot (Figure 5.12). Group 1 waters plot in the top right with Na^+/Br^- ratios between 2,100 and 2,500, and Cl^-/Br^- ratios between 1,800 and 2,200. Group 2 formation waters plot in the lower left of the plot with Na^+/Br^- ratios between 300 and 700 and Cl^-/Br^- ratios between 400 and 800. Group 3 formation water plot more centrally with Na^+/Br^- ratios between 1,100 and 1,500 and Cl^-/Br^- ratios between 1,000 and 1,400.

In comparison to modern seawater composition (blue marker on Figure 5.13), Group 1 and Group 3 waters have higher Cl^-/Br^- and Na^+/Br^- ratios while Group 2

waters Cl^-/Br^- and Na^+/Br^- ratios approximate or are less than those of modern seawater. Group 1 and Group 3 waters plot along a slope of 0.73 while Group 2 waters plot along a 1:1 slope.

Cl^-/Br^- versus Na^+/Br^- plots have been criticized, and an alternative proposed. The isometric log-ratio transformation method of Engle and Rowan (2012) shows that Bakken Aquifer waters continue to plot in the same three distinct groups (Figure 5.14). Group 1 waters plot near Z_1 values of 0, and Z_2 values of 6.3. Three Group 2 waters plot slightly above modern seawater values (Z_1 -0.1, Z_2 5.2) with the rest further down on the SET (after McCaffery et al., 1987) with Z_1 values between -0.3 - -0.11, with Z_2 values between 4.7 and 5.4. Group 3 waters plot between Groups 1 and 2 with Z_1 values of approximately 0 and Z_2 values of approximately 5.8.

The three distinct water groups plot spatially within the Bakken Aquifer (Figure 5.15). Group 1 waters plot in the north near the Bakken Formation subcrop edge near the Saskatchewan Manitoba border. Group 2 waters plot to the south of Group 1 waters near the Canadian United States border. Group 3 waters plot centrally and are only found in the United States portion of the Bakken Aquifer. The interpreted origin of these different groups will be discussed in chapter 6.

5.2. Hydrogeological Results

5.2.1. Hydraulic Head

The equivalent freshwater hydraulic head distribution based on 137 pressure measurements in the Bakken Aquifer is shown in Figure 5.16. Hydraulic head values range from over 2,000 m to less than 400 m in the Bakken Aquifer. The highest hydraulic head values are located within a closed potentiometric surface mound centered near 103°W and 58°N. Outwards from the mound, hydraulic head values rapidly decrease (approximately radially outwards) indicating a steep hydraulic head gradient. Excluding the closed mound, the highest values of hydraulic head are located

in the southwest of the study area approaching 1300 m. Hydraulic head values gradually decrease toward the northeast (as indicated by widely spaced equipotentials) reaching a regional low of less than 400 m near the Saskatchewan–Manitoba border.

Flow being normal to the equipotentials, is from the southwest towards the northeast within most of the Bakken Aquifer.

The permeability of the Bakken Formation is limited especially in the more deeply buried portions. Figure 5.17 shows the locations of Bakken Formation DSTs which showed no response during shut-in periods. When comparing the locations with extremely low permeability, it aligns with the closed potentiometric high.

Section 5.1.1 showed that within the Bakken Aquifer, high salinity brines are present. The effects of the high salinity brines on flow within the Bakken Aquifer are discussed in the next section.

5.2.2. Density Dependent Flow

Following the theoretical developments in section 2.6 water driving force vectors (WDFV) representing both the direction and magnitude of the two flow components were superimposed over top of the equivalent freshwater hydraulic head map (Figure 5.18). Blue vectors represent the EFWH and red vectors represent the net WDFV for the Bakken Aquifer. Areas where density effects are present are where the net WDFV diverges from the EFWH vectors. The magnitude and angular difference between the EFWH and WDF vectors have been calculated and contoured. Bright colours represent areas with significant deviations from the predicted flow direction.

Density-corrected flow in the Bakken Aquifer is from the southwest towards the northeast over most of the study area. However, significant density effects are present in northeast Montana and in two parts of southeastern Saskatchewan (Figure 5.18). Locally, flow directions are modified and in some cases, the direction of flow

can be up to 170 degrees deviated from what is interpreted from the equivalent freshwater head.

5.2.3. Pressure Depth Relationships

To better understand the pressure gradient distribution in the Bakken Aquifer a regional pressure-depth (P(d)) plot was constructed from DST data (Figure 5.19). Due to the large variation in TDS in the Bakken Aquifer (Section 5.1.1), the nominal hydrostatic gradient for freshwater (9.8 kPa/m) as well as for brines over 100,000 mg/L (11.6 kPa/m) are plotted for reference.

The Bakken Aquifer is slightly underpressured at depths of <1,500 m with pressures plotting to the left of the hydrostatic gradient with few exceptions. Pressure points plot along a single pressure gradient of 9.8 kPa/m; equal to the slope of the freshwater nominal gradient. Between 1,500 and 2,800 m pressures plot above the nominal fresh water gradient but still along the nominal brine gradient of 11.6 kPa/m.

Below 3,000 m there is an abrupt change in the observed pressures from normally pressured to overpressured with data clustering to the right of the nominal curve.

Pressure depth gradients for individual DST pressure measurement were calculated, plotted, and contoured (Figure 5.20). The Bakken Aquifer contains a large area (22,000 km²) with greater than hydrostatic pressures. Pressure gradients in the overpressured area increase from hydrostatic levels of 11.6 kPa/m to >14.5 kPa/m. The maximum overpressure gradient in the Bakken Aquifer is centered in North Dakota. Pressures decrease radially outward extending partially into Montana.

5.2.4. Oil Buoyant Force

Oil migration in the Bakken Aquifer can be examined using maps of oil migration vectors. Oil driving force vectors (Section 2.8) were calculated across the

entire Bakken Aquifer. Two such maps were constructed using 36 and 44 API gravity oil as these represent the ranges observed in the Bakken Formation (Cwiak et al., 2015).

The oil driving force vectors for 36 API oil in the Bakken Aquifer (Figure 5.21) shows oil migrating from the centre of the Bakken Aquifer, radially outwards and north toward Canada. A large area of vector convergence where multiple vector arrows intersect is located in northeast Montana (104.2°W, 48.3°N). Northwest of this convergence is an area of vector divergence (near 105.5W 49N). A third area of interest is located near the Saskatchewan Manitoba border where vector converge and the magnitude decreases approaching stagnation (101.9°W, 49.8°N).

The oil driving force vectors for 44 API oil in the Bakken Aquifer are nearly identical to those for 36 API oil. The oil buoyancy vectors show migration to be in the same direction differing only slightly in magnitude. As a result, the map for 44 API oil is shown (Figure 5.22) but not discussed.

5.2.5. Production Behaviours

Analysis of fluid (oil and water) production behaviours from selected wells revealed that there are four distinct production behaviours that are observed in oil wells producing from the Bakken Formation (Figure 5.23, Figure 5.24). Type 1 production behaviour is characterized by high initial oil production and low initial monthly water production (Figure 5.23a). As production continues, monthly oil production decreases and monthly water production increases, eventually surpassing monthly oil production. This reversal from high monthly oil production to high water production typically occurs within the first 5 years of production and this trend continues for the remainder of the wells production lifespan.

Type 2a production behaviour (Figure 5.23b) is characterized by a high initial monthly oil production and low/no monthly water production. Monthly oil production

decreases over the life of the well, however, monthly water production does not increase even in advanced stages of depletion in the reservoir.

Type 2b production behaviour is characterized by a high initial oil and water production in the early stages of production with a rapid decline in monthly production within the first three years (Figure 5.24a). Production volumes then stabilize and experience a much more gradual decline going forward. Unlike the Type 1 production behaviour, wells with Type 2b production behaviour do not experience an increase in monthly water production even in advanced stages of depletion.

Type 3 production behaviour is characterized by high initial production rates followed by a steep decline within the first three years(Figure 5.24b). Like the Type 2b production behaviour, monthly production rates then stabilize and gradual decline over the remainder of the production life. Type 3 production wells consistently produce more water than oil, but do not have a large increase in water production in advanced stages of reservoir depletion.

Well production plots were classified into one of the four previous groups and their spatial extent within the Bakken Formation was mapped (Figure 5.25). Type 1 production behaviour is found exclusively in the northern portion of the Bakken Formation in Saskatchewan and Manitoba. Type 2a and Type 2b production wells are dominantly located in the southern portion of the Bakken Formation in Montana and North Dakota. Wells displaying a Type 3 production behaviour are located throughout the Bakken Formation surrounding Type 2a and Type 2b production wells in the southern portion of the Bakken Formation.

Implications of the production behaviours in terms of hydrogeology and hydrochemistry will be discussed in a later section.

Water Type	Type 1	Type 2a	Type 2b	Type 2c
Water Classification	$Na\text{-}SO_4$	Na-Cl	Na-Cl	Na-Cl
SO_4^{2-} (%)	> 50%	< 50%	< 50%	<5 0%
Ca^{2+} (meq/L)	< 400	< 400	> 400	> 400
TDS (mg/L)	< 10,000	10,000-280,000	250,000-344,000	200,000-235,000

Table 3: Classification scheme for Bakken Aquifer waters.

Group	TDS (mg/L)	Cl^- (mg/L)	Br^- (mg/L)	Na^+ (mg/L)	Na/Br	Cl/Br	Z_1	Z_2
Group 1	30,000-40,000	15,000-24,000	15-25	11,000-16,000	2100-2500	1800-2200	-0.033	6.2-6.3
Group 2	250,000-350,000	150,000-210,000	420-1080	80,000-110,000	300-700	400-800	-0.3-0.1	4.7-5.5
Group 3	135,000-255,000	80,000-155,000	115-265	46,000-98,000	1100-1500	1000-1400	-0.10-0	5.7-6

Table 4: Summary of ion ranges; Na/Br and Cl/Br ratios; and Z_1 and Z_2 values for Na-Cl-Br systematics Group 1, Group 2, and Group 3 waters.

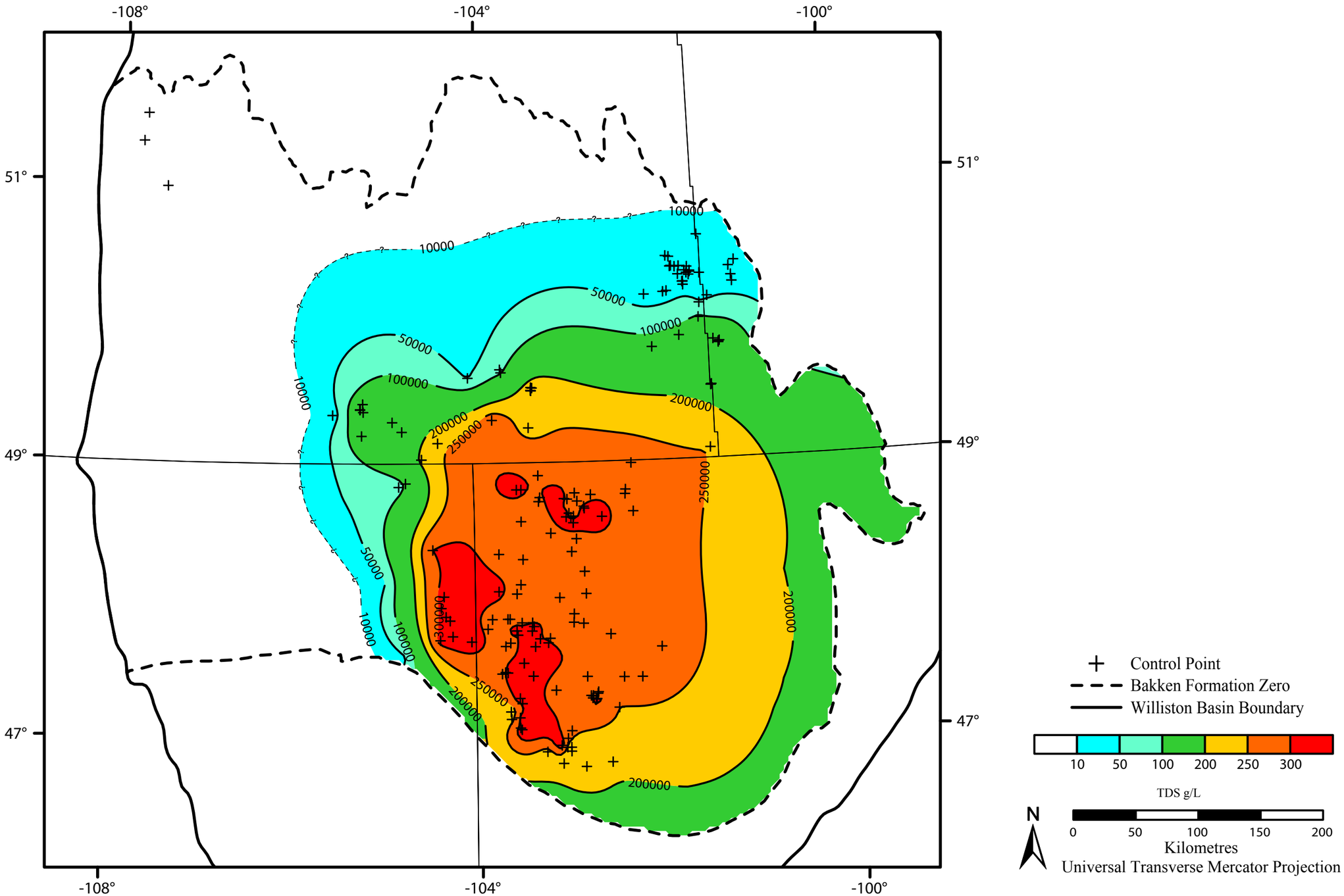

Figure 5.1: Total dissolved solids distribution in the Bakken Aquifer.

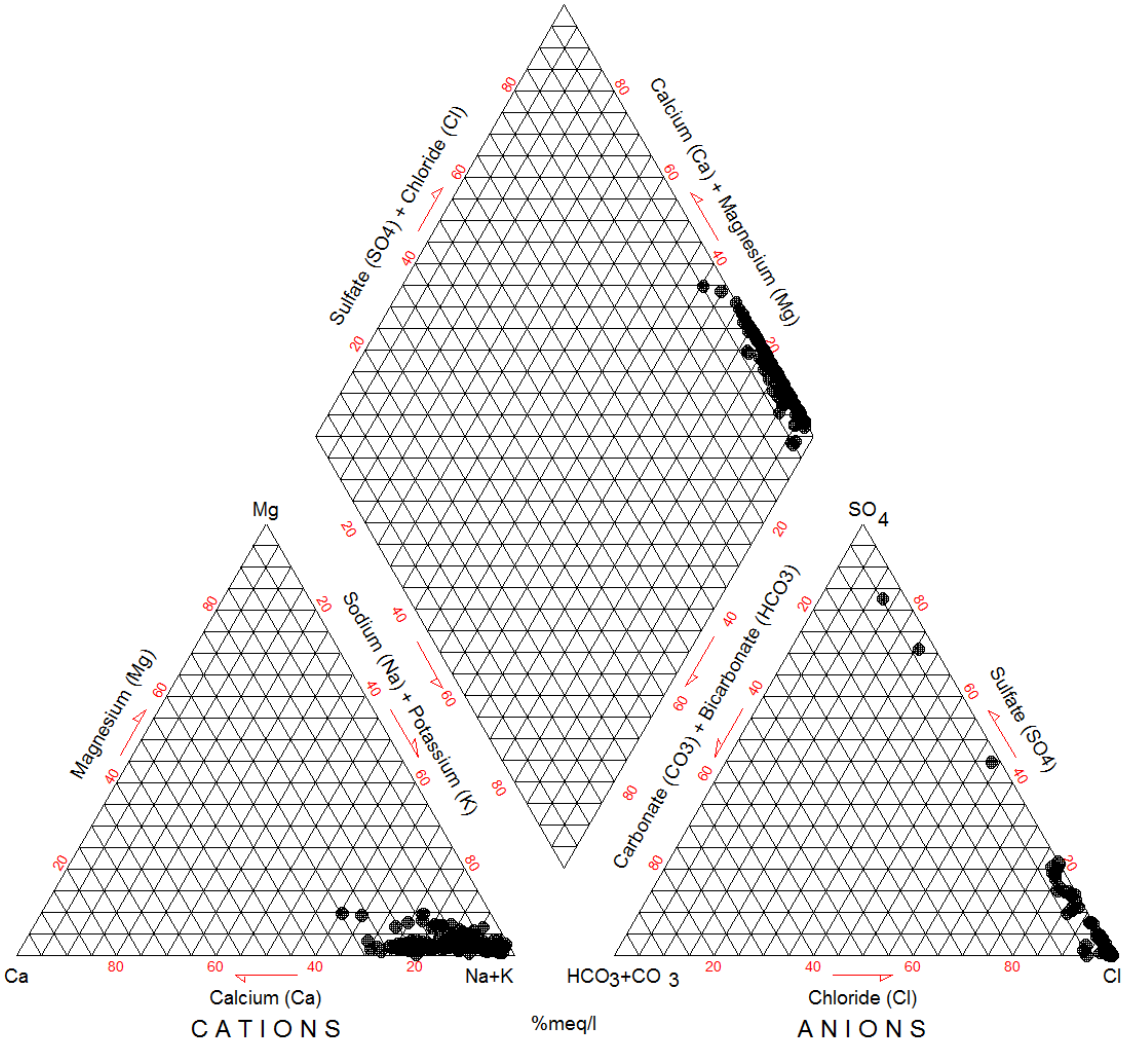

Figure 5.2: Piper diagram for Bakken Aquifer waters.

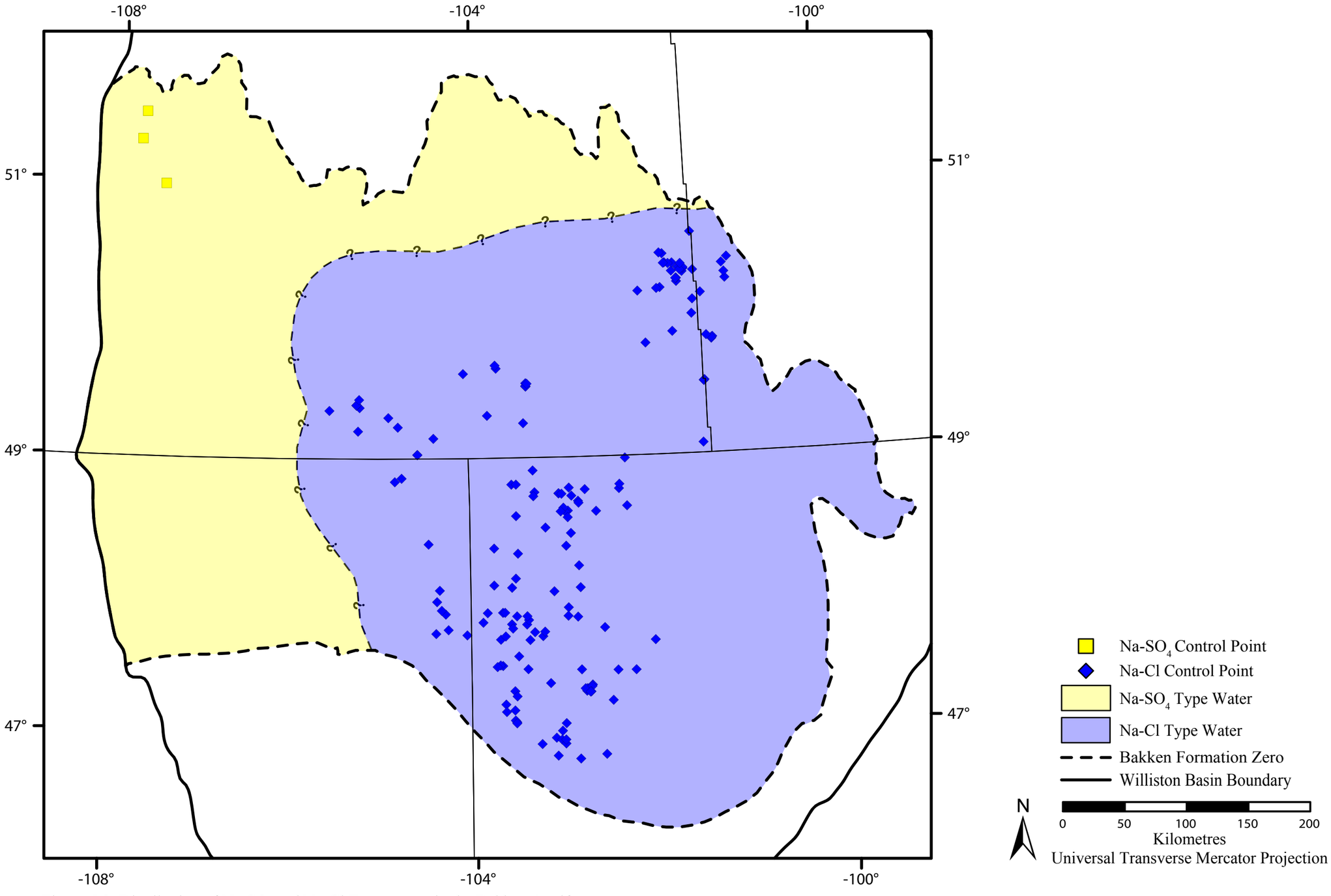

Figure 5.3: Distribution of Na-SO_4 and Na-Cl Type waters in the Bakken Aquifer.

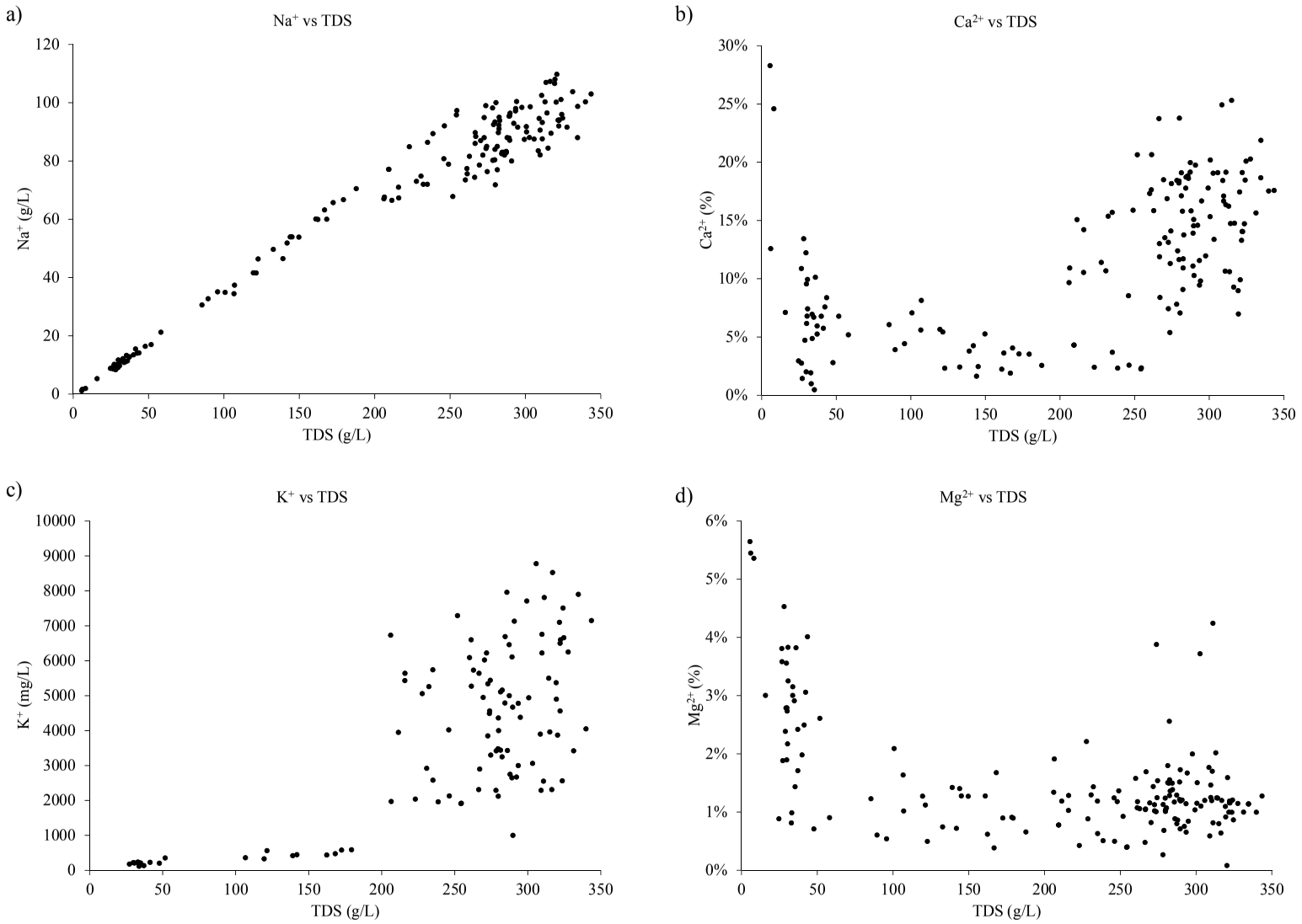

Figure 5.4: Total dissolved solids (g/L) versus: a) Sodium (g/L), b) Calcium (%), c) Potassium (mg/L), d) Magnesium (%).

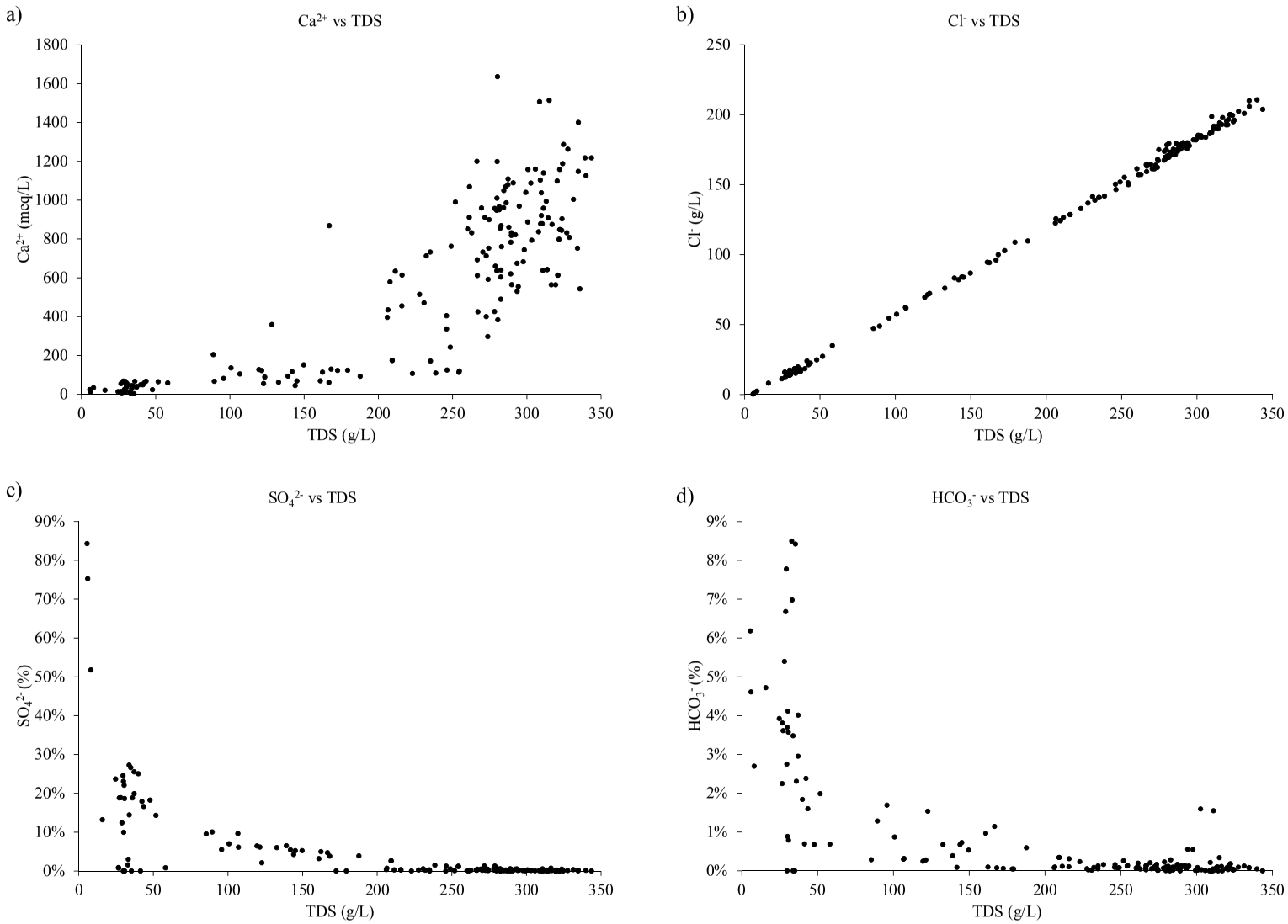

Figure 5.5: Total dissolved solids (g/L) versus: a) Calcium (meq/L), b) Chloride (g/L), c) Sulfate (%), d) Bicarbonate (%).

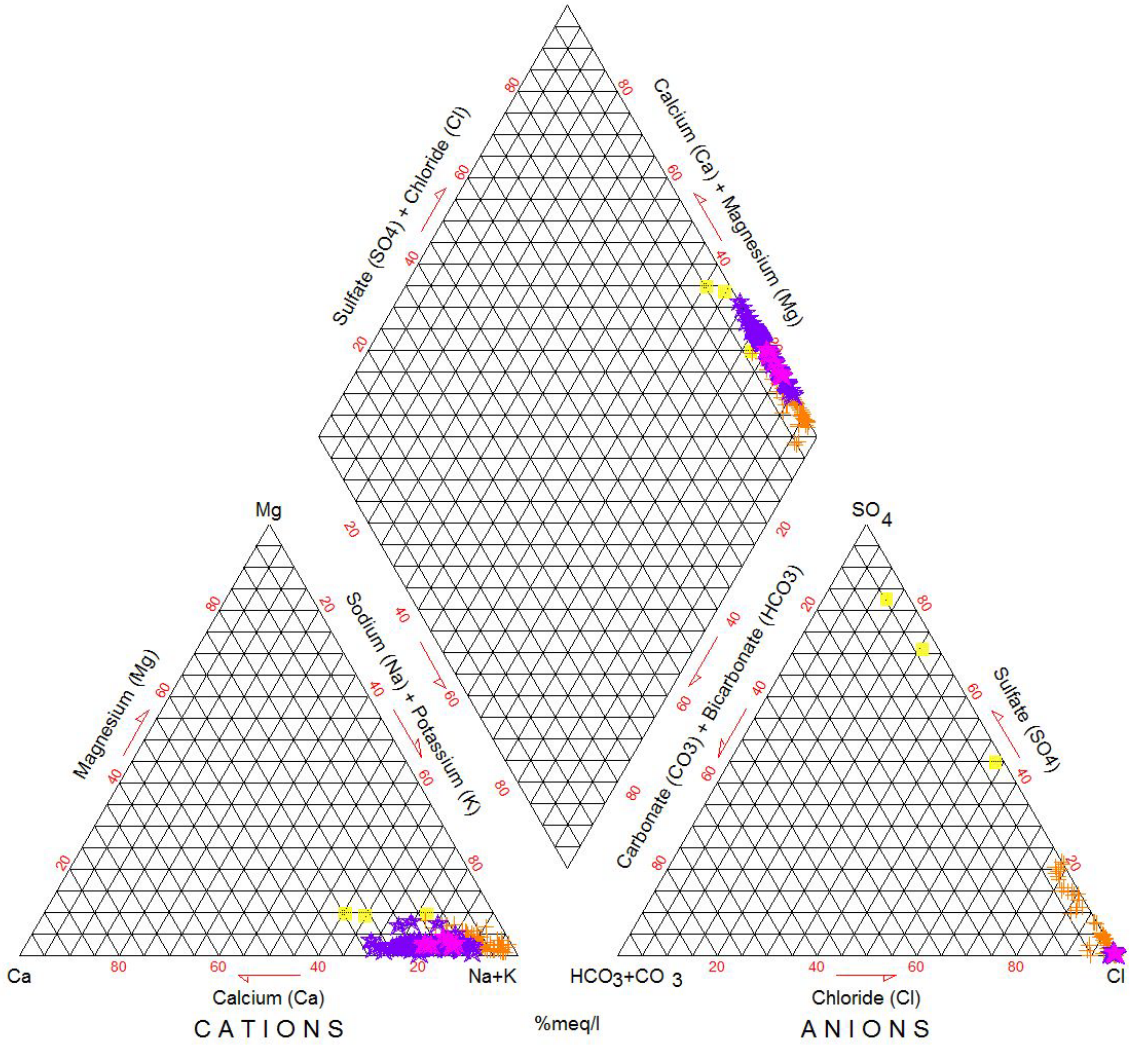

Figure 5.6: Piper diagram for Bakken Aquifer waters classified by waters type.

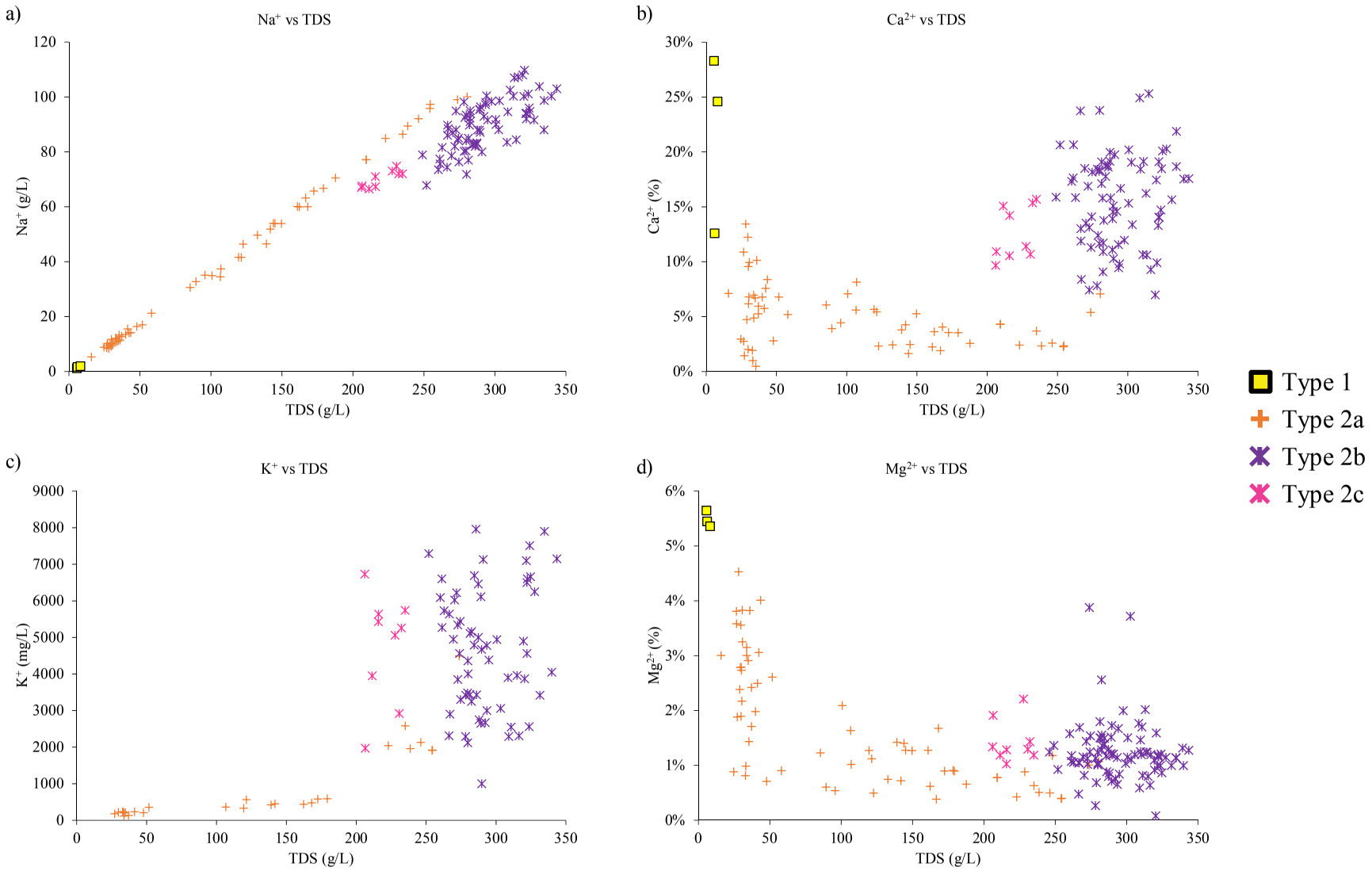

Figure 5.7: Total dissolved solids (g/L) versus: a) Sodium (g/L), b) Calcium (%), c) Potassium (mg/L), d) Magnesium (%) for classified Bakken Aquifer waters.

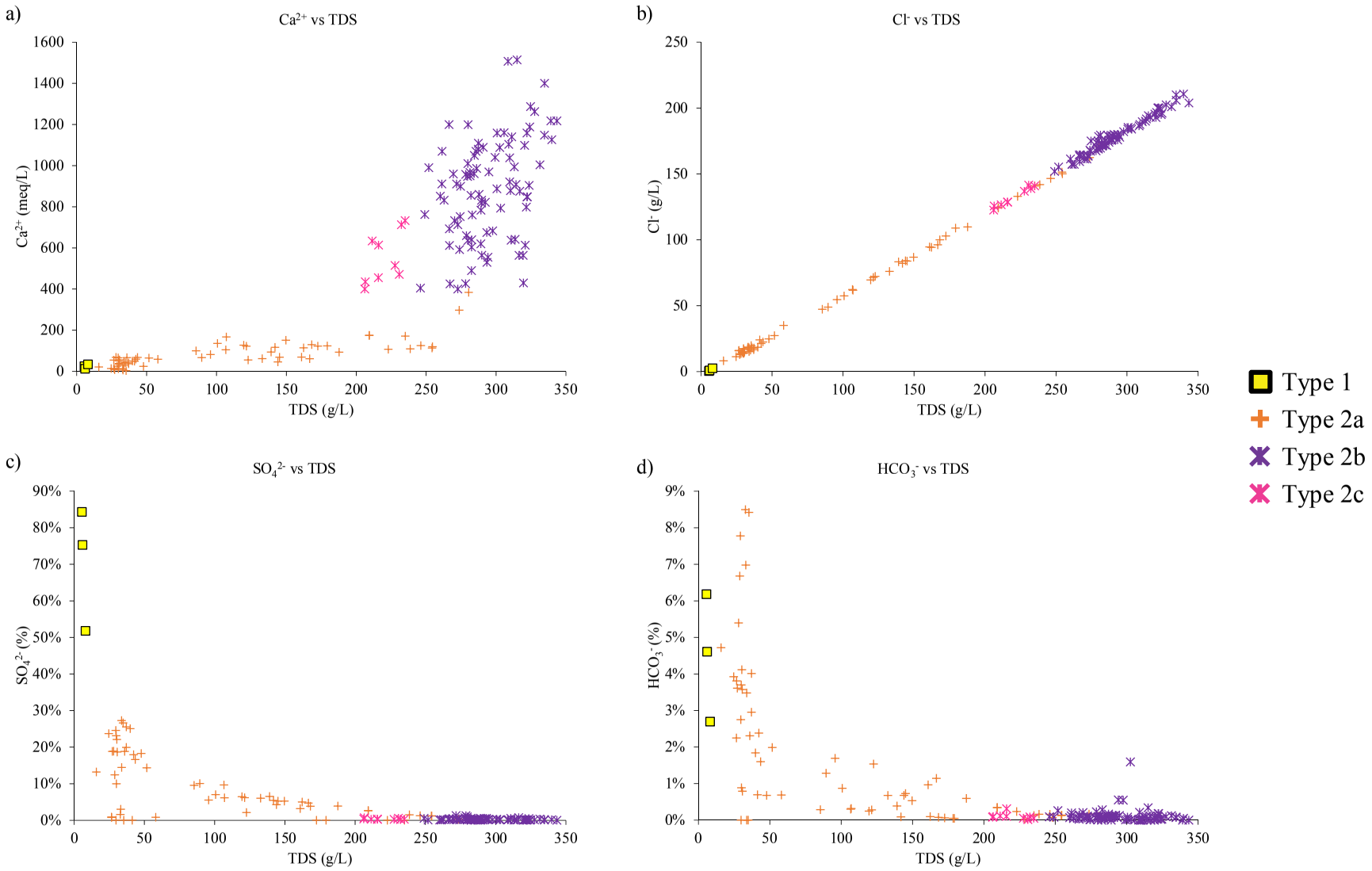

Figure 5.8: Total dissolved solids (g/L) versus: a) Calcium (meq/L), b) Chloride (g/L), c) Sulfate (%), d) Bicarbonate (%) for classified Bakken Aquifer waters.

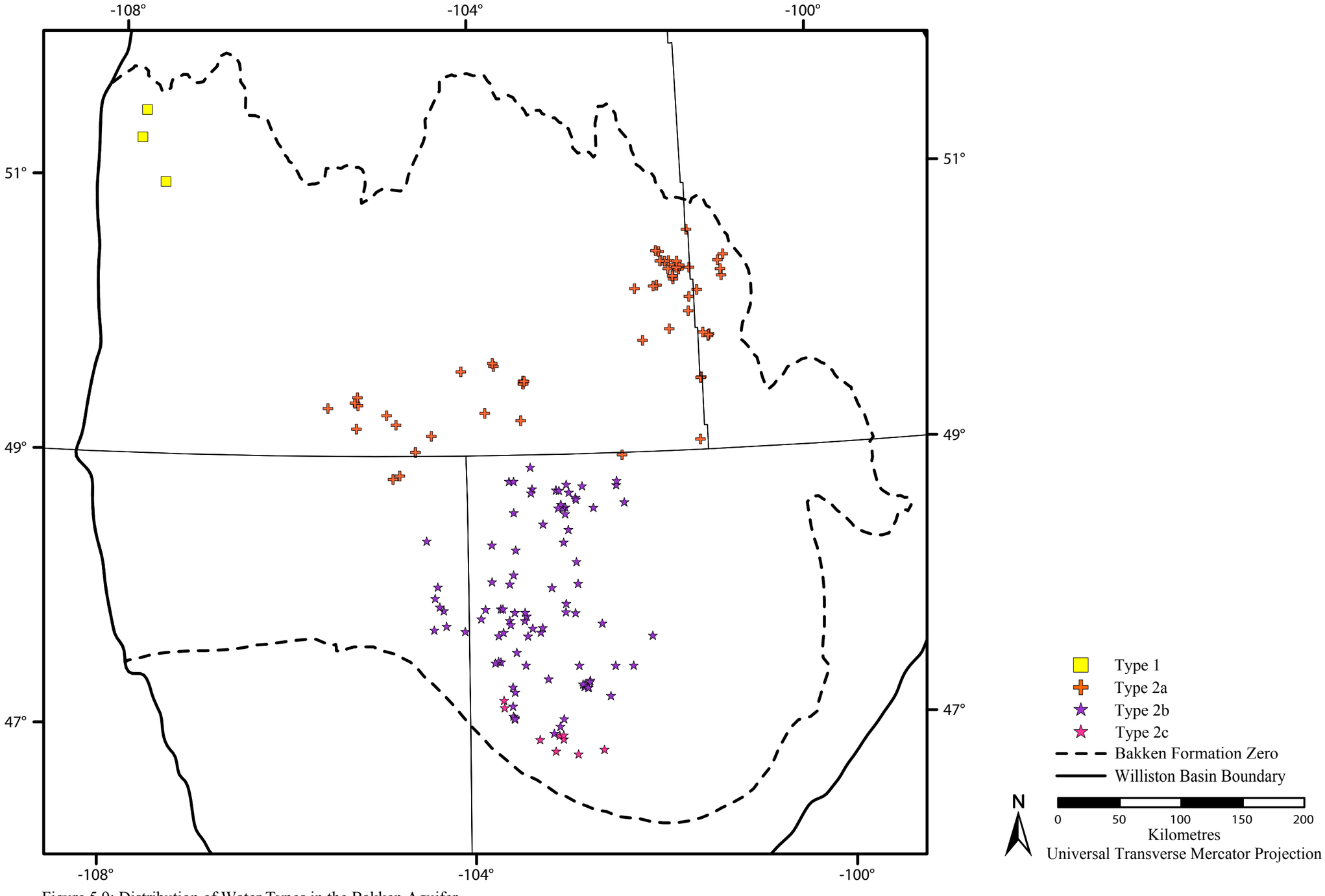

Figure 5.9: Distribution of Water Types in the Bakken Aquifer.

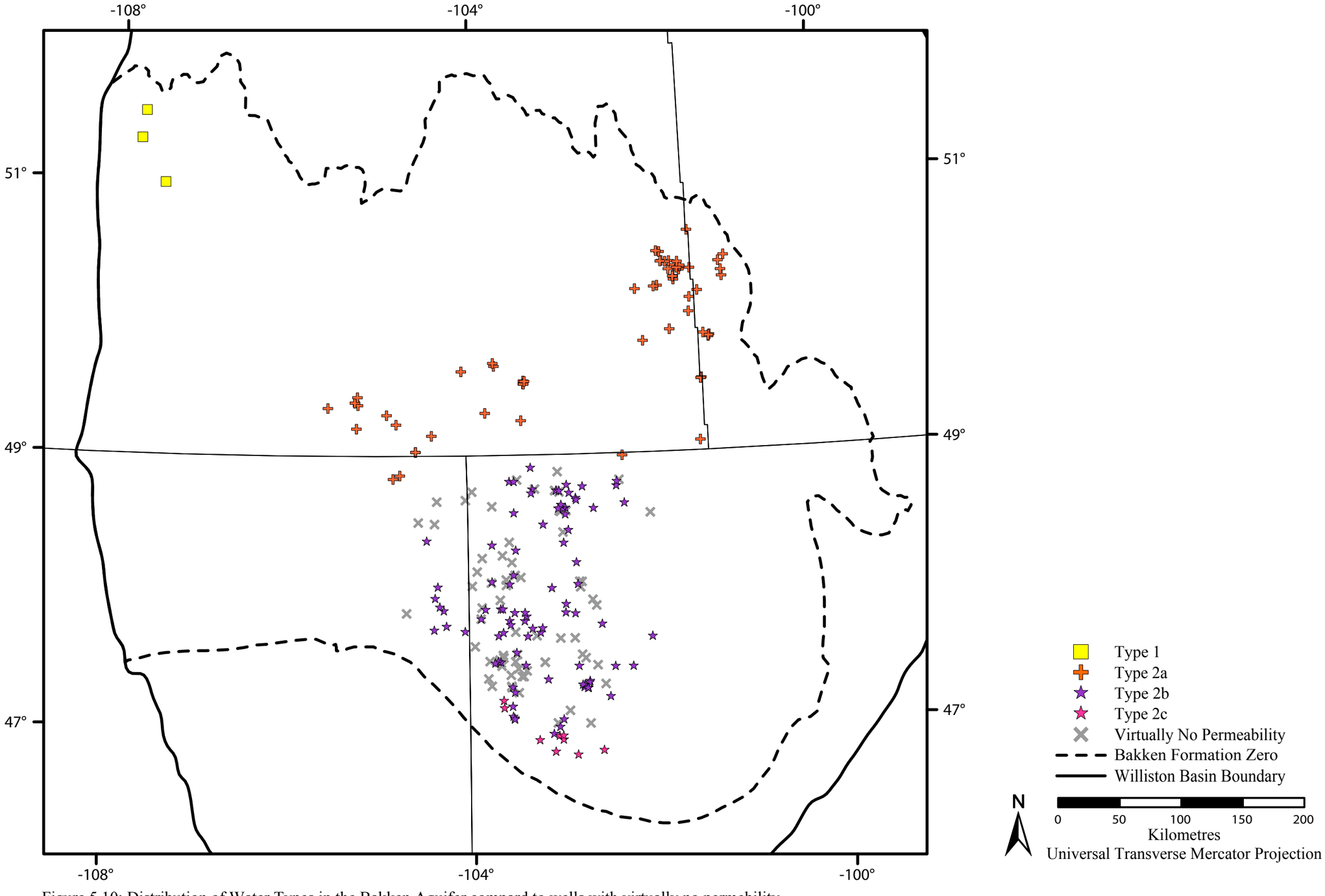

Figure 5.10: Distribution of Water Types in the Bakken Aquifer compard to wells with virtually no permebility.

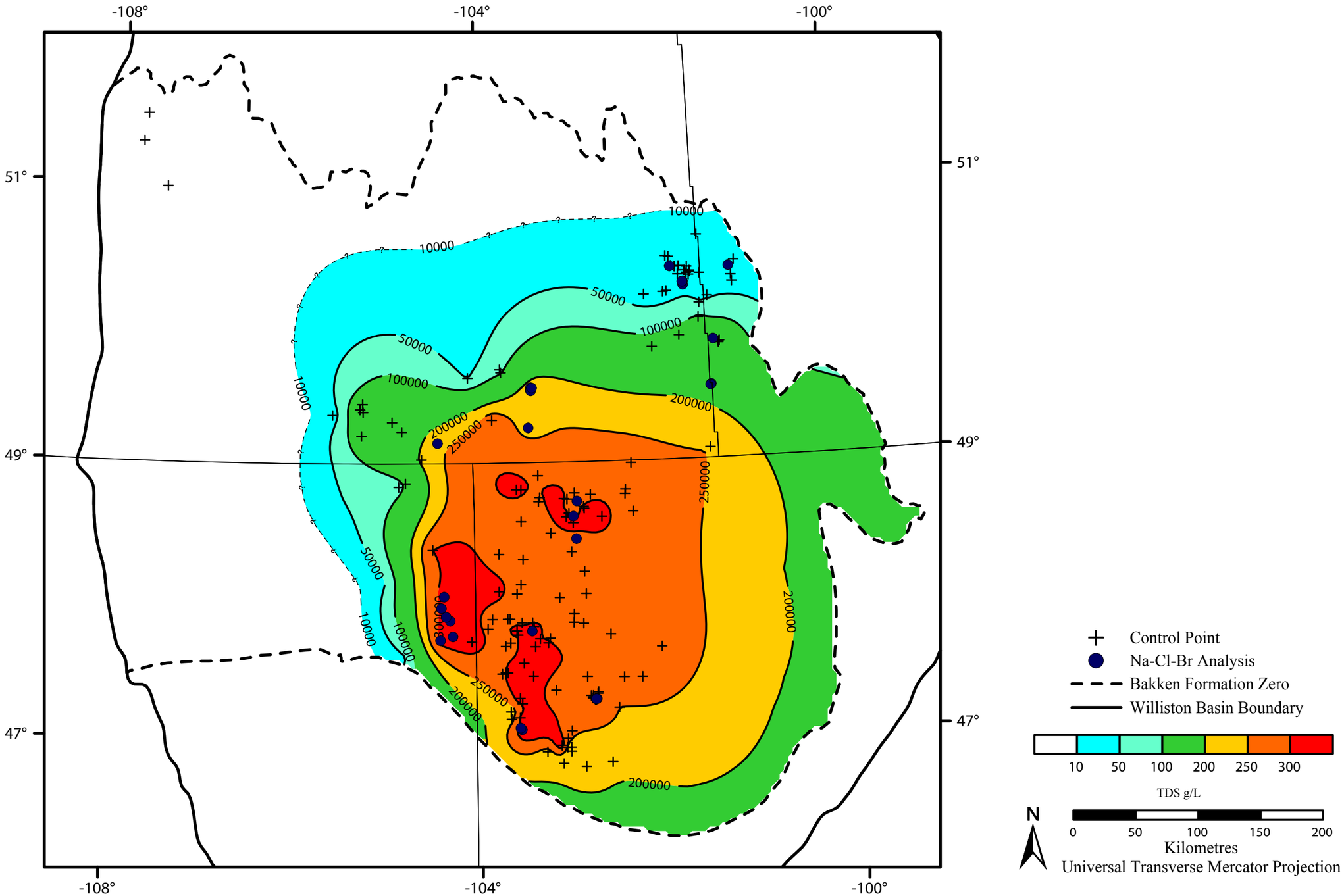

Figure 5.11: Distribution of water samples with Br⁻ analysis in the Bakken Aquifer.

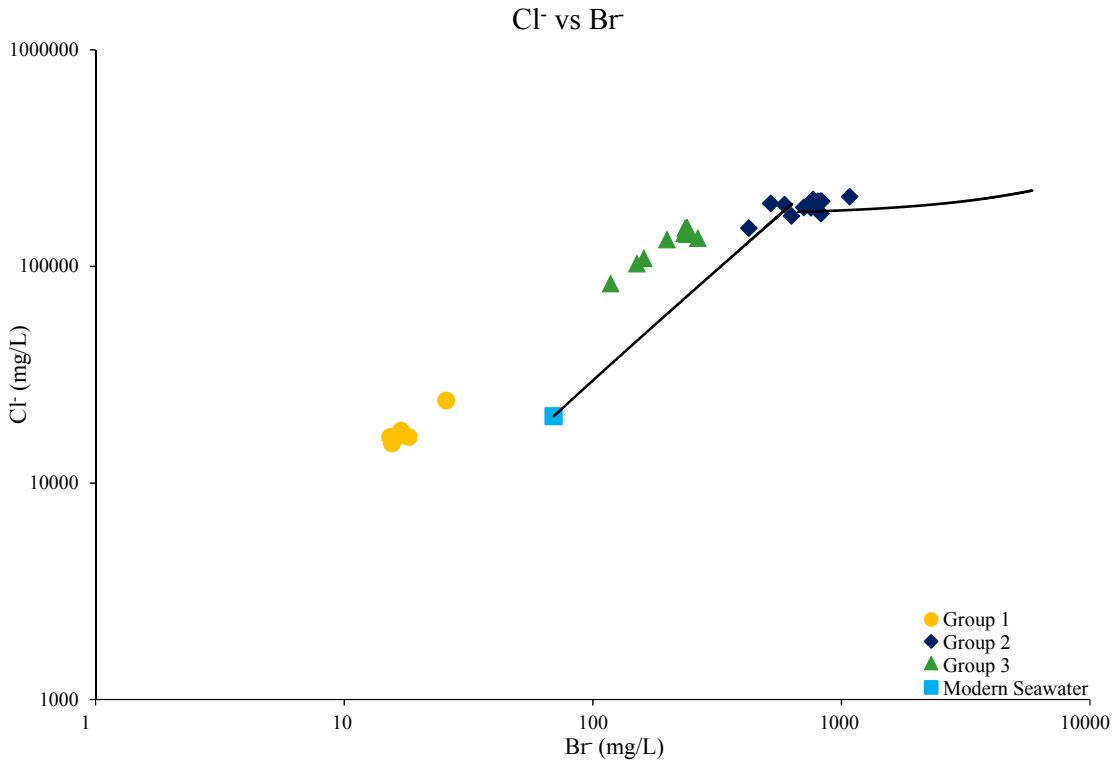

Figure 5.12: Chloride versus Bromide for 30 water samples analyzed for Bromide in the Bakken Aquifer. Seawater composition, and seawater evaporation trajectory from McCaffery et al., (1987).

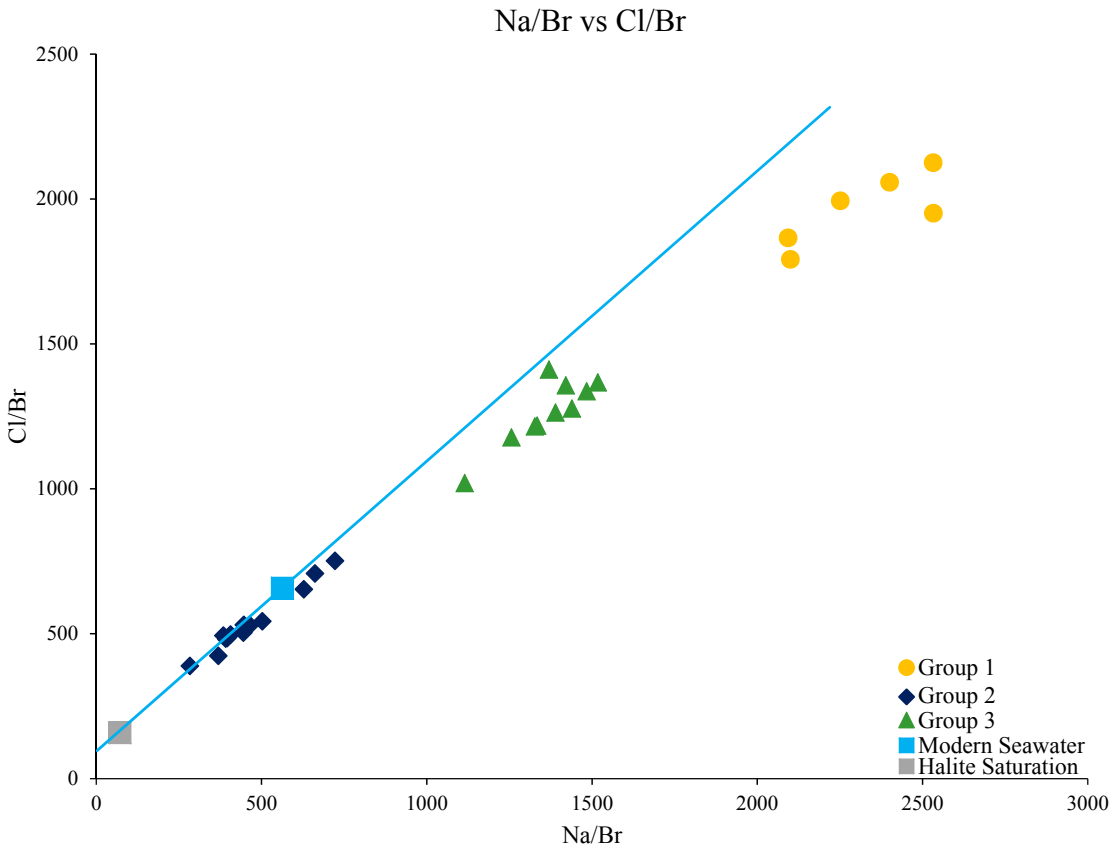

Figure 5.13: Cl/Br versus Na/Br for Bakken Aquifer waters with Bromide analysis. Modern seawater and SET data from McCaffery et al., 1987. Group 2 waters plot near the expected 1:1 SET however, Group 1, and Group 3 waters plot along a slope of 0.72.

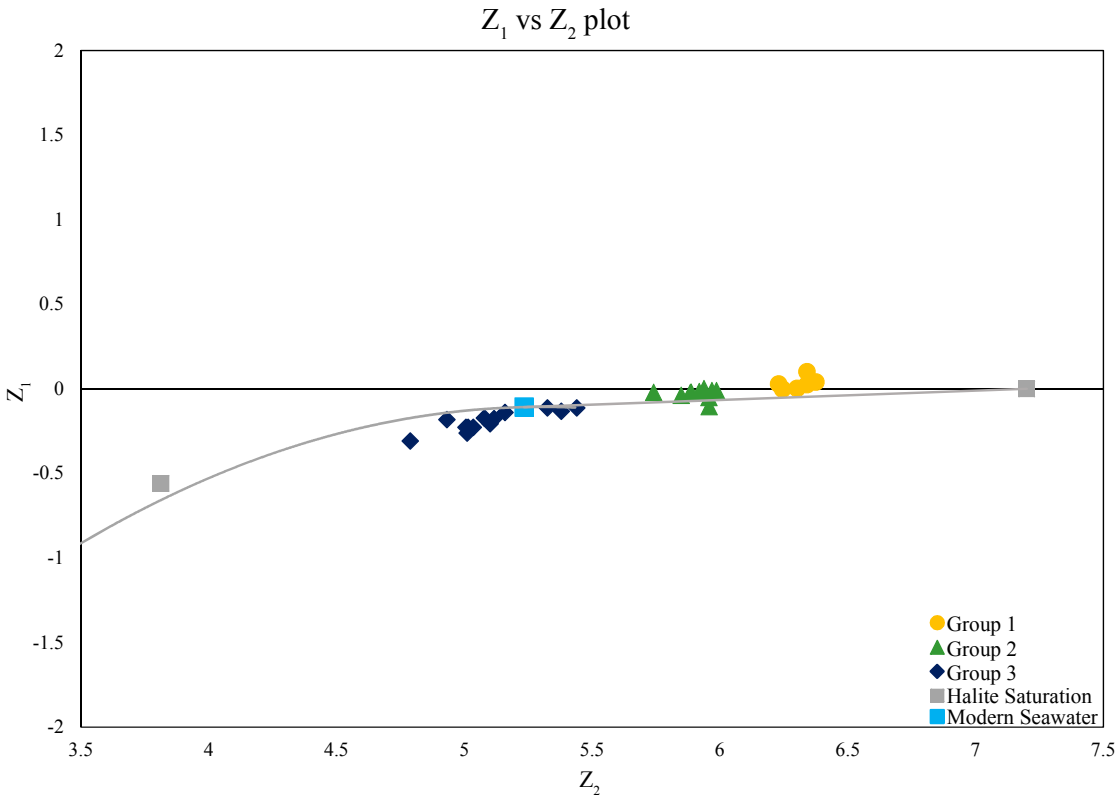

Figure 5.14: Z_1 versus Z_2 plot of Bakken Aquifer waters. SET and modern seawater composition from McCaffery et al., (1987).

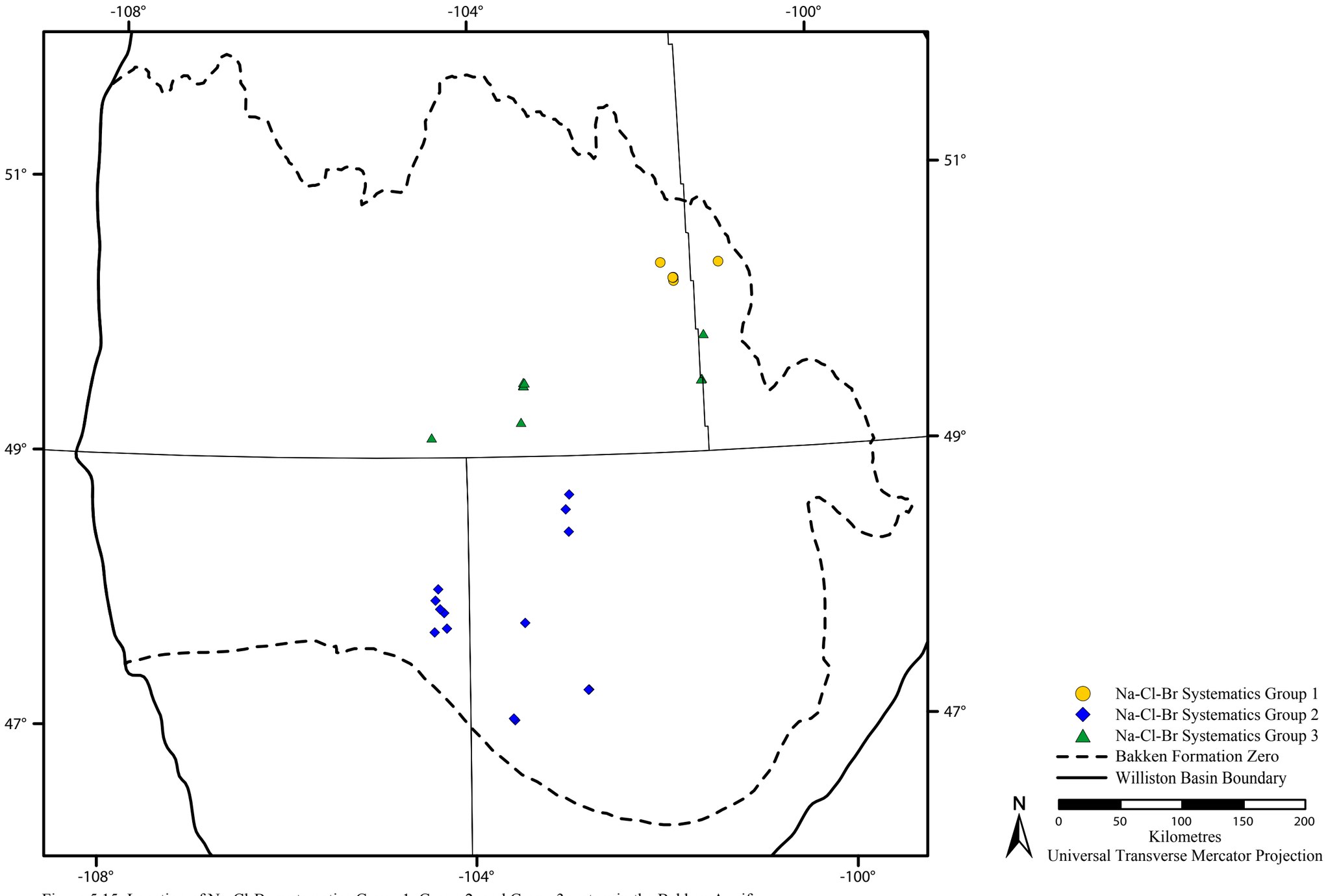

Figure 5.15: Location of Na-Cl-Br systematics Group 1, Group 2, and Group 3 waters in the Bakken Aquifer.

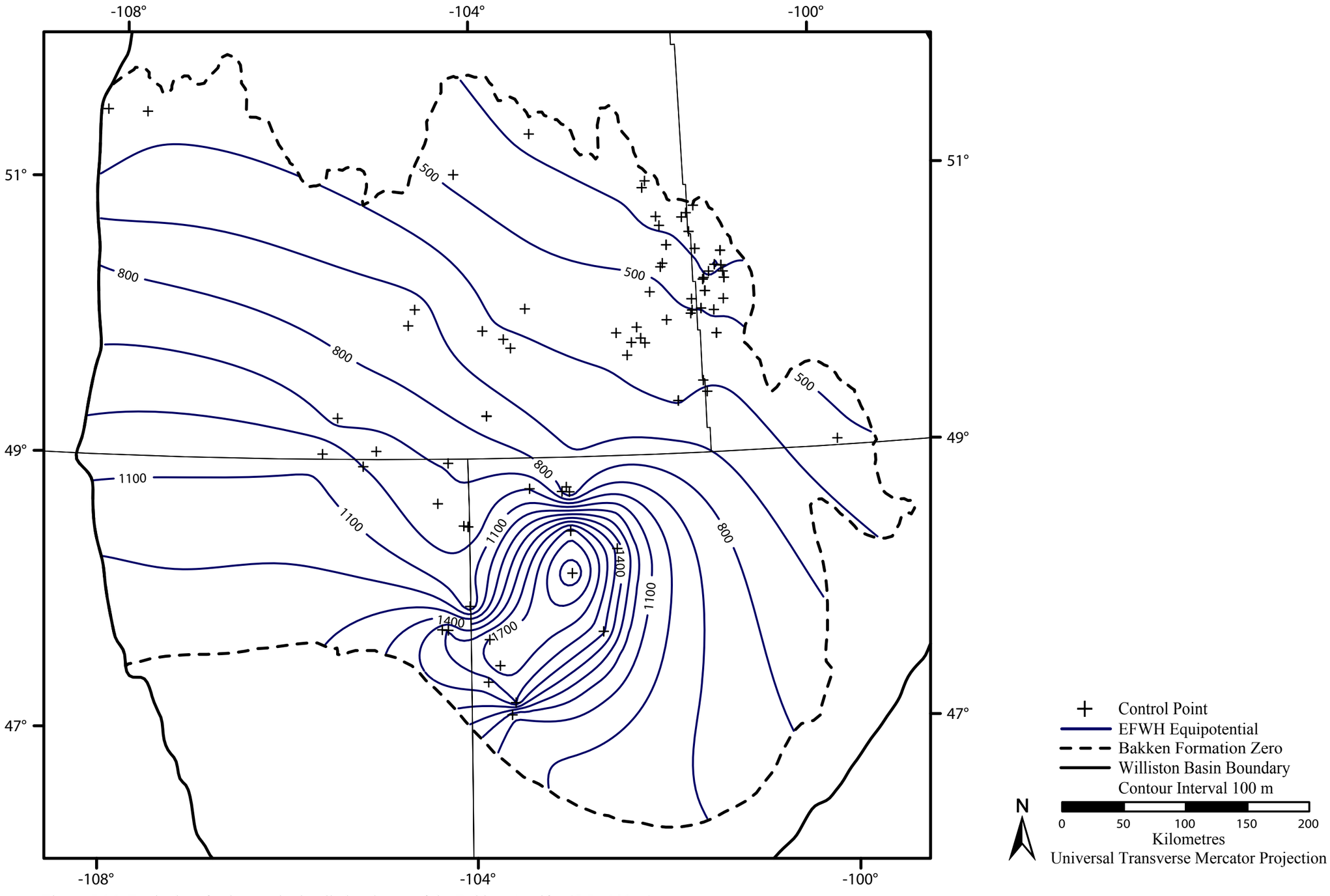

Figure 5.16: Equivalent freshwater hydraulic head map of the Bakken Aquifer (C.I.=100 m).

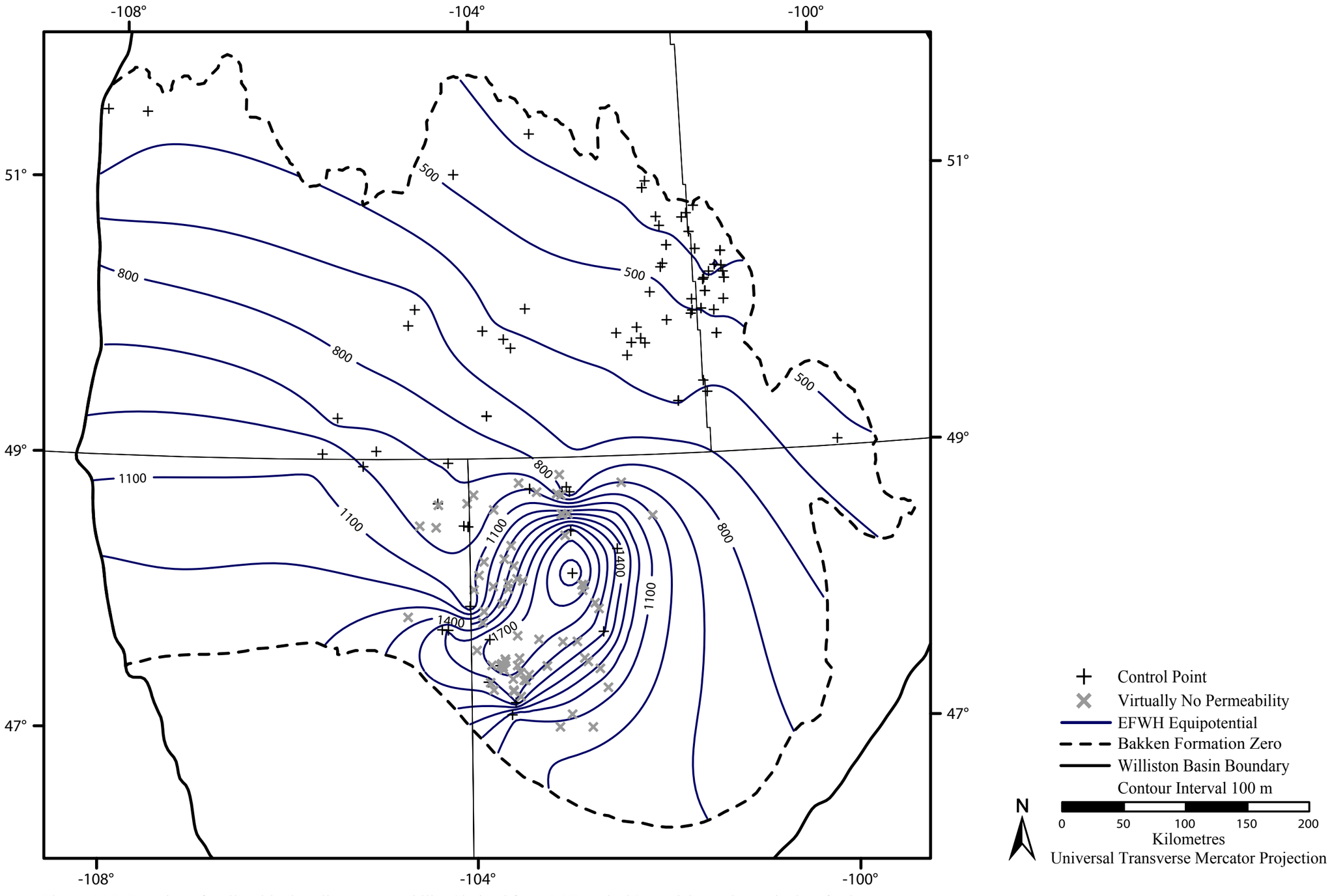

Figure 5.17: Location of wells with virtually no permeability (derived from DST analysis) overlain on the equivalent freshwater hydraulic head map of the Bakken Aquifer (C.I.=100 m).

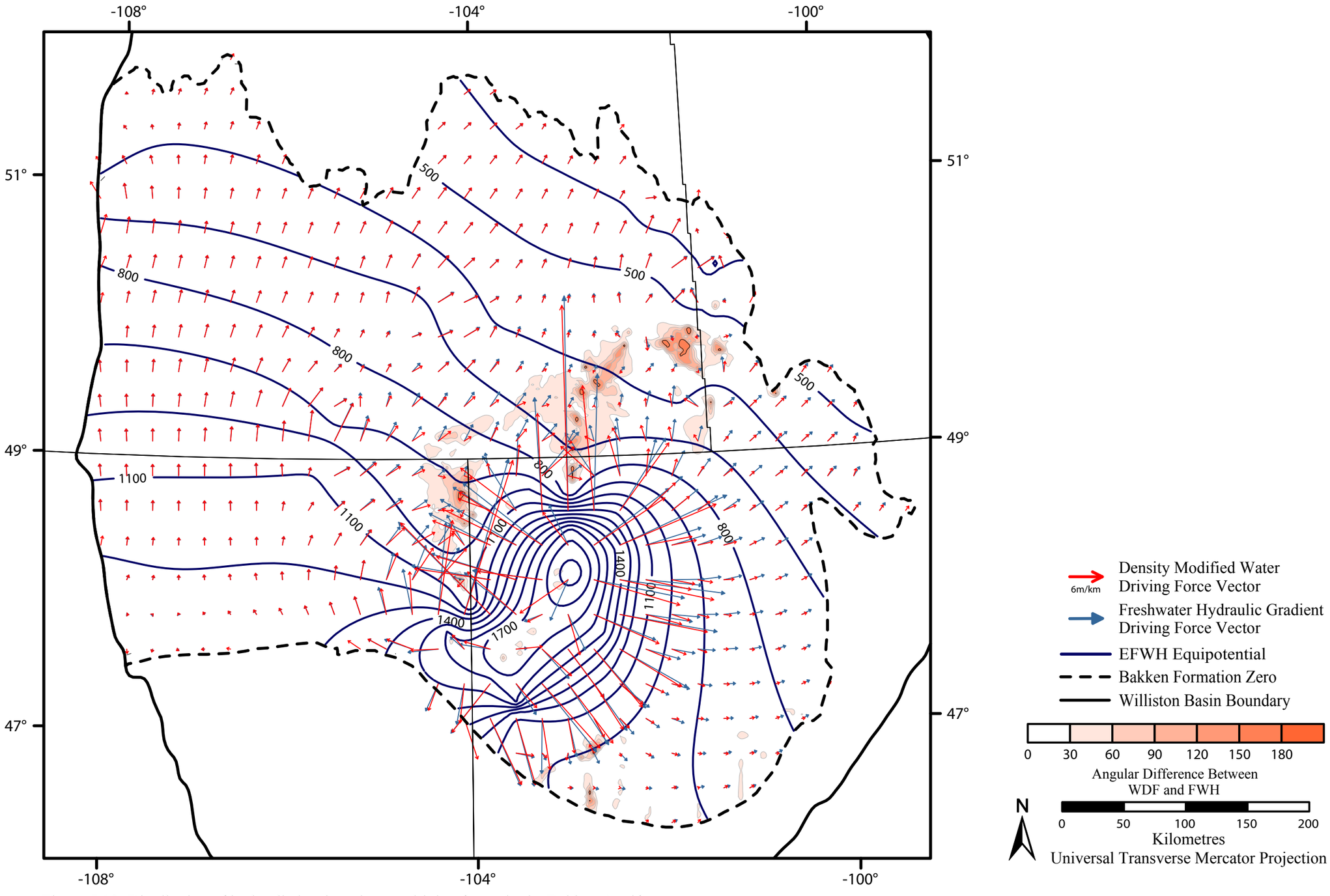

Figure 5.18: Distribution of hydraulic heads and water driving forces in the Bakken Aquifer.

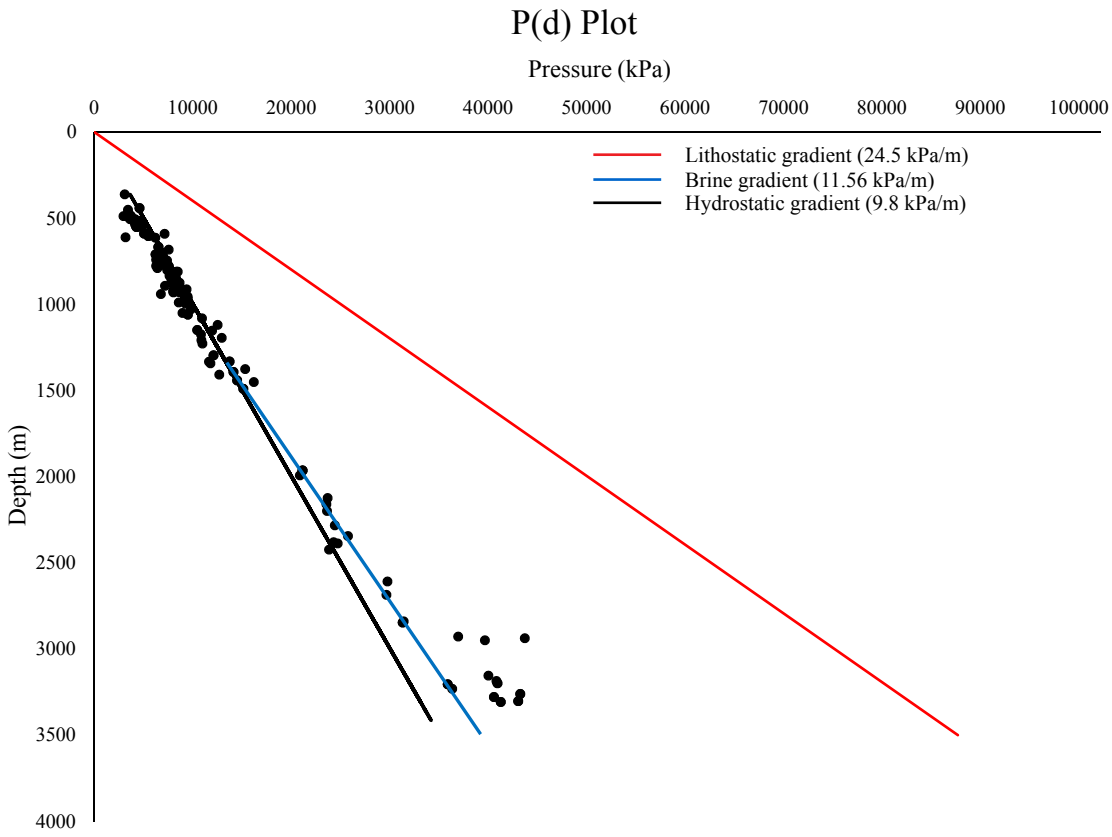

Figure 5.19: Regional pressure versus depth plot for the Bakken Aquifer.

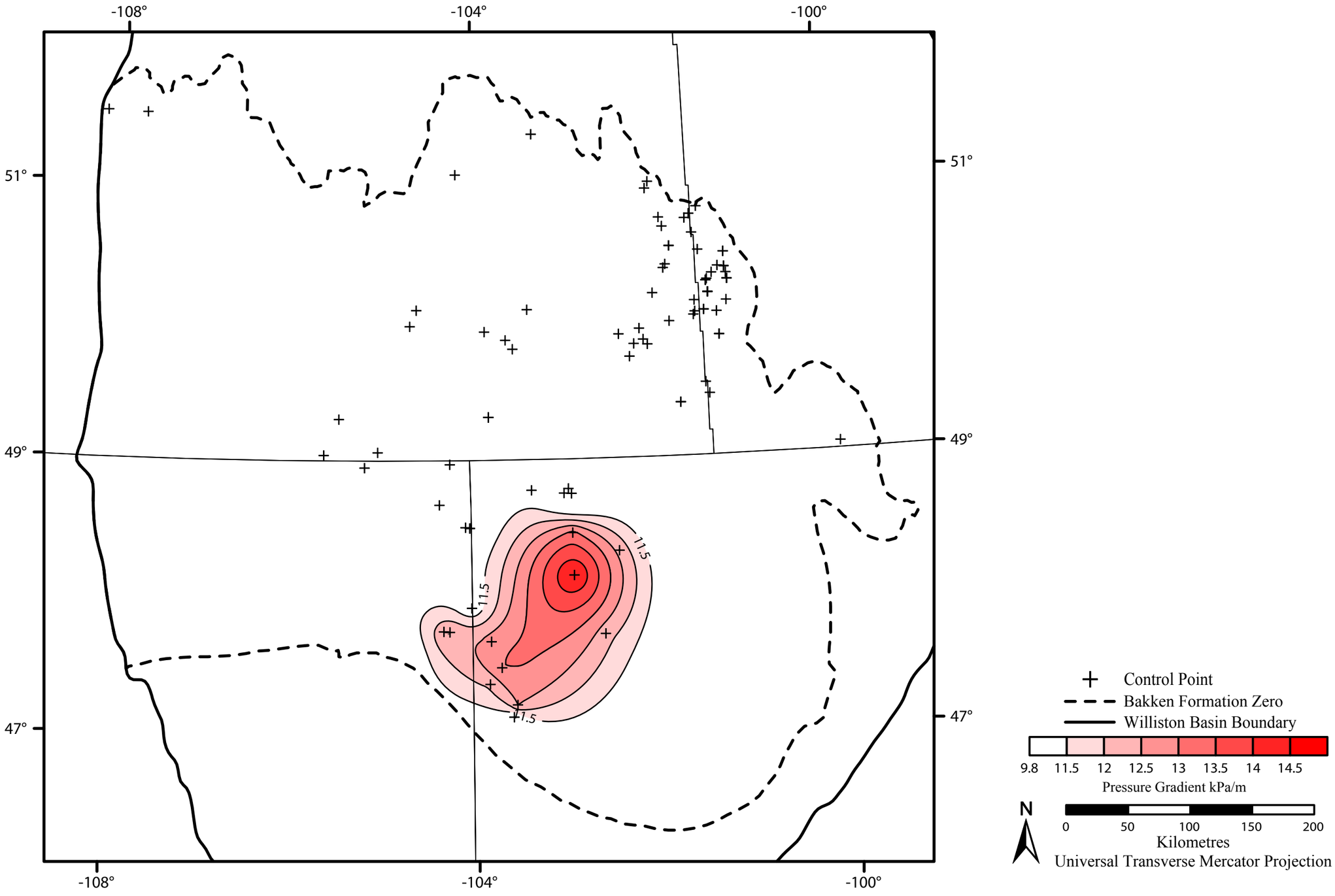

Figure 5.20: Pressure gradient distribution in the Bakken Aquifer. Shaded areas represent areas with greater than hydrostatic formation pressure, non-shaded areas are represent areas with hydrostatic/neary hydrostatic conditions.

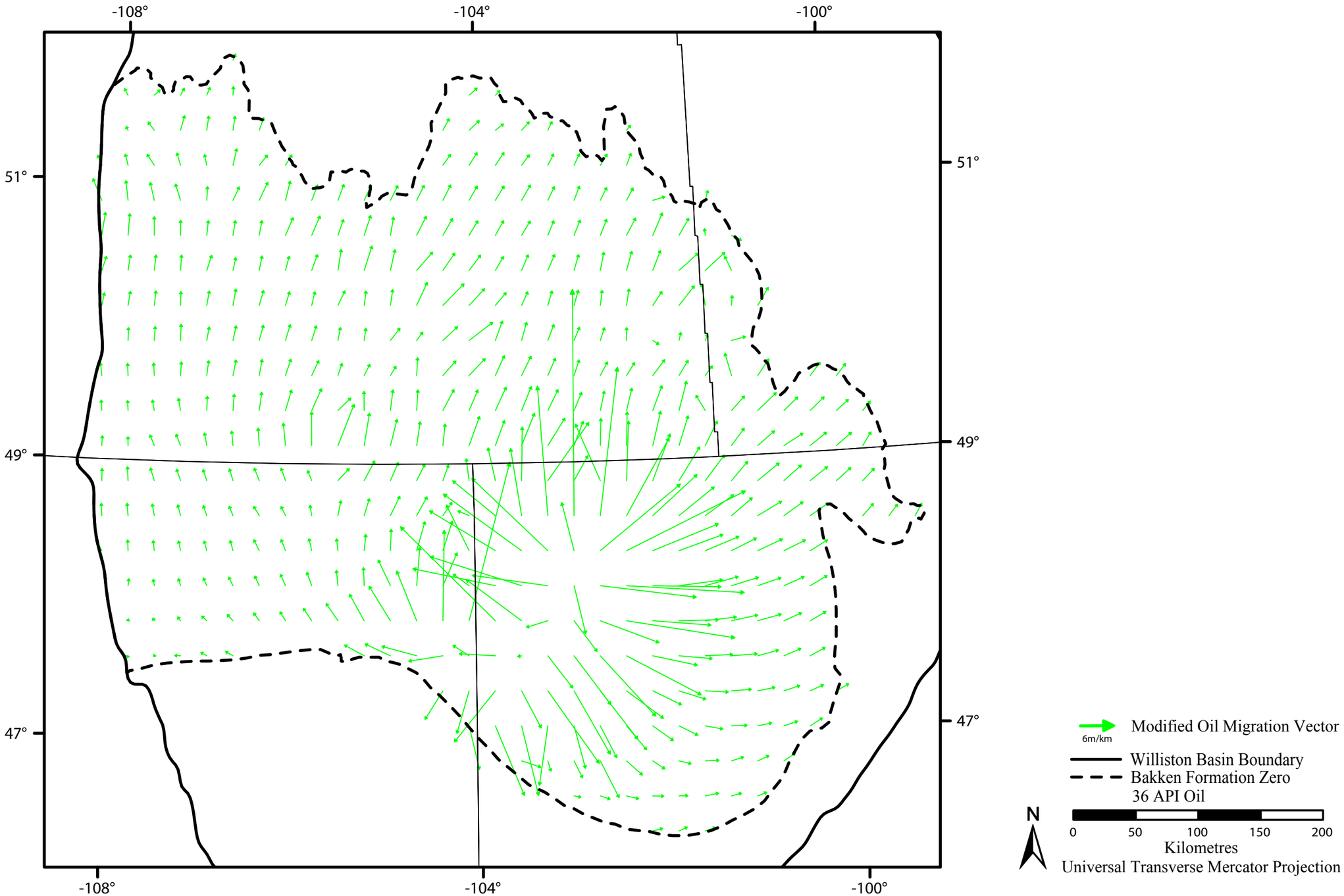

Figure 5.21: Map of water driving force modified oil migration vectors for 36 AIP oil in the Bakken Formation.

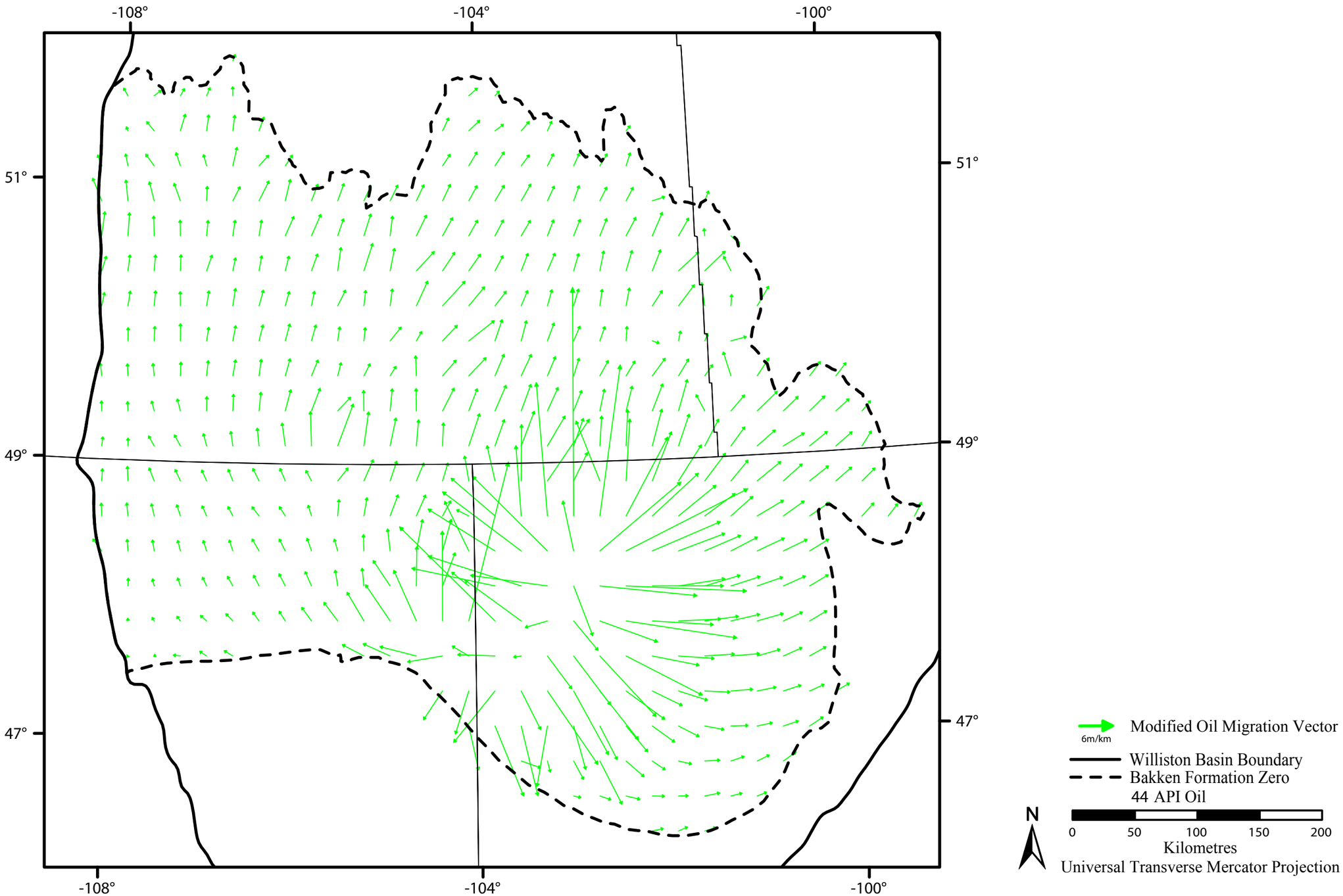

Figure 5.22: Map of water driving force modified oil migration vectors for 44 AIP oil in the Bakken Formation.

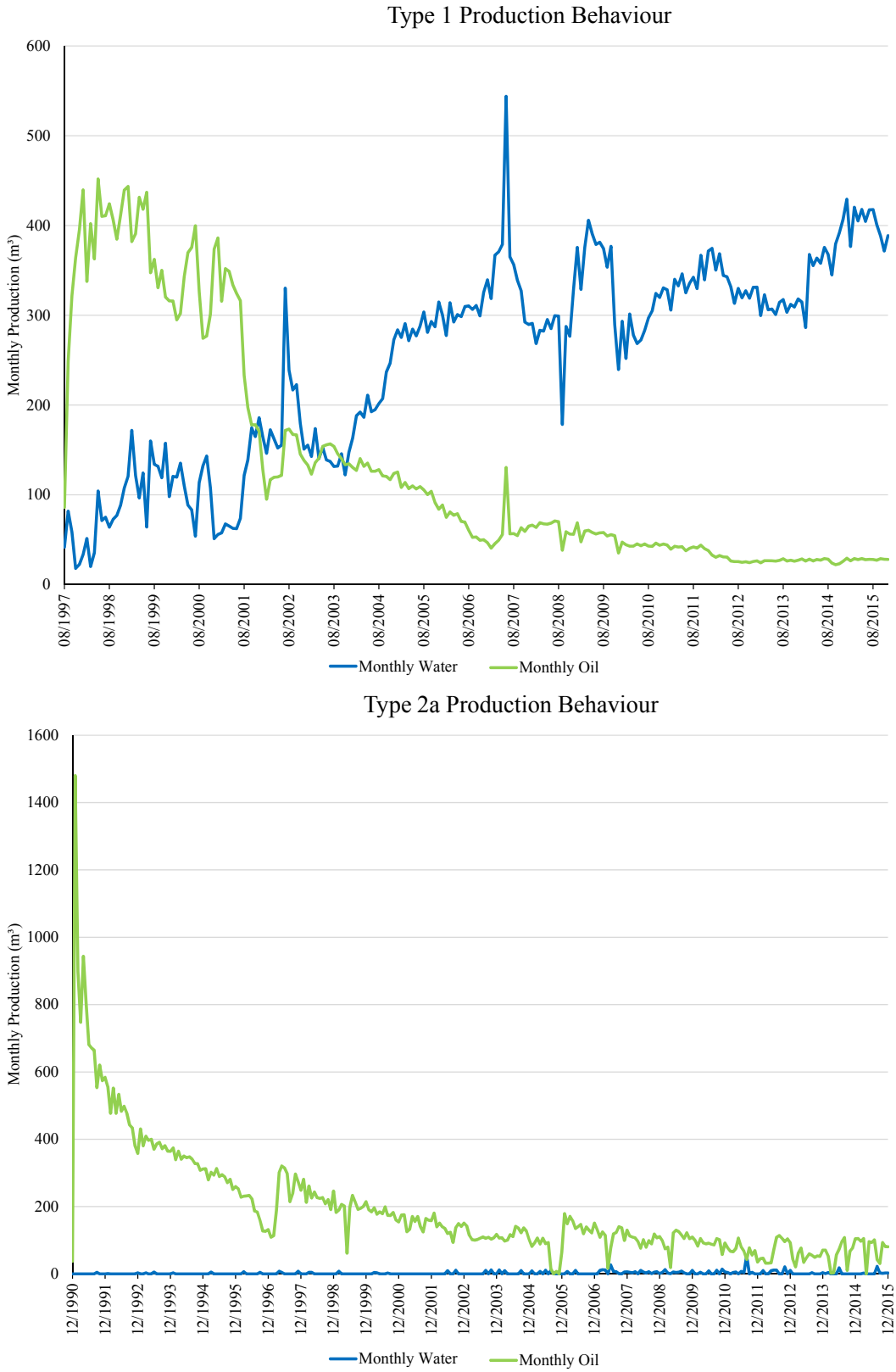

Figure 5.23: Representative Type 1 and Type 2a production behaviours observed in Middle Bakken oil wells (production data sourced from AccuMap).

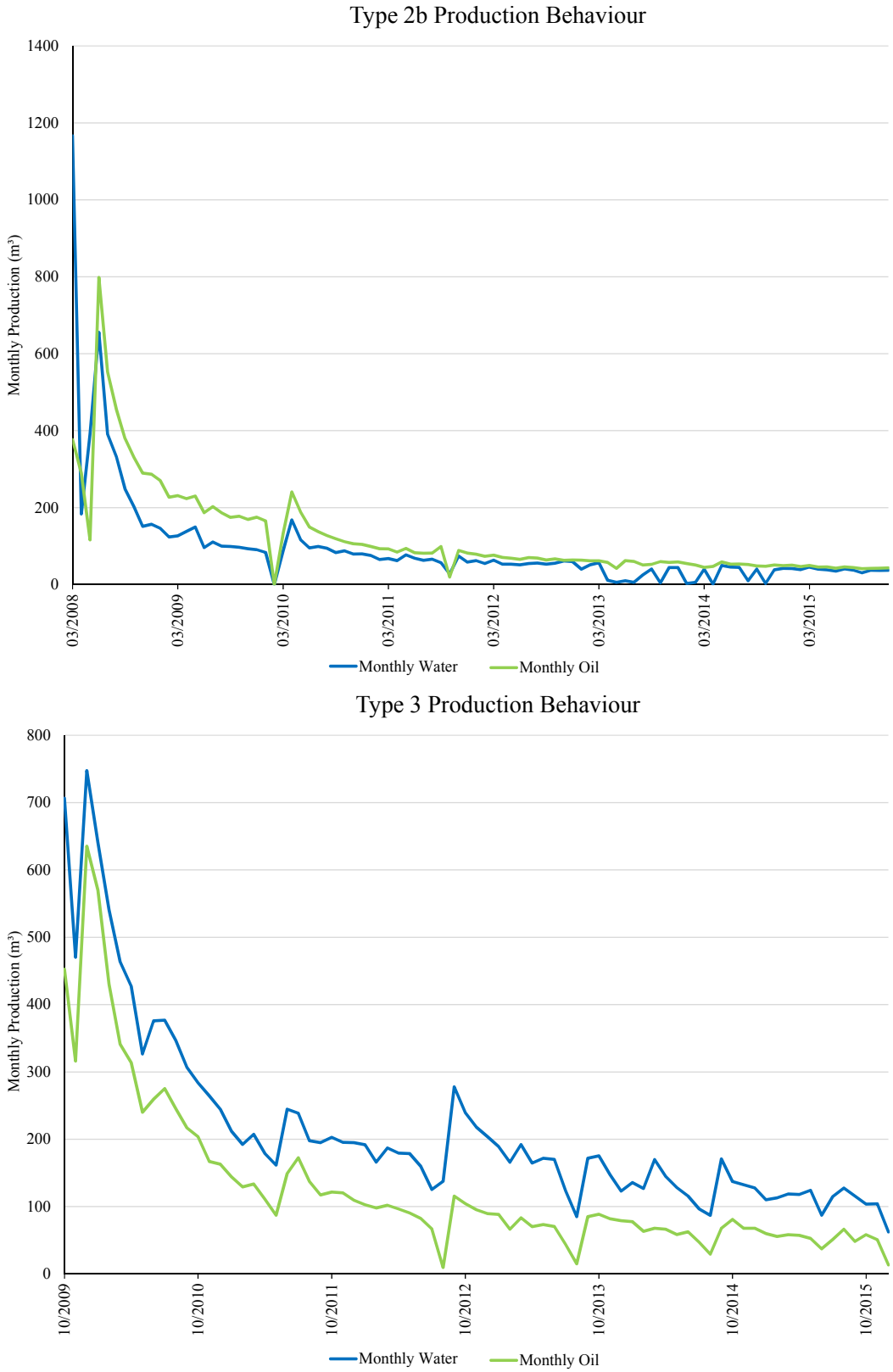

Figure 5.24: Representative Type 2b and Type 3 production behaviours observed in Middle Bakken oil wells (production data sourced from AccuMap).

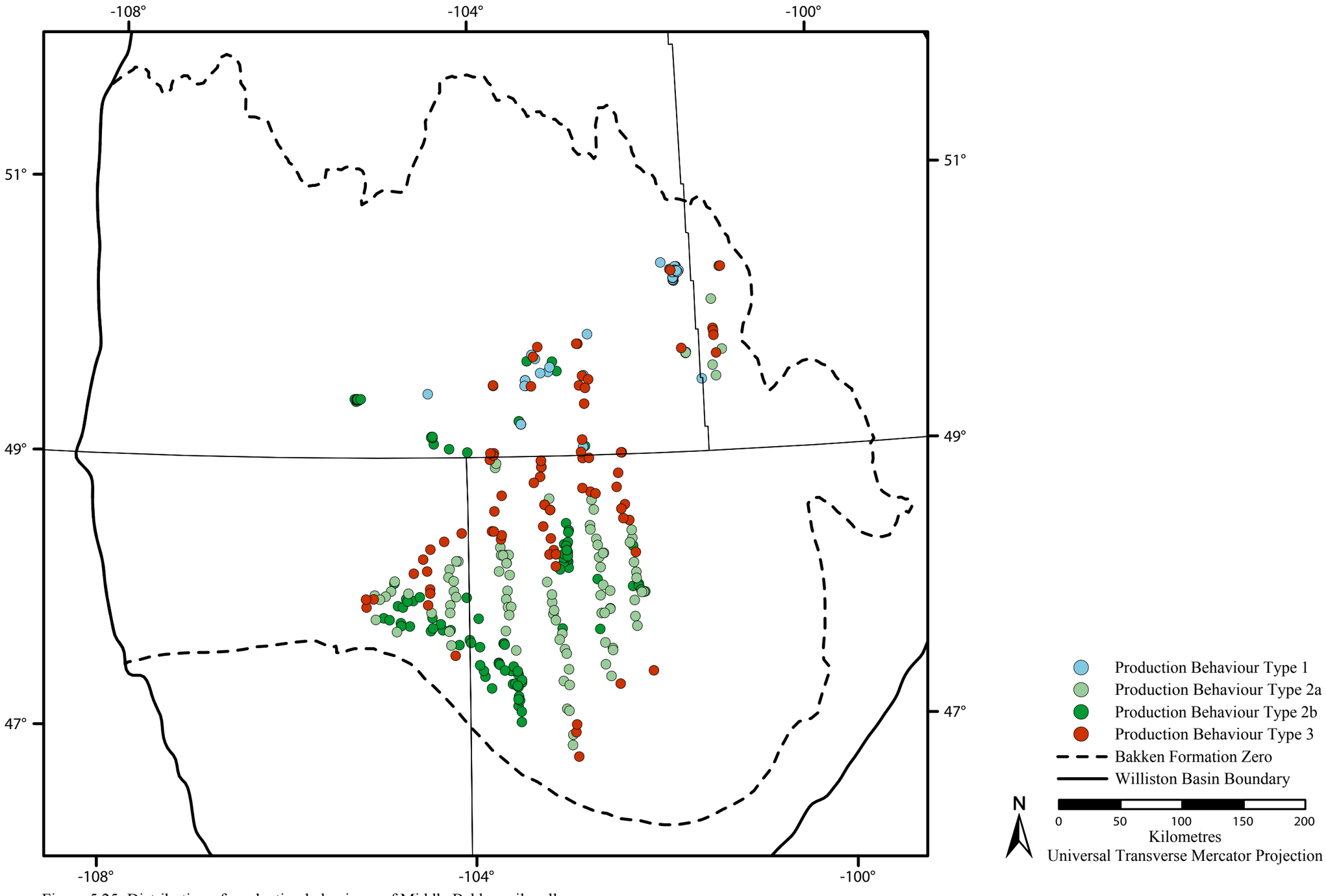

Figure 5.25: Distribution of production behaviours of Middle Bakken oil wells.

6. Hydrogeochemical Discussion and Synthesis

6.1. Origin of Formation Water in the Bakken Aquifer

Sodium-Chloride-Bromide systematics, as well as an investigation of the ion concentrations in the Bakken Aquifer were used to determine the origin of the Bakken Aquifer fluids. Results show that the Bakken Aquifer contains fluids of two distinct origins as well as a mix between them. In the following discussion on the origins and mixing of these waters Type 1, Type 2a, 2b, and 2c waters refer to the water classification in section 5.1.3 and Group 1, 2, 3 waters refer to the water groups based on Na-Cl-Br systematics (section 5.1.5)

6.1.1. Non-Marine Formation Waters

Hydrochemical analysis suggests that some Bakken Aquifer water samples are of non-marine origin. This is supported by several lines of evidence.

First, the chemical concentration of Type 1 ($Na\text{-}SO_4$) waters are less than seawater samples with TDS less than seawater (35,000 mg/L) point to a non-marine origin.

Second, Type 2a Bakken Aquifer waters belonging near 101.5°W and 50.3°N have ion ratios which do not reflect a marine origin. These water samples have a TDS range between 30,000 and 41,000 mg/L averaging 33,370 mg/L. While the TDS is similar to that of modern seawater, they do not share the same chemical composition. Modern seawater Cl^- concentrations are approximately 20,000 mg/L (Carpenter, 1978), while these water samples contain an average of 17,600 mg/L. These waters also have K^+ concentrations averaging 220 mg/L, Mg^{2+} concentrations averaging 358 mg/L, and Br^- concentrations averaging 18 mg/L while the corresponding concentrations in modern seawater are approximately 400 mg/L, 1,300 mg/L, and 68 mg/L respectively (Carpenter, 1978). Additionally, the expected SO_4^{2-} content in modern seawater is

approximately 2,800 mg/L with these samples reaching approximately 6,000 mg/L (Table 5).

Third, examining the Cl^- versus Br^- concentration plot (Figure 5.12) Group 1 waters do not plot near modern seawater, nor do they plot along the SET. Group 2 waters contain approximately the same Cl^- concentration as seawater however they are heavily depleted in Br^-. Group 2 waters are located near the Saskatchewan Manitoba border near 101.5°W and 50.3°N (Figure 5.15).

Fourth, Group 1 waters have larger Cl^-/Br^- and Na^+/Br^- ratios than seawater (Figure 5.13). A seawater sample that dissolves halite with a fixed Br^- concentration (as found in the halites of the Williston Basin (Wardlaw and Schwerdtner, 1966) will plot along a 1:1 line with increasing Cl^-/Br^- and Na^+/Br^- ratios on the Cl^-/Br^- versus Na^+/Br^- plot (McCaffery et al., 1987). Thus, waters with Cl^-/Br^- and Na^+/Br^- ratios greater than seawater are interpreted to have obtained their salinity from halite dissolution rather than the evaporation of seawater (McCaffery et al., 1987; Engle and Rowan, 2012). The further from modern seawater the larger the amount of halite dissolution.

Assuming that the only source of Na^+, Cl^- and Br^- in the water samples is from the dissolution of halite, or from the evaporation of seawater, waters will plot on a 1:1 line. However, Groups 1 waters plot on a line with a slope of 0.77 (Figure 5.13); below the 1:1 pure dissolution line. As such, Group 1 waters must have gained their salinity from a combination of halite dissolution and from other sources.

Fifth, using isometric log-ratio transformation method of Engle and Rowan (2012), Group 1 waters plot with a Z_1 value near 0 and Z_2 value of 6.3 (Figure 5.14). Formation waters showing evidence of halite dissolution have Z_1 values approaching 0 and Z_2 values approaching 7.1 (Engle and Rowan, 2012). These waters therefore show evidence of halite dissolution.

Finally, Group 1 waters are located in the northeastern portion of the Bakken Aquifer, near the Saskatchewan Manitoba border (Figure 5.15). In this area of the basin,

Grasby and Chen (2005) proposed that during the Paleocene glaciation, high fluid pressures at the base of the ice sheet allowed subglacial meltwaters to recharge the Williston Basin. As meteoric waters recharge the aquifer they may dissolve portions of the rock matrix in which they flow. Water dissolves minerals according to their solubility constants attempting to reach a chemical equilibrium between the formation water and the rock matrix (Chebotarev, 1955). Geochemical evidence in the northeast Williston Basin show that these meltwaters were able to dissolve the Prairie Evaporite Formation (Palombi, 2008).

While these waters show that there is a non-marine endmember in the Williston Basin, they are not the result of pure halite dissolution with meteoric water because there is evidence of mixing with other formation waters in the Bakken Aquifer. The TDS versus Br^- plot (Figure 6.1) for Group 1 waters shows meteoric waters dissolving halite containing 68 mg/L Br^- would contain approximately 2.5 to 3.4 mg/L Br^- at 30,000 to 40,000 mg/L TDS (Rittenhouse, 1967). However, Group 1 waters contain between 15 and 25 mg/L Br^-.

Thus, one possible explanation for the water chemistry found in this area of the Bakken Aquifer is that the waters originated as the connate Bakken water and was then mixed with recharging meteoric waters resulting in waters with approximately the TDS of modern seawater enriched in Cl^- and depleted in Br^-.

The dataset for this study had limitations. One limitation was that there were many water samples with incomplete water analyses. Only 30 of the 167 Bakken Aquifer waters were analyzed for Br^-. In order to obtain a more representative distribution of water origins in the aquifer, water samples with Br^- analysis were highlighted on ion concentration plots (Figure 6.2, Figure 6.3). Group 1 waters correspond to the Bakken Aquifer water Type 2a with TDS <50,000 mg/L. Thus, within the Bakken Aquifer, areas with Na-SO_4 type waters are of meteoric origin and Na-Cl Type 2a waters with TDS <50,000 mg/L are of mixed origin.

6.1.2. Brines from Seawater Evaporation

In sedimentary basins, seawater can evaporate at the surface or subaerially (Hannor, 1994). Seawater evaporated to approximately four times its original concentration can be classified as a brine (McCaffery et al., 1987). During evaporation, minerals begin to precipitate out of solution according to the solubility of the mineral. This progressive evaporation results in the residual brine becoming enriched in some ions relative to others creating a unique fingerprint. This fingerprint can be used to interpret the origin of various waters.

During the progressive evaporation of seawater, Na^+, Cl^- and Br^- concentrations increase by the same factor until a degree of evaporation of 10. At this point, halite begins to precipitate removing Na^+ and Cl^- from the residual brine. Sodium the limiting ion decreases in concentration relative to Cl^- which continues to increase until a degree of evaporation of 80 times is reached when potash is precipitated (McCaffery, 1987).

Salinities in Group 2 waters are between 250,000 and 350,000 mg/L. Sodium concentrations range between 80,000 to 110,000 mg/L, Cl^- concentrations are between 150,000 and 210,000 mg/L, K^+ concentrations are between 3,900 and 7,900 mg/L. Sodium, Cl^- and Br^- concentrations in Group 2 waters are within 2, 7, and 10% respectively (Figure 6.4) (based on McCaffery et al., 1987).

Group 2 waters plot along and reach halite saturation on Cl^- versus Br^- plot (Figure 5.12). On the Na^+/Br^- versus Cl^-/Br^- plot Group 2 waters have smaller Na^+/Br^- and Cl^-/Br^- ratios than modern seawater with the exception of three water samples. Waters plotting below modern seawater are indicative of evaporated seawater (Walter et al., 1990). Group 2 waters plot along the 1:1 line on the Na^+/Br^- versus Cl^-/Br^- plot strongly indicating a seawater origin.

The seawater evaporation signature of Group 2 waters is supported by isometric log-ratio transformations (Figure 5.14). Group 2 waters have smaller Z_1 and Z_2 ratios than modern seawater (-.1 and 5 respectively) with the exception of three points. Waters

with Z_1 and Z_2 values less than seawater are interpreted to be have a enriched seawater origin (Engle and Rowan, 2012).

As mentioned previously only some waters were analyzed for Br^-. Comparing the waters analyzed for Br^- against other Bakken waters it was determined that Group 2 waters belonged to the Type 2b Na-Cl aquifer waters (Figure 6.3).

Waters with this chemical signature (Na-Cl-Br Group 2 and Na-Cl Type 2b) are found in the center of the Bakken Aquifer (Figure 6.5). The location of these waters coincide with the area of virtually no permeability (Figure 6.5) and is strongly overpressured (Figure 5.20). A plausible explanation for the origin is they are original evaporated seawater (due to the strong agreement with the SET) that have not moved because of the low permeability and related residual overpressure.

6.1.3. Evidence of Brines from Halite Dissolution and Seawater Mixing

As shown in the previous section, halite dissolution waters have mixed with other saline waters in the Bakken Aquifer.

Group 3 waters have TDS between 135,000 and 255,000 mg/L, with Cl^- concentrations between 80,000 and 155,000 mg/L, and Na^+ concentrations between 46,000 and 98,000 mg/L. Group 2 waters have up to 20% excess Na^+ and an excess of 40% Cl^- compared to seawater values evaporated to the equivalent salinity. However, Br^- concentrations for Group 3 waters are 40% deficient compared to seawater values (McCaffery et al., 1987) (Figure 6.6).

As mentioned previously, Group 3 plot above the SET and are enriched in Cl^- relative to Br^- (Figure 5.12). Cl^-/Br^- versus Na^+/Br^- ratios for Group 3 waters are larger than those of modern seawater and plot along a slope of 0.72 (Figure 5.13). Waters with Cl^-/Br^- and Na^+/Br^- ratios larger than seawater are interpreted to show a halite

dissolution signature. However, because Group 3 waters plot below the 1:1 SET these waters have also experienced other water rock interactions (Figure 5.13).

The presence of a significant percentage of halite dissolved seawater is supported by using isometric log-ratio transformations. Group 3 waters have Z_1 values approaching 0 and Z_2 values approaching 6 (Figure 5.14). With increasing halite dissolution, waters will move towards Z_1 and Z_2 values of 0 and 7.2 respectively (Engle and Rowan, 2012).

Waters that have dissolved significant amounts of halite can produce the salinities observed in Group 3 waters. Dissolving the Prairie Formation using meteoric waters to generate waters with the equivalent salinities of Group 3 would result in Br^- concentrations reaching 8.5 to 10.2 mg/L (Figure 6.1). However, Br^- concentrations in Group 3 waters range from 115 and 265 mg/L. Due to the limited quantity of Br^- incorporated into the halite lattice and the Br^- concentrations in Group 3 waters, the dissolution of halite does not explain the water chemistry observed.

Spatially, Group 3 waters are located in a wide band from 102-104°W near 49°N. These waters are located more centrally in the basin than those of Group 1. From the chemical signature of these wasters it can be interpreted that Group 3 waters are likely the result of paleoseawaters which evolved along the SET to approximately 100,000 mg/L prior to mixing with halite dissolution brines (Figure 6.7).

Comparing Na-Cl-Br Group 3 waters to Na-Cl Type 2a waters both chemically (Figure 6.2, Figure 6.3) and spatially (Figure 6.8) show an interesting pattern. In the northeast, there is a stronger halite dissolution signature as highlighted by Na-Cl-Br systematics. In the south waters are of higher salinity but show a smaller contribution from halite dissolution. This is evident from the Br^- concentrations being closer to those of evolved seawaters of equivalent salinity. From this, we can interpret that in the Bakken aquifer, the closer to the center of the aquifer, the larger the original water composition while the closer to the aquifer margin the greater the amount of halite dissolution.

Near the Canada United States border, this area can be interpreted as a mixing zone between original aquifer waters and recharging meteoric waters based on Na-Cl-Br systematics.

6.1.4. Summary

Formation waters in the Bakken aquifer are of multiple origins and have experienced multiple evolutionary histories. There are three groups, each with their own history.

Group 1 waters are located only in the northeast of the study area near the Manitoba Saskatchewan border where subglacial recharge is proposed to have taken place. Group 1 waters are interpreted to be the result of a subglacial meltwaters infiltrating the Bakken Aquifer after dissolving the Prairie Formation subsequently mixing with partially evaporated seawaters. Due to the high Na^+ and Cl^- content relative to Br^-, these samples show a larger component of halite dissolution than Group 3 waters. These waters represent a small portion of the formation waters in the Bakken Formation, limited to the areas of subglacial melt water infiltration.

Salinities in the Bakken Aquifer are at their lowest in the northwest of the study area near the transition of the Bakken Formation of the Williston Basin to the Bakken/Exshaw Formation of the Alberta Basin. In this location, meteoric waters originating in central Montana dissolved away the Prairie Evaporite Formation leaving behind a relatively low salinity tongue of formation waters (Hitchon, 1996).

Group 2 formation waters are of a marine origin. These waters are located in the center of the basin, where permeability is very low and the Bakken Formation is overpressured. Fluids in this area likely represent the original Bakken Aquifer water composition during the time of deposition. It is unlikely that other waters would be able to infiltrate this area and alter the formation waters in this area. Group 2 formation

waters appear to be present where ever the Bakken Formation is low permeability and overpressured.

Outside of the area of extremely limited permeability and overpressure are formation waters which have a different evolutionary history than Group 2 waters. Group 3 waters are of mixed origin. Some of the Na^+ and Cl^- in these waters was derived from halite dissolution and some from evaporated seawater. Due to the high salinity of these samples, and the relatively high Br^- content in these waters, they must be the result of a mixture between partially evaporated paleoseawater and other high salinity brines which have dissolved halite. These brines are likely present over most of the Bakken Formation.

6.2. Secular Variations in Seawater Chemistry

The major ion composition of seawater has fluctuated over the Phanerozoic Eon and these fluctuations have been recorded in the composition of marine carbonates and marine evaporite sequences (Lowenstein et al., 2014).

Over geologic time, two distinct types of saline brines have been produced, $CaCl_2$ and $MgSO_4$ brines. $CaCl_2$ brines are Na-Ca-Cl rich and Mg-K-SO_4 poor. $CaCl_2$ brines are found in the Cambrian, Ordovician, Silurian, Devonian, Jurassic, and Cretaceous. The evaporation of modern seawater results in $MgSO_4$ brines. Brines with this chemical signature are also present in the Pennsylvanian, Permian, Triassic, and Cenozoic. These waters are rich in Na-Mg_2-K-Cl-SO_4 (Lowenstein and Timofeeff 2008).

Lowenstein et al. (2003) predict the reversal between Ca^{2+} and SO_4^{2-} seas occurred within sometime during the Mississippian. The Bakken Formation straddles the Devonian/Mississippian boundary and therefore can help constrain the time of this reversal.

As discussed in section 5.1.3, the Bakken Aquifer contains four water types. However, only Type 2a and Type 2b are of interest for this discussion. Type 2b waters are located in the center of the Bakken Aquifer where it is over pressured and permeability is very low (Figure 6.5). Type 2a waters are found surrounding this area where the Bakken Formation is normally pressured and permeability is higher.

Type 2b waters reflect a $CaCl_2$ brine composition while Type 2a waters reflect a $MgSO_4$ brine composition. The significance being that that Type 2b formation waters are only found in the center of the Bakken Aquifer, where permeability is limited and the formation is overpressured. Due to the low permeability and overpressured nature of the aquifer, waters located in this area represent the original waters present at the time of deposition. Outward from this area, permeability is higher and pressures are hydrostatic allowing for the moving and mixing of fluids in this area. Therefore, during the time of Bakken Formation deposition, there was a higher Ca^{2+} in the seas than SO_4^{2-} but not to the extent of the high Ca^{2+} brines found elsewhere in the Williston Basin (Jensen, 2007; Melnik, 2012).

6.3. Correlation Between Hydrochemistry and Formation Well-Log Resistivity

There is a distinctive pattern in the resistivity measured with well-logs across the Bakken Formation. Murray (1968) observed the anomalously high resistivity in the Bakken shales and attributed it to hydrocarbon saturated pore space. In a landmark paper Meissner (1978) correlated source rock maturity and hydrocarbon generation with overpressure in the Bakken Formation. Utilizing resistivity and sonic velocity logs Meissner (1978) mapped thermal maturity and overpressure in the Bakken Formation. He observed a correlation amongst them concluding that the highly resistive thermally mature portion of the Bakken Formation was overpressured, while the low resistivity, thermally immature area is normally pressured.

Meissner's study was followed up by Schmoker and Hester (1990). Using rock-eval pyrolysis they determined that 35 ohm-m represents the onset of oil generation in the Bakken Formation. This value is in good agreement with Meissner (1978) who used a separate method but determined that significant hydrocarbon production from Bakken Shales begins at 40 ohm-m.

Kreis et al. (2006) later mapped the resistivity in upper and lower Bakken shales in southern Saskatchewan. They too attributed the high resistivity of the shales to be the result of hydrocarbon saturation.

To the author's knowledge, there has never been a comparison of the resistivity of the Bakken Formation to the hydrochemistry of the Bakken Aquifer. First a regional "resistivity" line was created for the Bakken Aquifer by combining the 35 ohm-m resistivity contour of the Lower Bakken Shale mapped by Kreis et al. (2006) and the 40 ohm-m contour mapped by Meissner (1978) as the boundary for the high resistivity area of the Bakken Formation (Figure 6.9).

Total dissolved solids concentrations in the Bakken Aquifer show a partial correlation to the high resistivity Bakken shales (Figure 6.9). The 250,000 mg/L salinity contour approximately follows the regional resistivity line along the northern and eastern portion of the Bakken Aquifer.

Thus, one possibility for the resistivity anomaly is that the well-logs are measuring the 250,000 mg/L formation waters and not the hydrocarbon saturated pore space in the Bakken Formation. This proposal is supported by the lack of correlation between the regional overpressure and the regional resistivity line (Figure 6.10).

Water Type	Na^{+}	Ca^{2+}	Mg^{2+}	K^{+}	Cl^{-}	SO_4^{2-}	Br^{-}	TDS
Type 2a average	11900	682	358	220	17600	5800	18	33370
Seawater	11300	422	1326	416	19870	2780	68.4	35932

Table 5: Average water chemistry values for Type 2a waters near 101.5W and 50.3N. These waters have approximately the same TDS as modern seawater (based on Carpenter, 1978) however, the chemical composition differes.

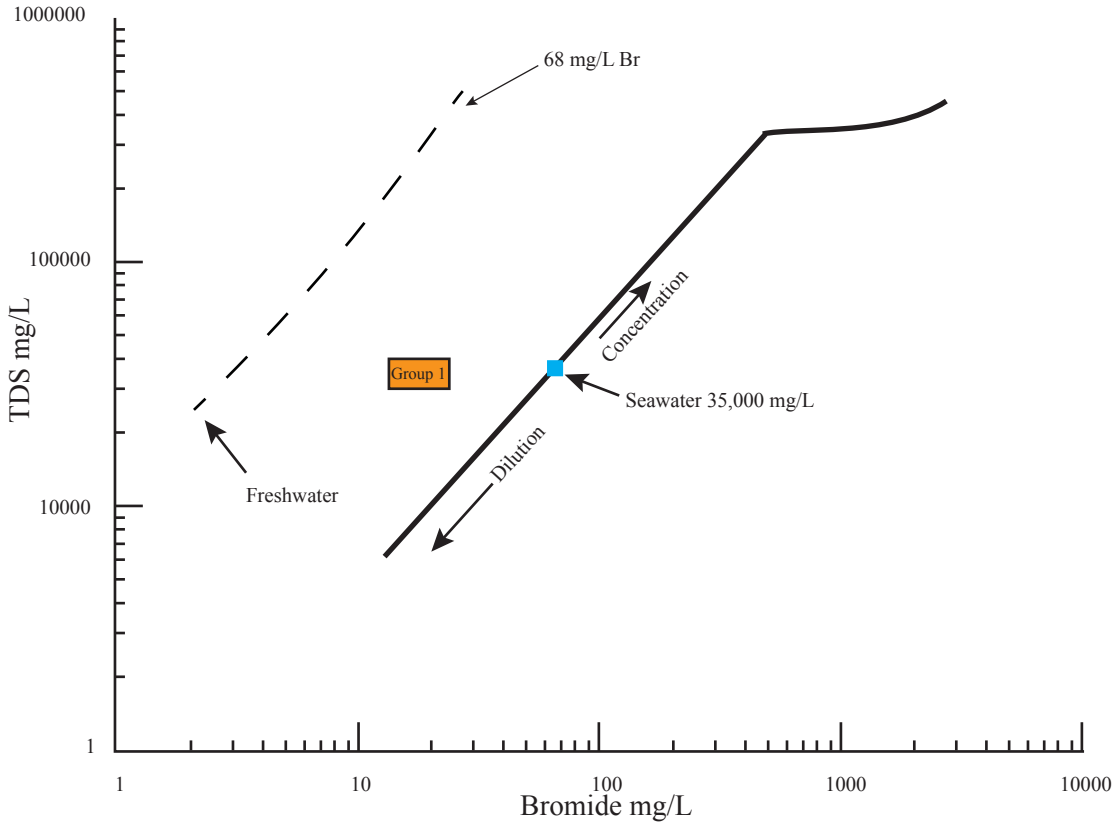

Figure 6.1: The total dissolved solids versus Bromide plot shows that Group 1 waters have approximately the TDS of seawater however, are significantly depleted in Br^-. Group 1 waters contain approximately 15-25 mg/L Br^-. Metoric waters dissolving the Prairie Formation to equivalent salinities of Group 1 would contain between 2.5 and 3.4 mg/L Br^-.

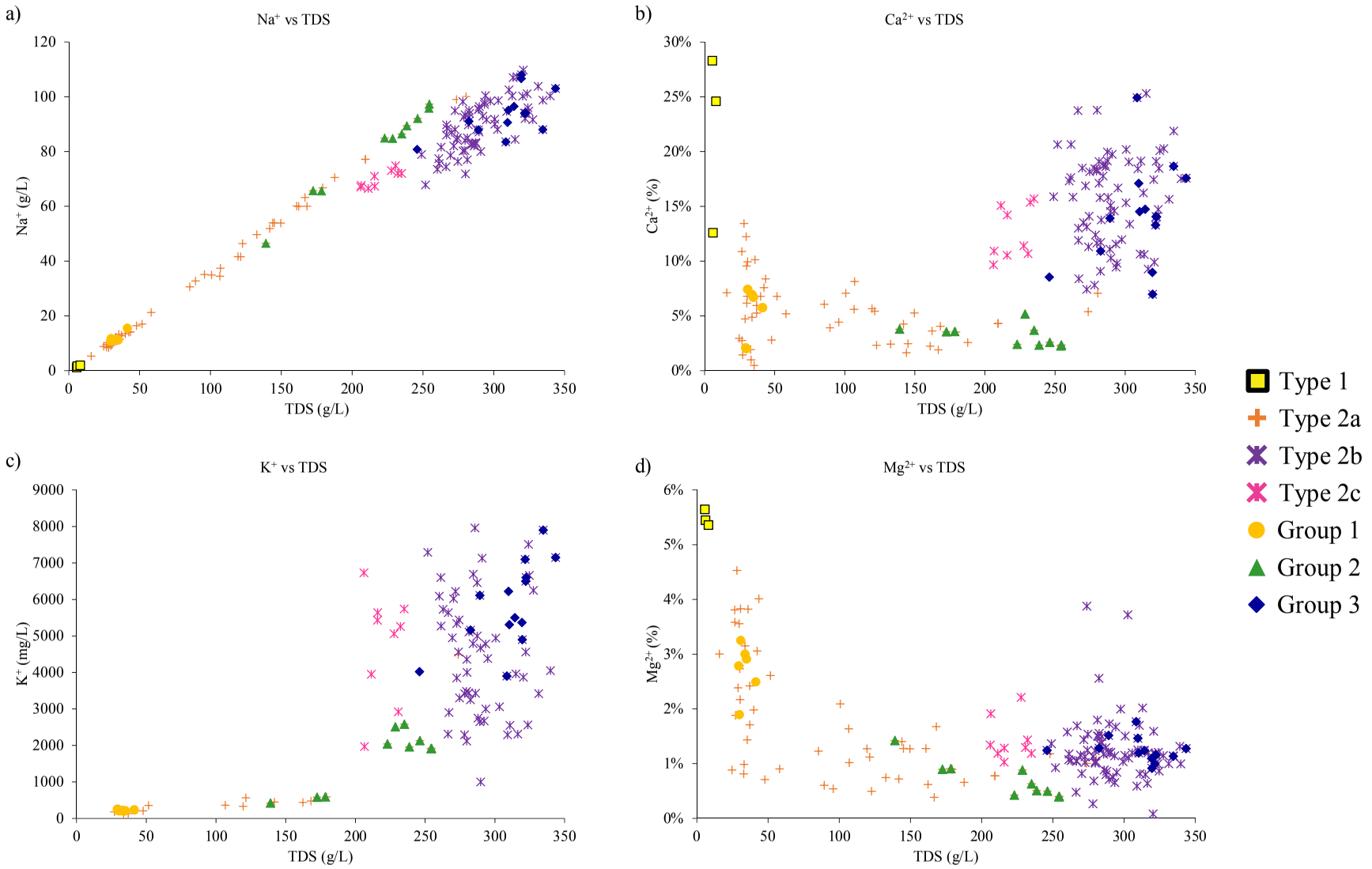

Figure 6.2: Total dissolved solids (g/L) versus: a) Sodium (g/L), b) Calcium (%), c) Potassium (mg/L), d) Magnesium (%) for Bakken Aquifer water types with Na-Cl-Br systematics water groups overlain.

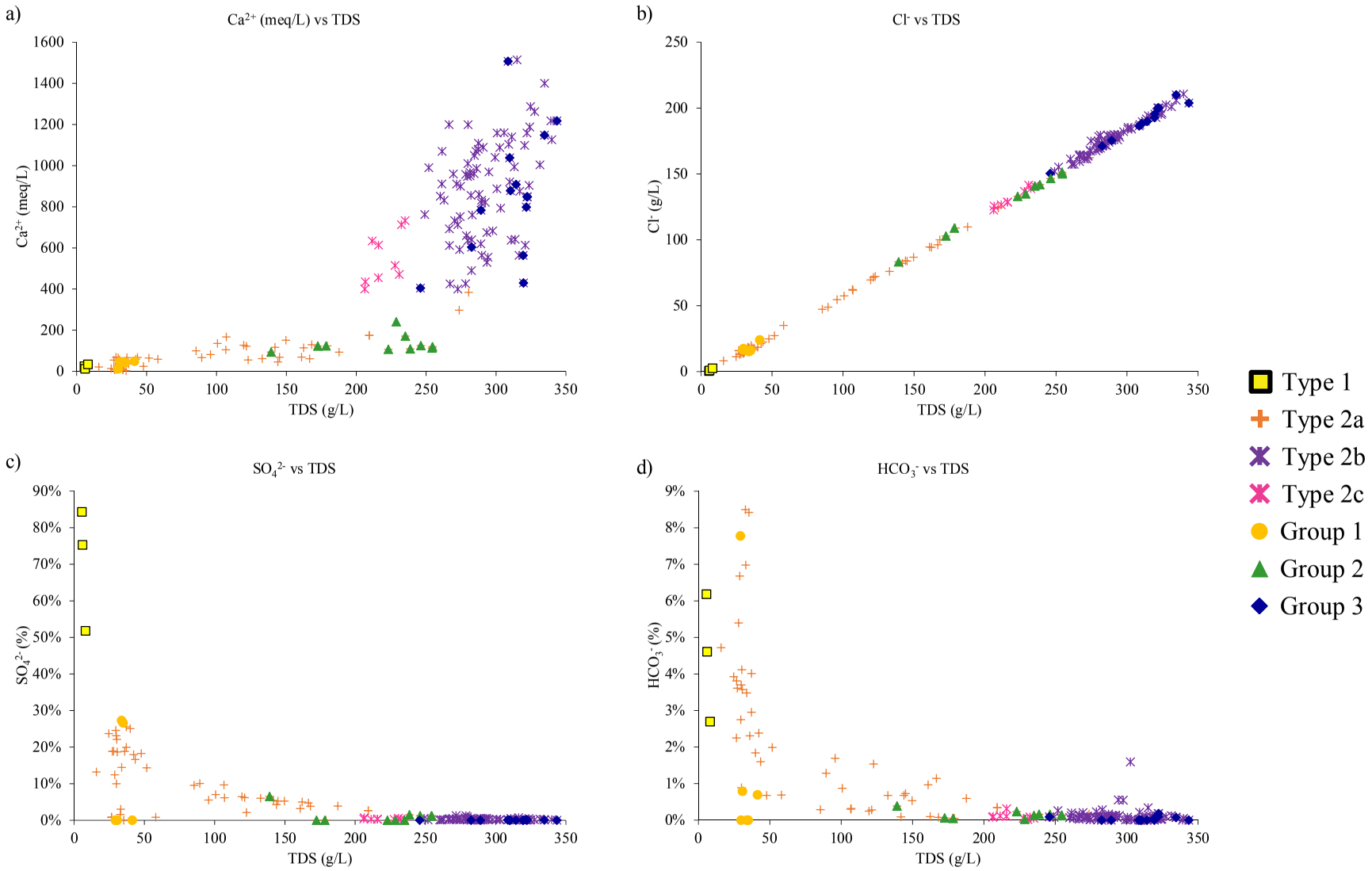

Figure 6.3: Total dissolved solids (g/L) versus: a) Calcium (meq/L), b) Chloride (g/L), c) Sulfate (%), d) Bicarbonate (%) for Bakken Aquifer water types with Na-Cl-Br systematics water groups overlain.

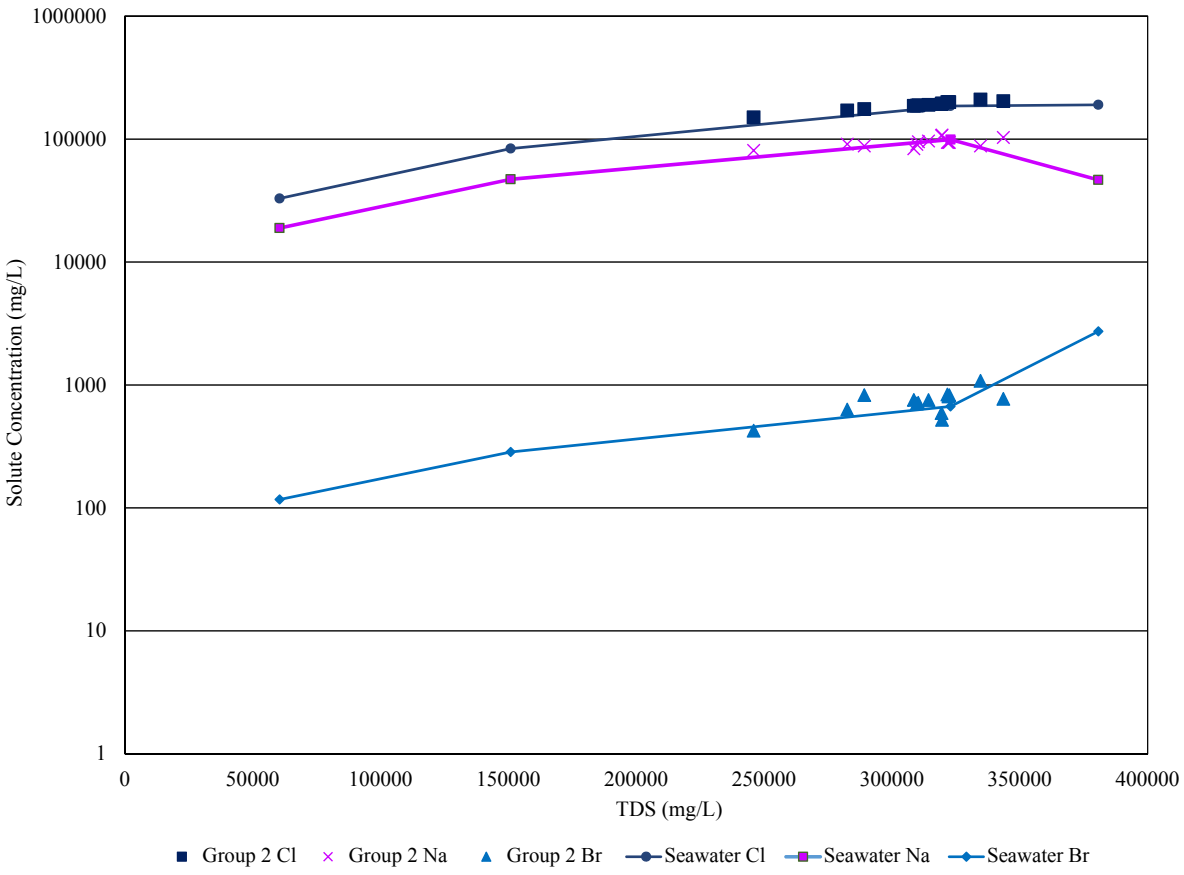

Figure 6.4: Comparison of Na-Cl-Br systematics Group 2 Chloride, Sodium, and Bromide concentrations with the evaporated seawater trends (data from McCaffery et al., 1987).

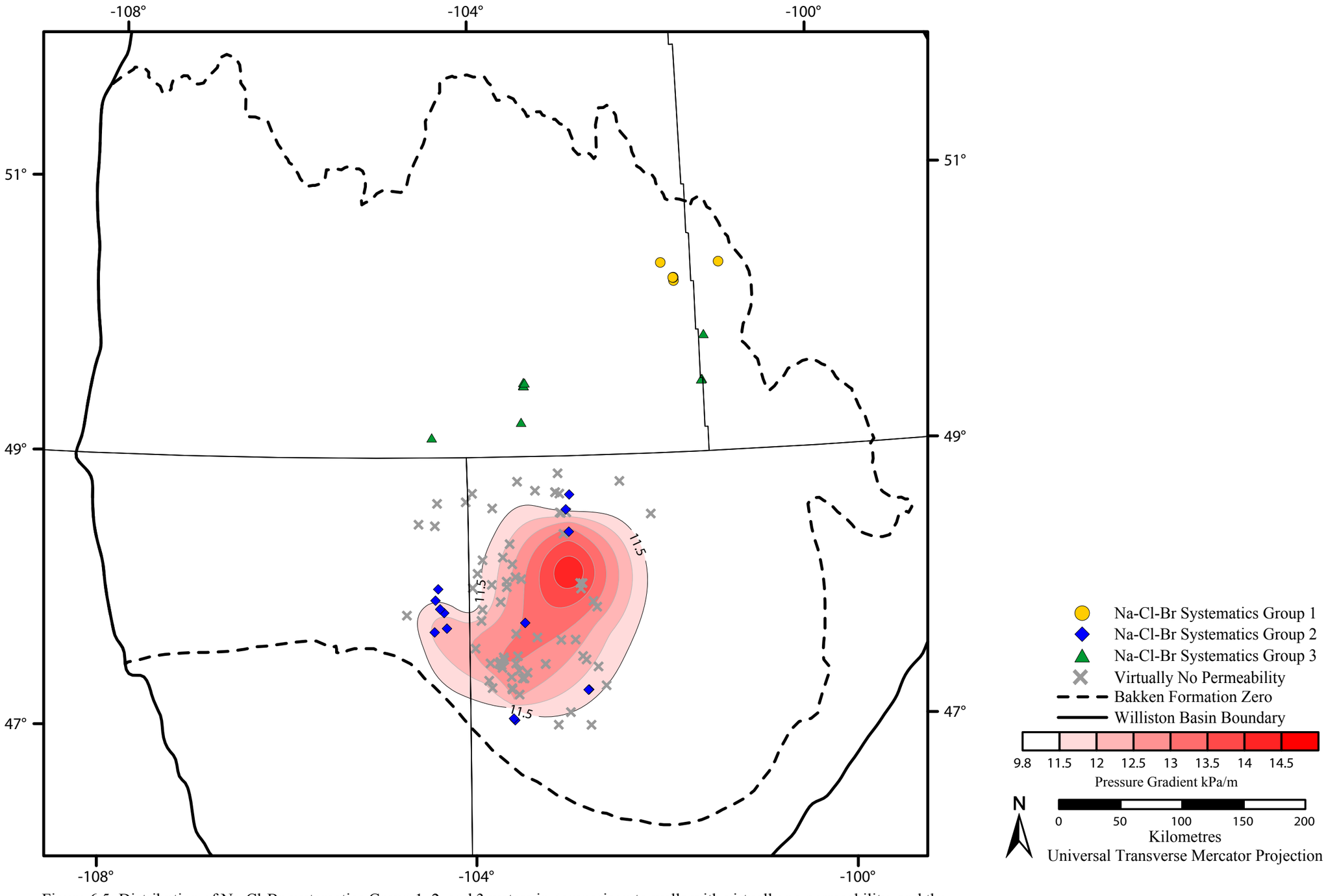

Figure 6.5: Distribution of Na-Cl-Br systematics Group 1, 2, and 3 waters in comparison to wells with virtually no permeability, and the overpressured portion of the Bakken Aquifer.

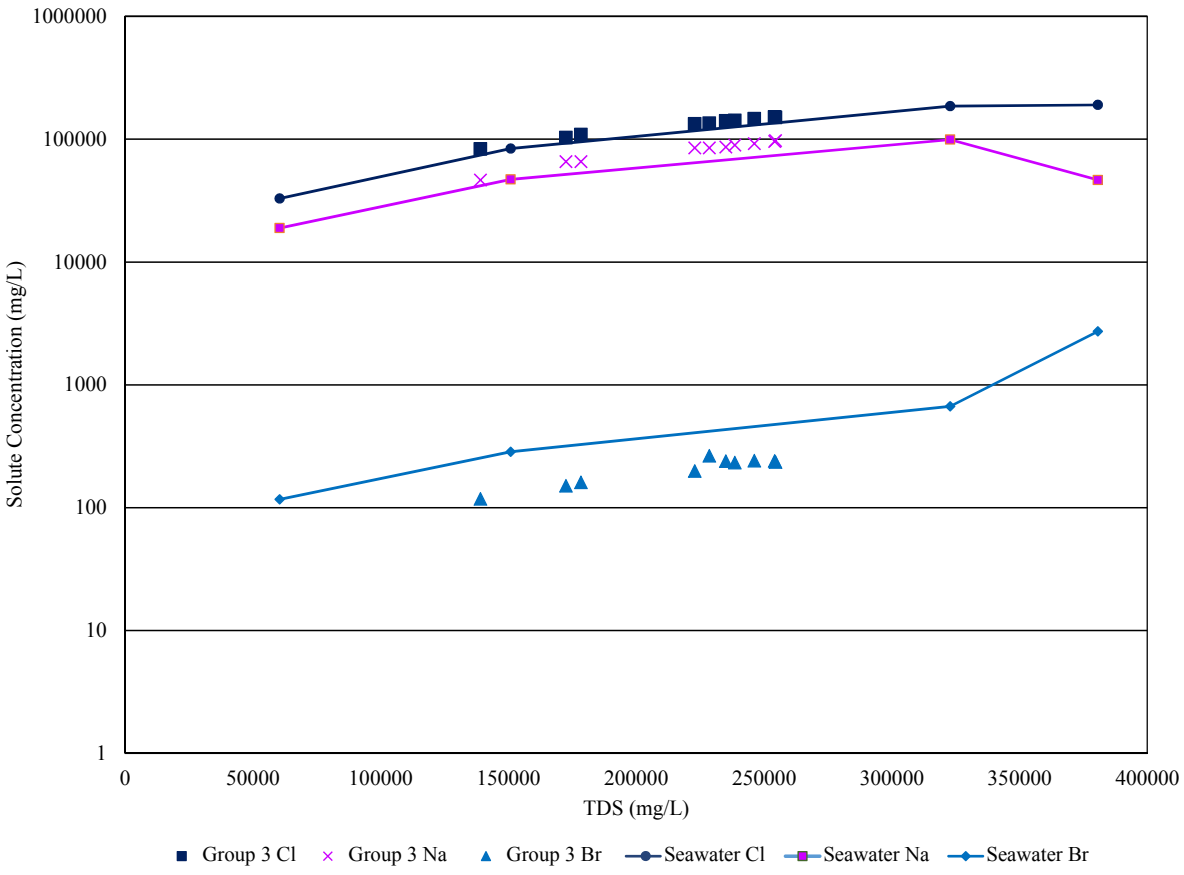

Figure 6.6: Comparison of Na-Cl-Br systematics Group 3 Chloride, Sodium, and Bromide concentrations with the evaporated seawater trends (data from McCaffery et al., 1987).

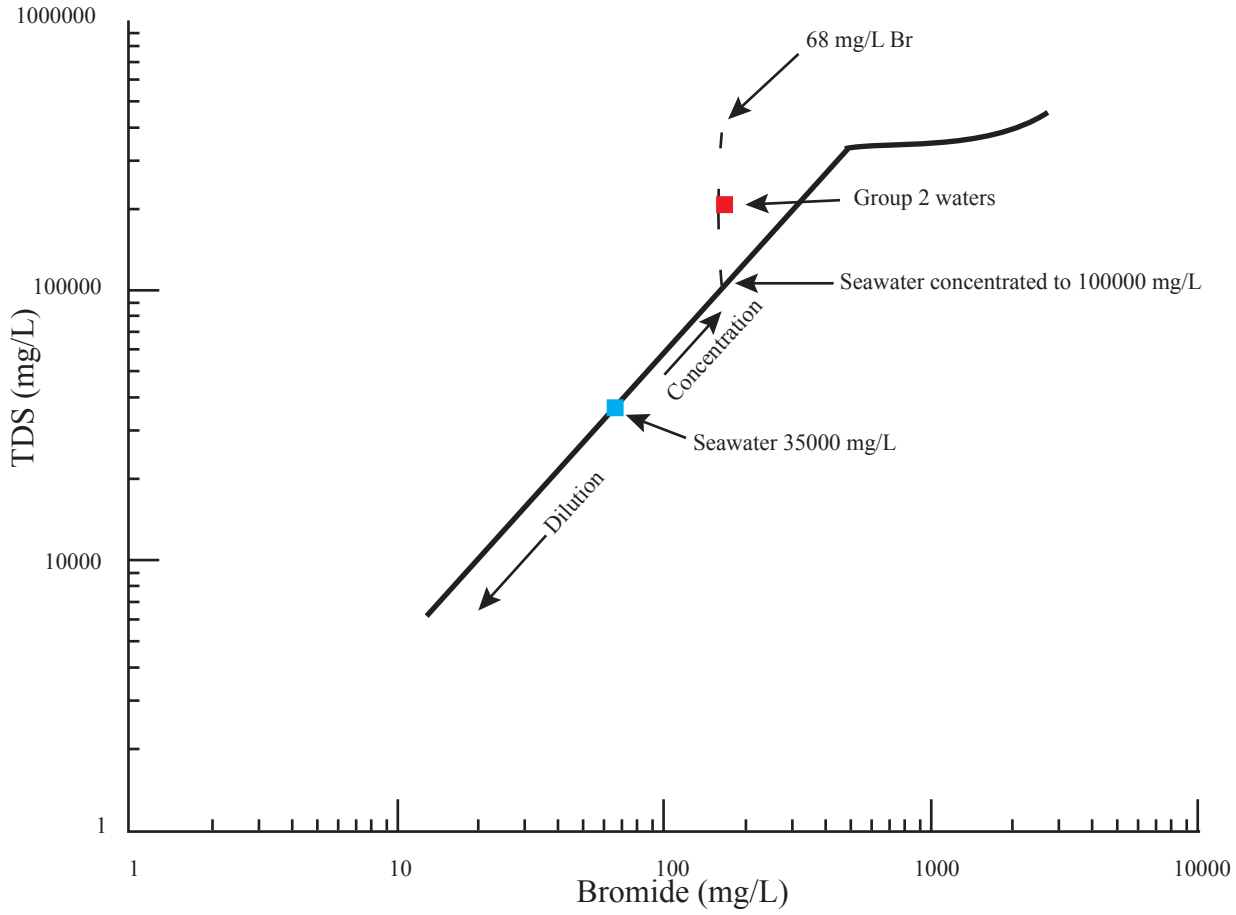

Figure 6.7: Total dissolved solids versus Bromide plot showing a possible evolutionary history of Na-Cl-Br Group 2 waters. Starting with modent seawater, TDS increases to 100,000 mg/L, then mixes with waters that dissolved halite containing 68 mg/L Br^- (Prairie Formation) resulting in a brine enriched in Chloride (Rittenhouse, 1967).

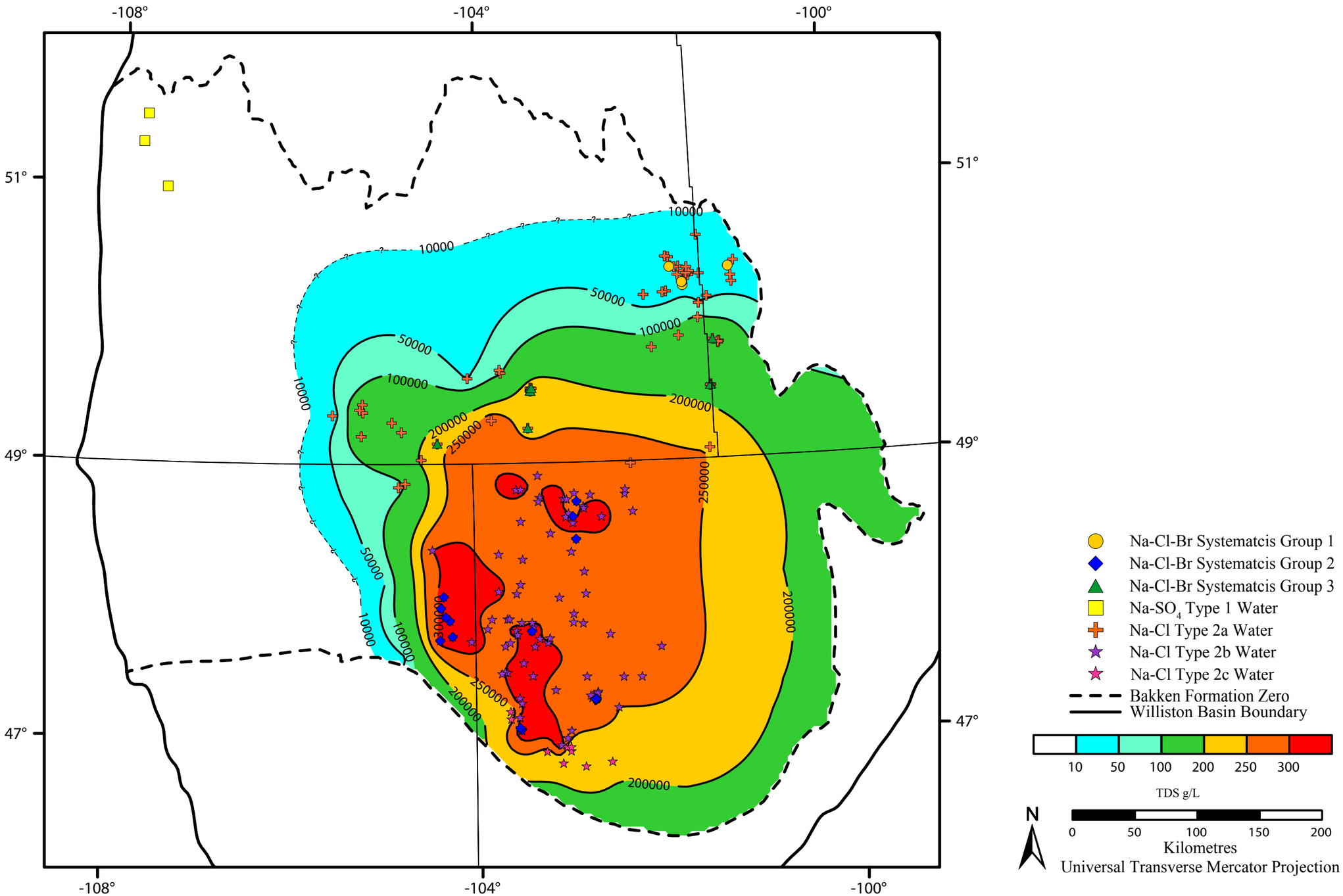

Figure 6.8: Distribution of Group 1, Group 2, and Group 3 waters (determined from Na-Cl-Br systematics) compared to Bakken Aquifer water classifications; Na-SO_4 Type 1 and Na-Cl Type 2a, 2b, 2c.

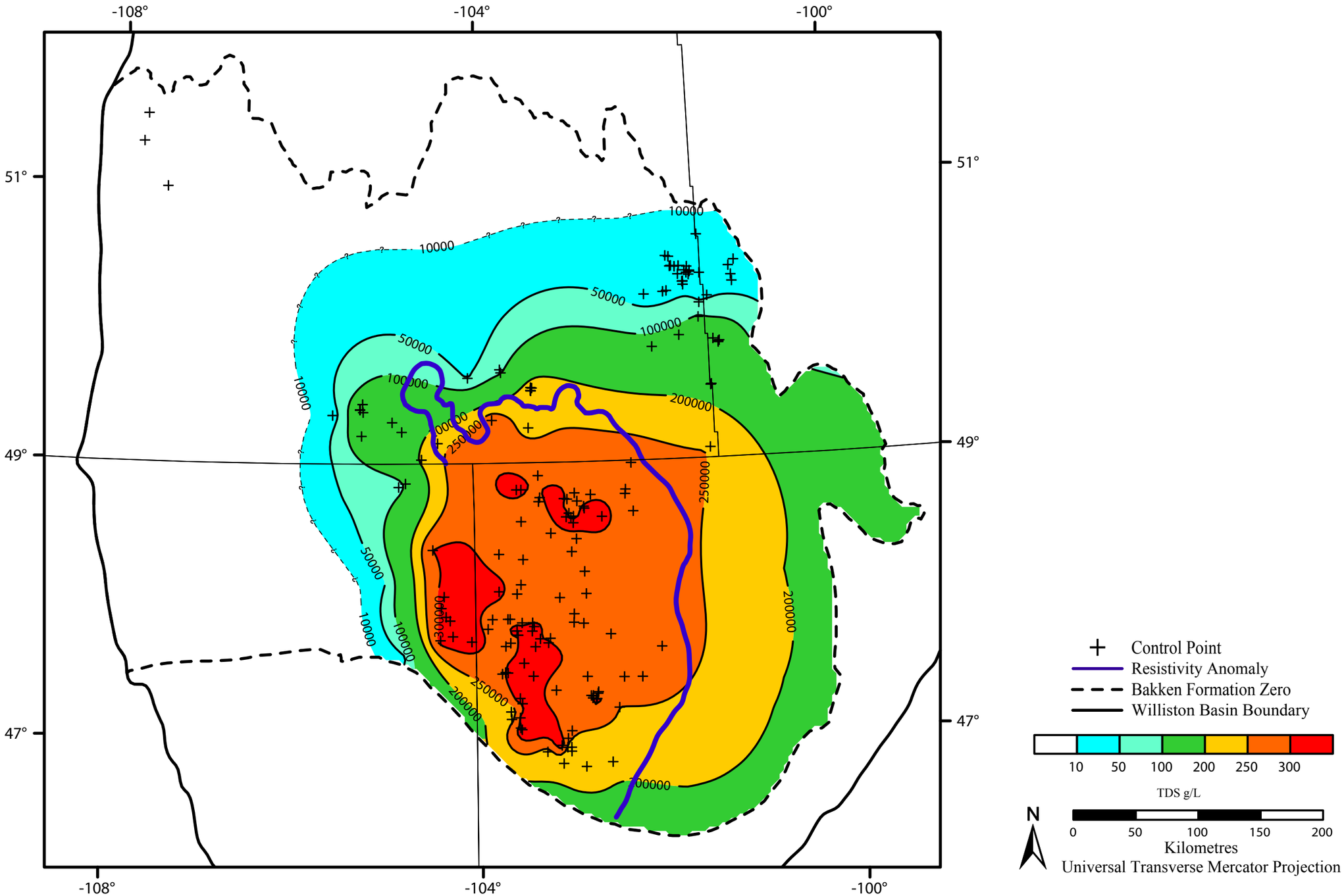

Figure 6.9: Total dissolved solids in the Bakken Aquifer compared to the highly resistive Bakken Formation in Saskatchewan (after Kreis et al., 2006) and North Dakota (after Meissner, 1978).

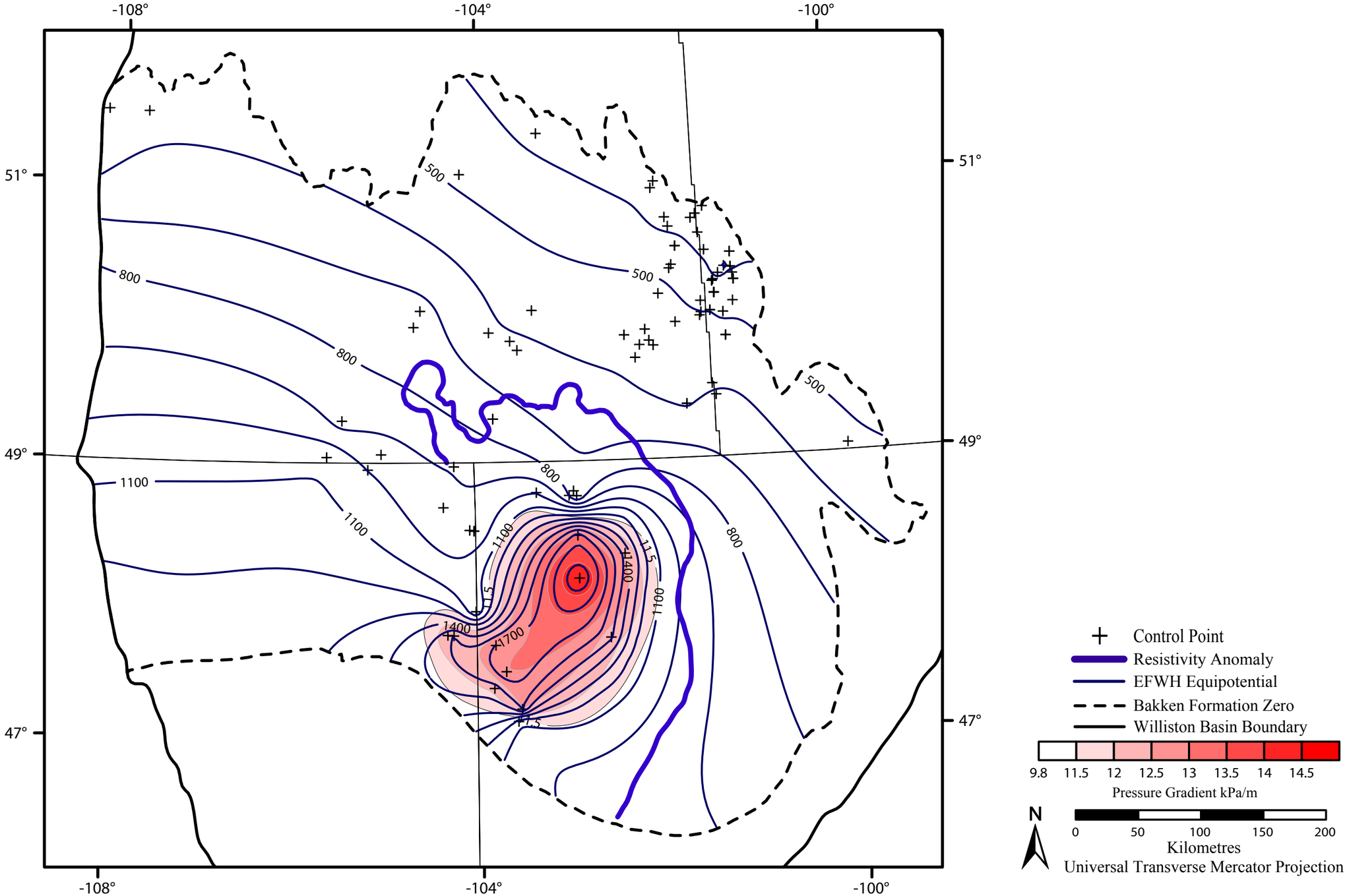

Figure 6.10: Equivalent freshwater hydraulic head in the Bakken Aquifer and pressure distribution compared to the highly resistive Bakken Formation in Saskatchewan (after Kreis et al., 2006) and North Dakota (after Meissner, 1978).

7. Hydrogeological and Petroleum Hydrogeological Synthesis

7.1. Fluid Driving Forces in The Bakken Aquifer

There are three distinct types of fluid flow in the Bakken Aquifer: topography driven groundwater flow, buoyancy driven flow resulting from density variations within the aquifer, and overpressure driven flow caused by hydrocarbon generation.

Section 5.2.1 presents the potentiometric surface of the Bakken Aquifer. Fresh meteoric waters recharge the Williston Basin in the southwest at the topographic highs. Fluids flow toward the center of the basin and continue to the northeast. High values on the potentiometric surface are located in the southwest of the Bakken Aquifer associated with the topographic high, while the regional low is located to the northeast where elevation is lower.

The direction of fluid movement in the Bakken Aquifer was investigated using a P(d) plot (Figure 7.1, Figure 7.2). In Manitoba near the Bakken Aquifer subcrop (101°W, 50.4°N) pressures are sub-hydrostatic plotting with a lower pressure than the nominal gradient, however, the slope is equivalent. In Saskatchewan near 104°W, 50°N pressures plot along and follow the nominal hydrostatic gradient for freshwater (9.8 kPa/m) (Figure 7.2). Pressures plotting along a single line following the nominal gradient are interpreted to show horizontal flow through the aquifer.

Flow in the Bakken Aquifer is horizontal, from the southwest towards the northeast in the topographic driven flow portion of the Bakken Aquifer.

Areas with significant density dependent flow in the Bakken Aquifer are highlighted on the water driving force map (Figure 5.18). Significant deviations from the equivalent freshwater hydraulic head map are present in northeast Montana and southeast Saskatchewan. In these areas, regional groundwater flow is retarded,

redirected and in some locations nearly reversed (up to 170° deviated) compared to the equivalent potentiometric surface generated using freshwater densities.

The final driving force of fluids in the Bakken Aquifer is the result of the pressure gradient in the overpressured area near the center of the aquifer. The overpressured area causes a disruption in the potentiometric surface compared to normally pressured portions of the aquifer. Due to the limited permeability of this portion of the aquifer, flow is limited, however, the potential for flow causes a disruption in the potentiometric surface. Fluid potentials decrease radially outwards from the center of the overpressured area and as permeability increases, the pressure decreases.

A P(d) plot was used to determine flow direction in the overpressured portion of the Bakken Aquifer (Figure 7.1, Figure 7.2). In this area pressures plot along a single trend exceed the nominal pressure gradient. Vertical flow is indicated by the P(d) plot however the extremely limited permeability confines flow to the aquifer. Instead, the pressures are interpreted to reflect hydrocarbon generation (Meissner, 1978; Osadetz et al., 1996).

7.2. Extent of Overpressure in The Bakken Aquifer

Pressure depth analysis reveals the Bakken Aquifer to be overpressured (i.e. >11.5 kPa/m) over a large portion of North Dakota extending partially into Montana (Figure 5.20). Overpressures range from 11.6 to 14.5 kPa/m decreasing radially outward from the maximum located at 103°W 48.1°N in North Dakota.

The Bakken Formation has long been known to be overpressured. Meissner (1978) constructed an overpressure map in the Bakken Formation utilizing sonic velocity data in 32 wells. Sonic velocities were compared in wells known to be overpressured with those known to be normally pressured. The magnitude of the velocity discrepancy between two measurements at the same depth being a direct

relation to the magnitude of the overpressure. Utilizing a series of control points, a calibration curve for overpressure as a result of the sonic velocity was constructed. Meissner mapped the extent and magnitude of the overpressured in the Upper and Lower shales of the Bakken Formation using this well-log derived relationship to obtain a distribution map of overpressures (Figure 7.3).

Meissner (1978) results show the Bakken Formation to be overpressured over a large portion of North Dakota extending into Montana with a pressure gradient of 15.8 kPa/m. The maximum overpressure calculated from the sonic velocity exceeds 18.1 kPa/m. A steep pressure gradient is present along the eastern margin of the overpressured area indicated by tightly spaced contours. Outwards from the central overpressured area pressures decrease returning to hydrostatic conditions.

A comparison the overpressure map generated from DST data in this study to Meissner's (1978) overpressure maps reveals two main differences: the shape and magnitude (Figure 7.4).

The overpressured area mapped by Meissner (1978) is significantly larger than in this study. Meissner's area of overpressure extends over a large portion of North Dakota, northeast Montana and north into Canada covering approximately 55,000 km². The overpressured area determined in this study covers a portion of North Dakota and partially extends into Montana, covering an area of approximately 22,000 km². The magnitudes of the pressure gradients determined in this study are less than those mapped by Meissner, with a maximum pressure gradient of 14.5 kPa/m obtained from stabilized DST pressures.

Furthermore, the shapes of the pressure distributions calculated from each method are not in agreement. The pressure distribution calculated from DST data shows the maximum pressure gradient located in the center of the Bakken Formation in North Dakota decreasing radially outwards. The maximum pressure gradient of Meissner (1978) is located to the south of what is shown from the DST data. Pressures decrease outwards, however, Meissner (1978) shows an area with a lower pressure gradient extending from the south into the center of the overpressured area.

This study provides the most accurate pressure distribution in the Bakken Aquifer to date based on the following reasons. First, this study was not constrained by political boundaries. By using a geological boundary rather than a political boundary potential edge effects are not present in the dataset. Second, the pressure distribution presented in this study is based on pressure data rather than geophysical methods. Third, the pressure data used in this study underwent an extensive culling procedure to remove any non-representative data. Finally, this study utilized significantly more data than previous studies spanning the entire Bakken Aquifer.

7.3. Hydrocarbon Migration and Accumulation

The migration of hydrocarbons from source rocks to traps and reservoirs occurs in three successive steps. First hydrocarbons are generated and expelled from thermally mature source rocks in a process known as primary migration (Tisspt and Welte, 1978). During this phase, expelled hydrocarbons migrate out of the source rock as a separate hydrocarbon phase (Palciauskas, 1991). Following primary migration, hydrocarbons move through relatively high permeability carrier beds towards the hydrocarbon trap in a process known as secondary migration. Hydrocarbons are capable of migrating in many forms (i.e. droplets, continuous phase, in solution) all of which are effected by the differences in mechanical energy between the fluids within the sediments. Secondary migration stops when hydrocarbons are trapped due to the combination of structural, stratigraphic, lithologic, or hydrodynamic changes (Tóth, 1988).

Under hydrostatic conditions the primary control on hydrocarbon migration is buoyancy, resulting in the updip migration of hydrocarbons. The magnitude of this impelling force increases with the dip of the carrier bed as well as the density contrast between the two fluid phases. For hydrodynamic conditions, hydrocarbon migration is influenced by both the buoyant force and the head gradient (Figure 2.2).

7.3.1. Hydrocarbon Migration and Accumulation in the Bakken Formation

The migration of Bakken Formation hydrocarbons has been discussed extensively within the literature. Initially, it was believed that the Bakken Formation was the source of oils found in Madison group reservoirs (Dow, 1974; Williams, 1974; Meissner, 1978; Leenheer, 1984; Price et al., 1984). However, recent research shows the Bakken Formation to be a closed system with hydrocarbon expulsion primarily into the Middle Bakken Member (Kuhn et al., 2012 and references therein). However, to better understand potential influences on migration in the Bakken Formation, the effects of variable density formation water on buoyant hydrocarbon migration were investigated.

To show the effects of formation water movement on oil migration and accumulations within the Bakken Formation, oil driving force maps were constructed (Figure 5.21, Figure 5.22), and the UVZ method (Hubbert, 1953) employed (Figure 7.5, Figure 7.6). While oil migration vectors and the U surface have been calculated over the entire Bakken Formation, it is important to note that it does not mean oil is present over the entire Bakken Formation. These vectors represent the potential migration pathway oil would take if it was present at any given location. Oil specific gravities of 36 and 44 API were used as they represent the ranges of Bakken Formation crude oil (Cwiak et al., 2015).

Oil generated in the large thermally mature area located in Montana and North Dakota should migrate radially outward from the center of the Bakken Formation and updip toward Canada (Figure 7.5, Figure 7.6). Regionally, the U surface has the highest values in the south and southwest with lowest values in the north and northeast. Important features on these maps include: areas of convergence along the North Dakota/Montana border and the Saskatchewan/Manitoba border. A notable feature in Figure 7.5 is a closed depression in the U surface located in southern Saskatchewan. This closed depression highlights a local fluid potential minimum and is therefore a preferential hydrocarbon entrapment area.

Comparing the location of production wells (Figure 4.3) to the predicted migration path, there are several production wells drilled in locations highlighted in the potential areas of entrapment. While some of these areas have been targeted for development, there is the potential for further development of the Bakken Formation based on the findings of the UVZ method. These areas (outlines on Figure 7.7, and Figure 7.8) include:

1) The areas near 105°W and 49.5°N. This area is of interest due to the convergence of multiple flow vectors and closed U contour (36API).
2) The area in NE Montana near 104°W and 48.5°N. In this area there are multiple convergence flow vectors as well as a strong density dependent flow component resisting the updip migration of hydrocarbons.
3) The area near 102.5°W and 50.2°N. This area is chosen due to the migration pathway highlighted by the migration vectors and U surface, as well as the proximity to other production wells in the area (Figure 4.3). Production wells to the east indicate that long distance migration of oil from the thermally mature portion of the Bakken to distances of this length is possible.

7.4. Oil Production Behaviours and Hydrogeology.

It has long been known that production rates in Bakken Formation wells are spatially dependent and highly variable. Meissner (1978) mapped the resistivity of the Bakken Formation concluding that the change in well-log resistivity is related to the replacement of conductive formation waters with non-conductive hydrocarbons. In addition, Meissner (1978) also concluded that in the deeper portion of the Bakken Formation where hydrocarbon shows are widespread, oil and gas are essentially the only mobile fluids. While true in some areas, this was not the case even within the thermally mature portion of the Bakken Formation. In early development, production

was somewhat unpredictable with good wells, often offset with poor production wells (Sonnenberg and Pramudito, 2009).

Significant Bakken oil reserves have still been produced in the shallower, thermally immature portions of the Bakken Formation. In a study conducted in southeastern Saskatchewan, Dayboll (2010) attempted to determine the "Bakken water line", a line which serves as the boundary between portions of the Bakken Formation which produce significant volumes of water from those that do not. Using production data, a line separating high and low water producers was proposed; however, the regional extent of the "Bakken water line" was unclear.

To further the understanding of production behaviours in Bakken Formation wells and their spatial relation to various geological criteria, a regional study of production behaviours across the productive areas of the Bakken Formation was conducted. An attempt was made to relate observed production behaviours to: regional structure features (Figure 7.9); thermal maturity of source rocks (Figure 7.10); the hydrochemical distribution of formation waters in the Bakken Aquifer (Figure 7.11); the hydraulic head distribution within the Bakken Aquifer (Figure 7.12); the pressure distribution in the Bakken Aquifer (Figure 7.13); and mapped oil migration pathways in the Bakken Aquifer from UVZ analysis (Figure 7.14, Figure 7.15).

7.4.1. Relation to Geological Features

7.4.1.1. Structure

An understanding of the regional structural features within a basin is important for predicting areas of hydrocarbon migration and potential trapping locations. Preferential production behaviours (Type 2a and Type 2b) are observed around these large-scale features (Figure 7.9). Near the Billings and Nesson anticlines, wells display the Type 2a production behaviour. Near the Antelope Valley and Little Knife

anticlines, Type 2b production behaviour is dominant. Type 1 and Type 3 production behaviours are not observed near large, regionally extensive structural features.

7.4.1.2. Thermal Maturity

A comparison of production behaviours to the thermally mature portion of the Bakken Formation as determined by Meissner (1978) shows all production behaviours are present in the thermally immature Canadian portion of the Bakken Formation. Type 2a, Type 2b and Type 3 production behaviours are present in the thermally mature portion (Figure 7.10). While thermal maturity is crucial to the generation of hydrocarbons, it is not solely responsible for the distribution of production behaviours observed in the Bakken Formation.

7.4.2. Relation to Hydrogeological Features

7.4.2.1. Total Dissolved Solids

Comparing observed production behaviours to the TDS map, it is apparent that there is no correlation between salinity in the Bakken Aquifer and production behaviour of the Bakken Formation (Figure 7.11).

7.4.2.2. Hydraulic Head Distribution

Comparing the production behaviours and the hydraulic head map there is no relation between the hydraulic head distribution and the production behaviour (Figure 7.12).

7.4.2.3. Overpressured Area

A clear relationship between the overpressure in the Bakken Aquifer and production behaviour does exist (Figure 7.13). Within the overpressures area, Type 2a and Type 2b production behaviours are dominant. However, some wells display the Type 3 production behaviour. As pressure in the Bakken Aquifer decreases, returning

to hydrostatic conditions, Type 3 production behaviours become dominant, surrounding the overpressured area.

The agreement with the mapped overpressure in Montana is not as strong as it is in North Dakota; however, reliable pressure data in the area is sparse. With additional data, the overpressured area could be better refined and the trend may be similar to what is observed in North Dakota. Based on the observed production behaviour, the area of overpressure could extend northwest following Type 2a and Type 2b production behaviours.

In the United States portion of the Bakken Formation, production behaviours can largely be explained by their location in relation to the pressure distribution. Thermally mature Bakken source rocks generate hydrocarbons, subsequently increasing formation pressures. The Canadian portion of the Bakken Formation is thermally immature, not generating hydrocarbons therefore, pressures are hydrostatic, and do not influence production behaviours.

7.4.2.4. Hydrodynamic Oil Migration

Production behaviours in the Bakken Formation were compared to U surface maps for 36 and 44 API oils (Figure 7.14, Figure 7.15). In the United States portion of the Bakken Formation, Type 2a and Type 2b production behaviours are the dominant production behaviour over a large portion of North Dakota and Montana. Excluding the overpressured area (Figure 7.13) Type 2a and Type 2b production behaviours are only located in areas of U vector convergence (Figure 7.15). In the Canadian portion of the Bakken Formation, the Type 2a and Type 2b production behaviours are found in areas of vector convergence. In northern North Dakota and much of Canada, the Type 3 production behaviour is observed in locations where there are fewer U surface vectors converging.

7.5. Produced Water Availability

During the development of the Antelope field in North Dakota, DSTs and initial production results showed only small water cuts even in advanced depletions of the field (Meissner, 1978). Meissner suggested that this water was the result of capillary pore water and not suggestive of water encroachment or the presence of an oil water contact in the Bakken Formation concluding that hydrocarbons are the only mobile fluid in the deep portion of the Bakken Formation. While true in some thermally mature areas, observed production behaviours show that this is not the case in all thermally mature areas.

Bakken Formation oil wells little to no water production (Type 2a and Type 2b production behaviour) are typically located within the overpressured portion of the Bakken Formation (Figure 7.13). These wells produce limited quantities of formation water and never experience an increase in water production even in advanced stages of reservoir depletion (Figure 5.23, Figure 5.24). Wells with Type 2a and Type 2b production behaviours can also be found in migration pathways identified on oil migration maps (Figure 7.14, Figure 7.15).

Outward from the central overpressured area, water availability increases as evidenced by the presence of Type 3 wells (Figure 5.24), surrounding the overpressured area (Figure 7.13). These wells produce more water than oil for the entire production history, but do not exhibit a large increase in water production in advanced stages of depletion. Therefore, while there is more water available surrounding the overpressured area, water availability is still limited.

In the northern portion of the Bakken Formation, Type 1 production behaviour is observed (Figure 5.23, Figure 7.13). These wells show a large increase in monthly water production as the reservoir is depleted. In the area of these wells, we can therefore conclude that there is a large amount of free water in the Bakken Formation.

7.5.1. Bakken Water Line

Dayboll (2010) conducted a study examining the production behaviours of Bakken Formation oil wells in southern Saskatchewan. This study estimated the location of a proposed "Bakken water line", in the Canadian portion of the Bakken Formation. The Bakken water line as defined by Dayboll (2010) is a line separating production wells with significant versus insignificant water production. While a line was proposed, the regional extent was unknown. To determine if the Bakken water line was a regionally extensive feature, an investigation of production behaviours across all productive areas in the Bakken Formation was conducted.

Expanding the study area of Dayboll (2010) and integrating various hydrogeologic parameters it was determined that the "Bakken Water line" is not regionally extensive. There is no single feature which can be mapped across the Bakken Formation that can demarcate significant versus insignificant water production.

7.6. Production Anomaly Investigation

A large production anomaly is located in North Dakota in the northern portion of the overpressured area (Figure 7.16). Wells in this area exhibit a Type 3 production behaviour rather than the expected Type 2a or Type 2b production behaviour.

A detailed investigation was conducted to determine the cause of this production anomaly. Six possible explanations for the production anomaly were investigated.

7.6.1.1. Production Interval

The first possible mechanism investigated was production from the wrong interval or comingled production. The production interval of each well was verified two separate ways. The reported production interval was examined to ensure that the well was producing from the correct pool. Wells completed in multiple formations, or

wells with comingled production could not sufficiently explain the observed production behaviour anomaly.

7.6.1.2. Isopach Thickness

A second mechanism thought to be responsible for the anomalous production was the thickness of the upper and lower shale members. If either of the shale members were anomalously thin, or missing from the area, the sealing potential would be reduced. This would facilitate easier cross-formational flow into the middle member of the Bakken Formation from the overlying Lodgepole Formation or upwards from below. However, examination of the isopach thickness of each of the three members revealed that neither of the shale members are anomalously thin or missing in the area of the production anomaly. Therefore, it is unlikely that there is any relation between the thickness of the shale members and the production anomaly.

7.6.1.3. Structural Features

The third mechanism investigated was large regional scale structural features such as folds and faults. While the Nesson anticline is located just east of the anomaly, there are no apparent structural controls causing the production anomaly (Figure 7.9).

7.6.1.4. Water Saturation

Fourthly water saturation in the Middle Member of the Bakken Formation as well as the lower lying Three Forks Formation was examined. Using the maps of Millard and Dighans (2014) it was determined that the Middle Bakken has a calculated water saturation of between 0.3 and 0.6 and the Three Forks Formation is less than 0.2 in the area of the anomaly. There does not seem to be any correlation to the calculated water saturation in the area of the anomaly, compared to the area surrounding the anomaly exhibiting the expected production behaviour. Therefore, the higher than expected water production in this area can not be explained by the presence of a local water saturation anomaly in the Middle Member of the Bakken Formation or the lower lying Three Forks Formation.

7.6.1.5. Completion Technique

The fifth mechanism investigated was the completion techniques used in wells with anomalous production behaviour. Stimulation data including top, bottom, volume, proppant weight, pressure, and number of stages was obtained from the North Dakota DMR. Wells with normal and abnormal production behaviours were compared against each other to determine if there is a trend between the stimulation treatment and production behaviour. The results of this investigation were inconclusive; no obvious relationship between the stimulation properties and production behaviours was observed.

7.6.1.6. Hydrochemical Analysis

Water chemistry analyses from production wells within the anomaly were searched for in all public databases however, no water chemistry data was found. Without a water sample analysis, it is not possible to conclusively determine if the water produced from these wells is sourced from the Bakken Formation or elsewhere.

Although it is not possible to determine the origin of the waters in the anomalous area without a detailed chemical analysis, one possible mechanism is the ingress of out of zone waters sourced from the overlying Lodgepole Formation. The presence of stray formation fluids in production wells has been well documented in the literature (e.g. Rostron and Arkadaksky, 2014 and references within). Rostron and Arkadaksky (2014) analyzed 36 produced water samples from hydraulically fractured Bakken Formation wells in a Canadian portion of the Williston Basin. Stable isotope data showed that the produced waters from these wells were composed of up to 40% Lodgepole Formation waters. Subsequently, the most logical source for excess fluids produced in these wells is from the overlying Lodgepole Formation.

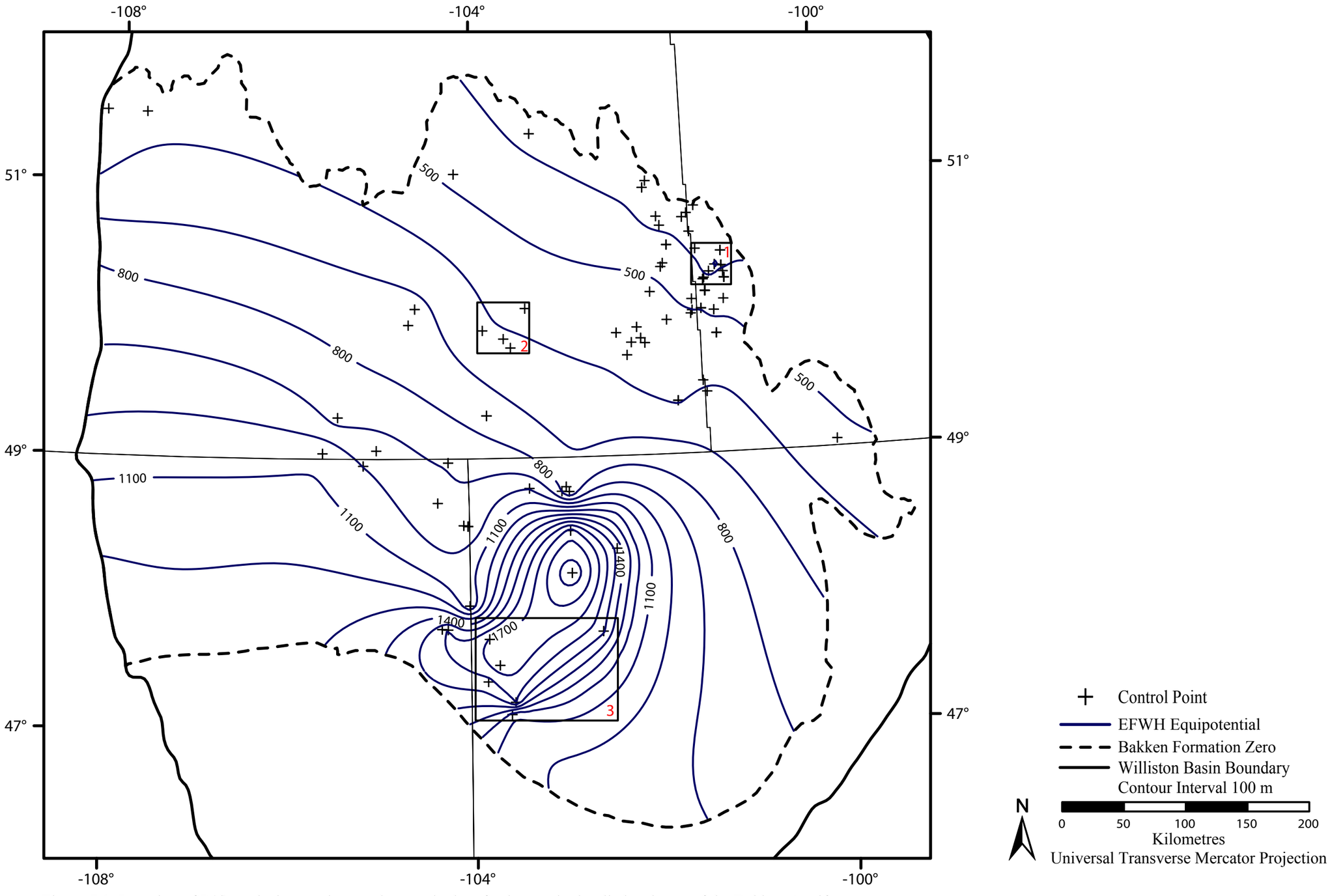

Figure 7.1: Location of P(d) analysis superimposed on equivalent freshwater hydraulic head map of the Bakken Aquifer.

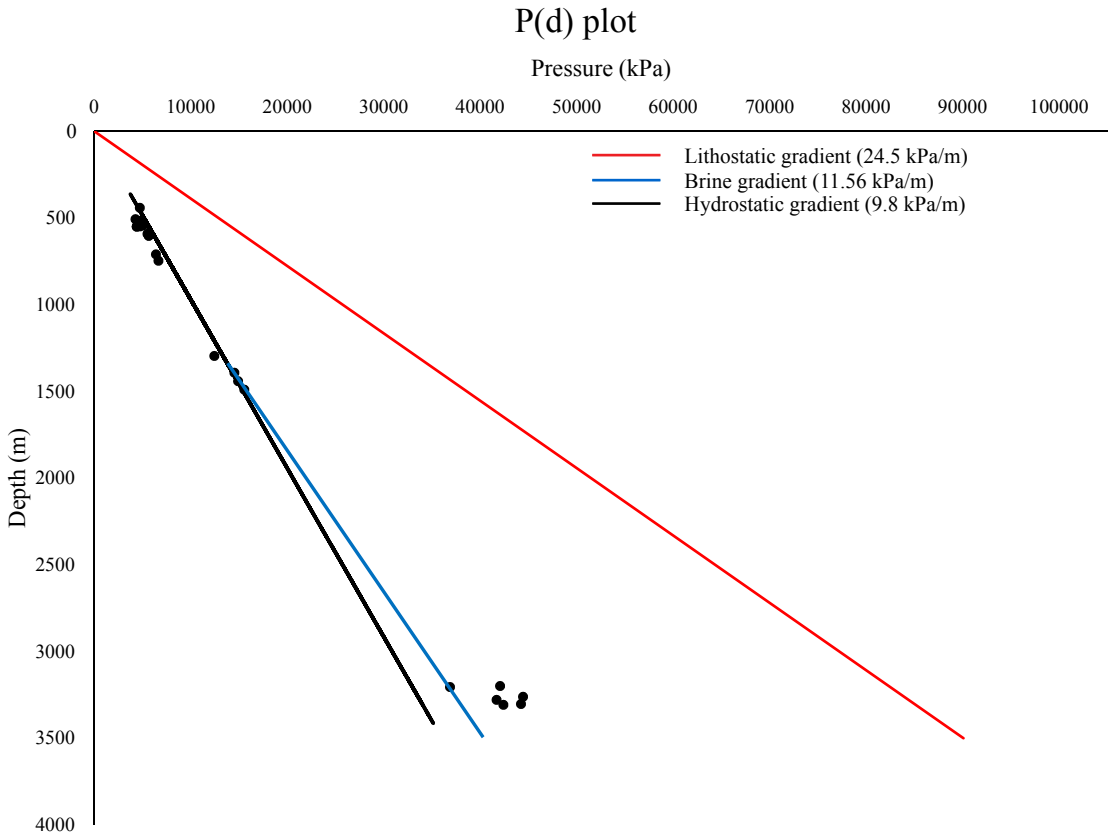

Figure 7.2: Pressure depth plot for the three areas highlighted in Figure 7.1. Area 1 corresponds to depths between 500 and 800 m. Area 2 corresponds to depths between 1,300 and 1,500 m. In these areas, pressures plot along the hydrostatic gradient indicating horizontal flow. Area 3 corresponds to depths between 3,200 and 3,300 m. Pressures exceed the brine gradient indicating overpressure conditions in the Aquifer. Vertical flow is indicated from the P(d) plot however, the extremely limited permeability confines flow to the Bakken Aquifer.

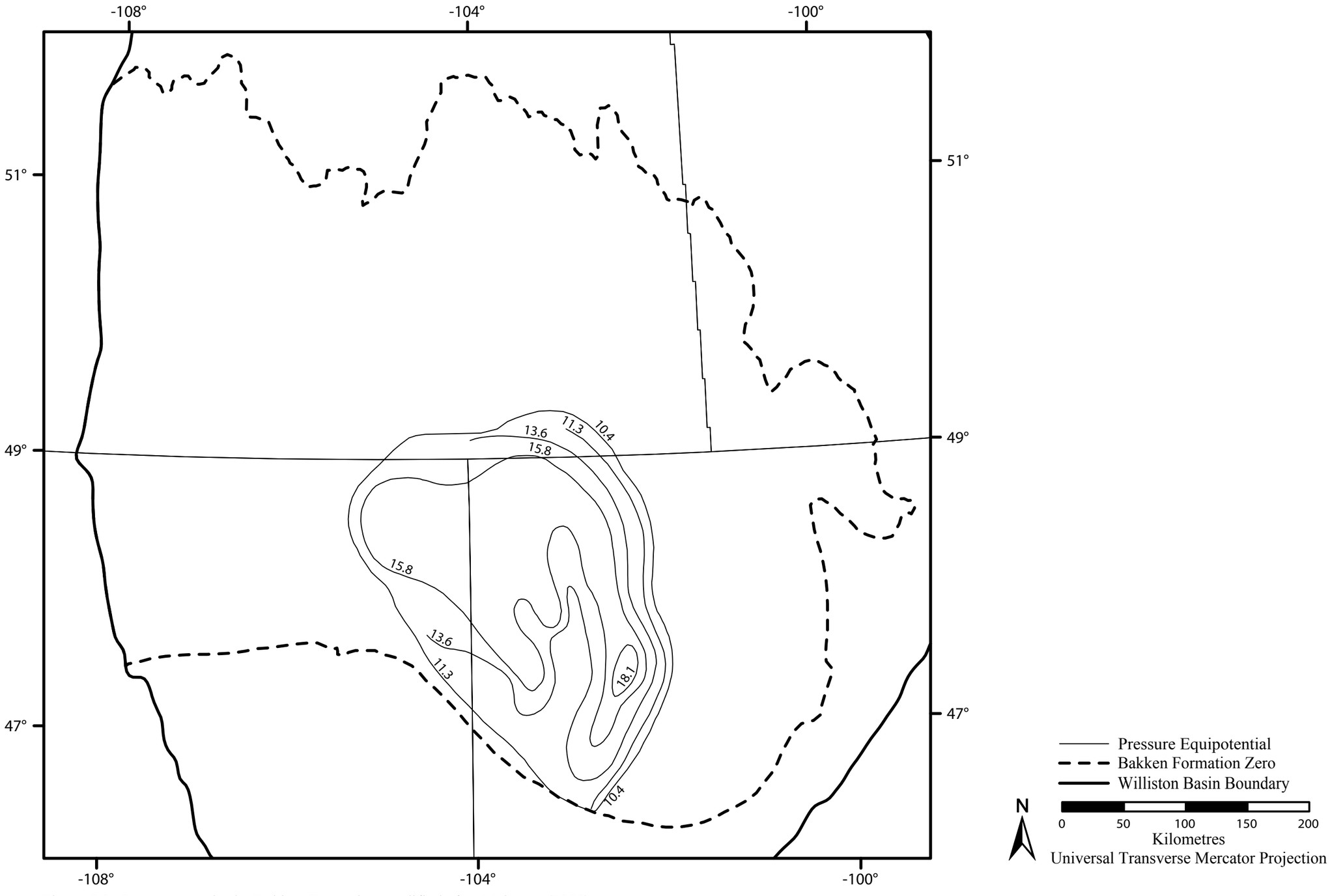

Figure 7.3: Overpressure in the Bakken Formation modified after Meissner (1978).

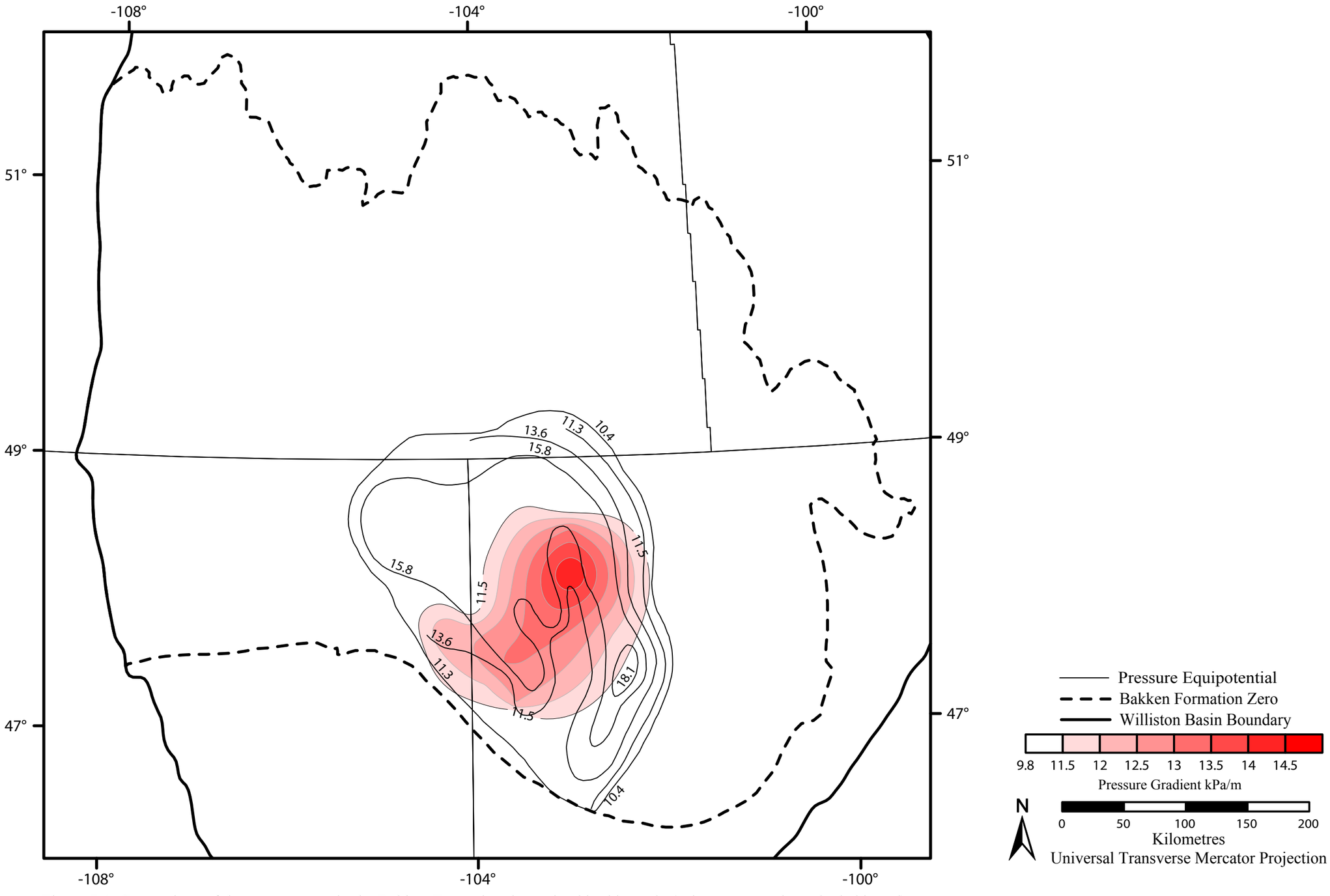

Figure 7.4: Comparison of the overpressure in the Bakken Formation determined in this study (using pressure data, shaded in red) to Meissner (1978) (from sonic velocity, unshaded).

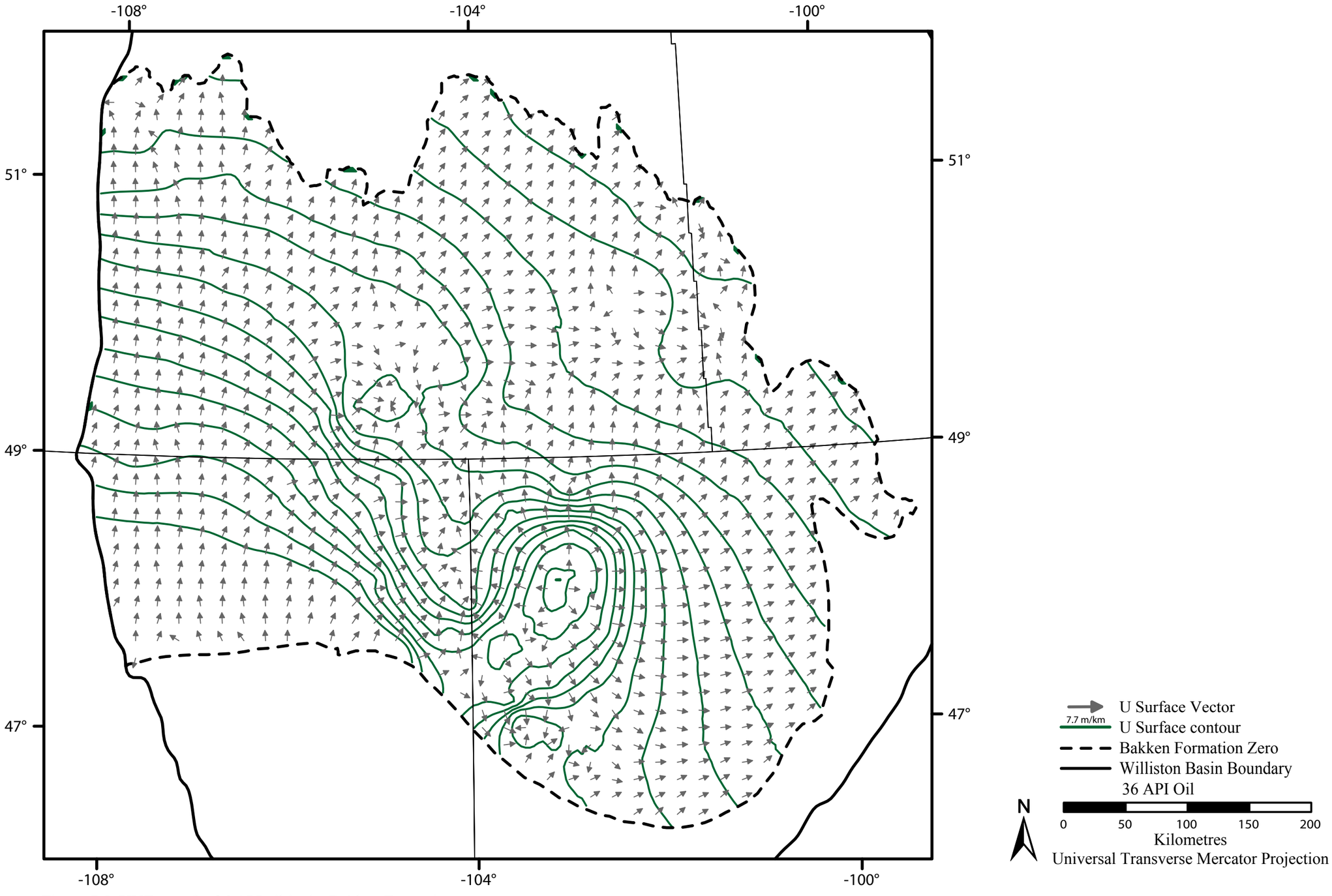

Figure 7.5: UVZ map for 36 API oil in the Bakken Formation.

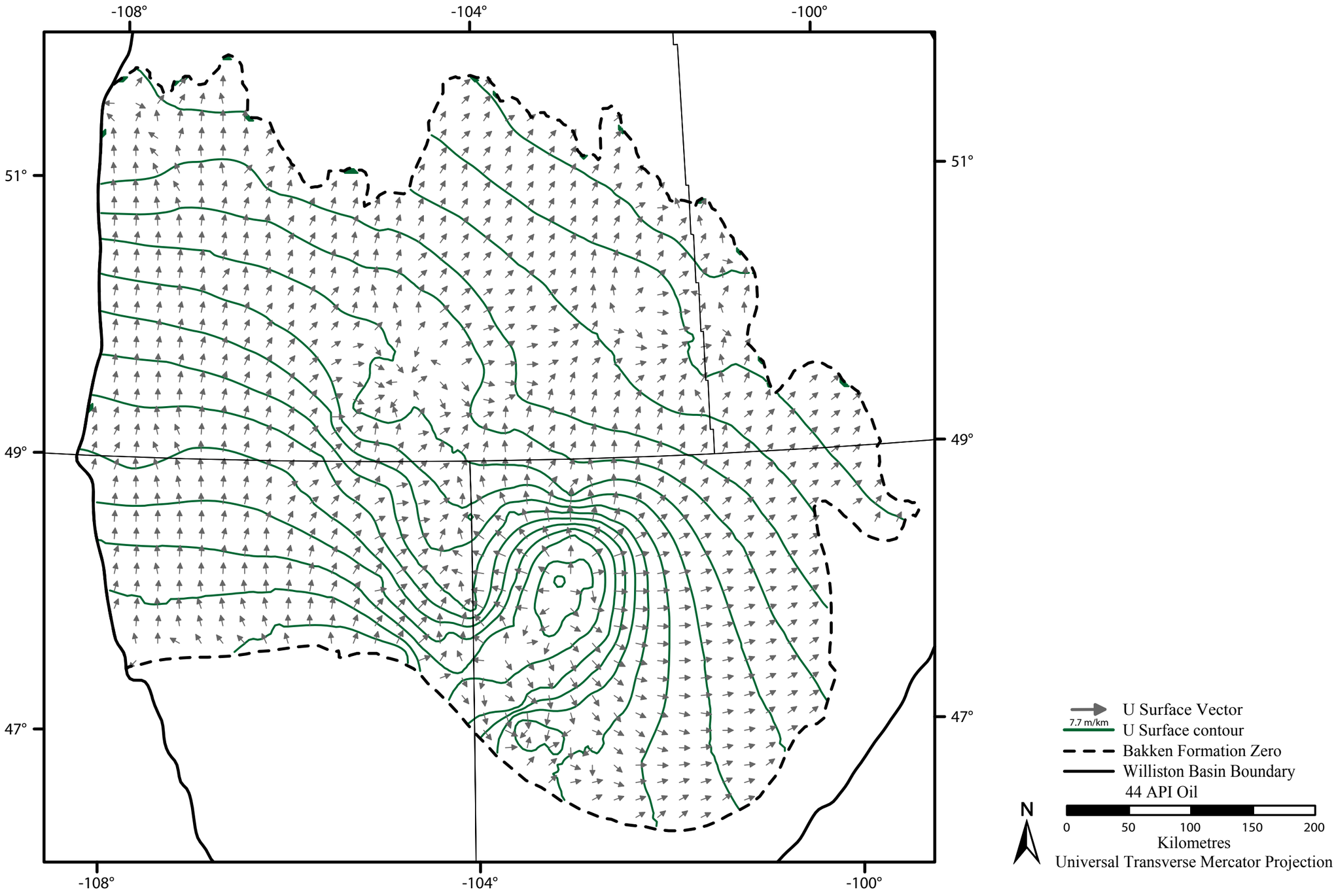

Figure 7.6: UVZ map for 44 API oil in the Bakken Formation.

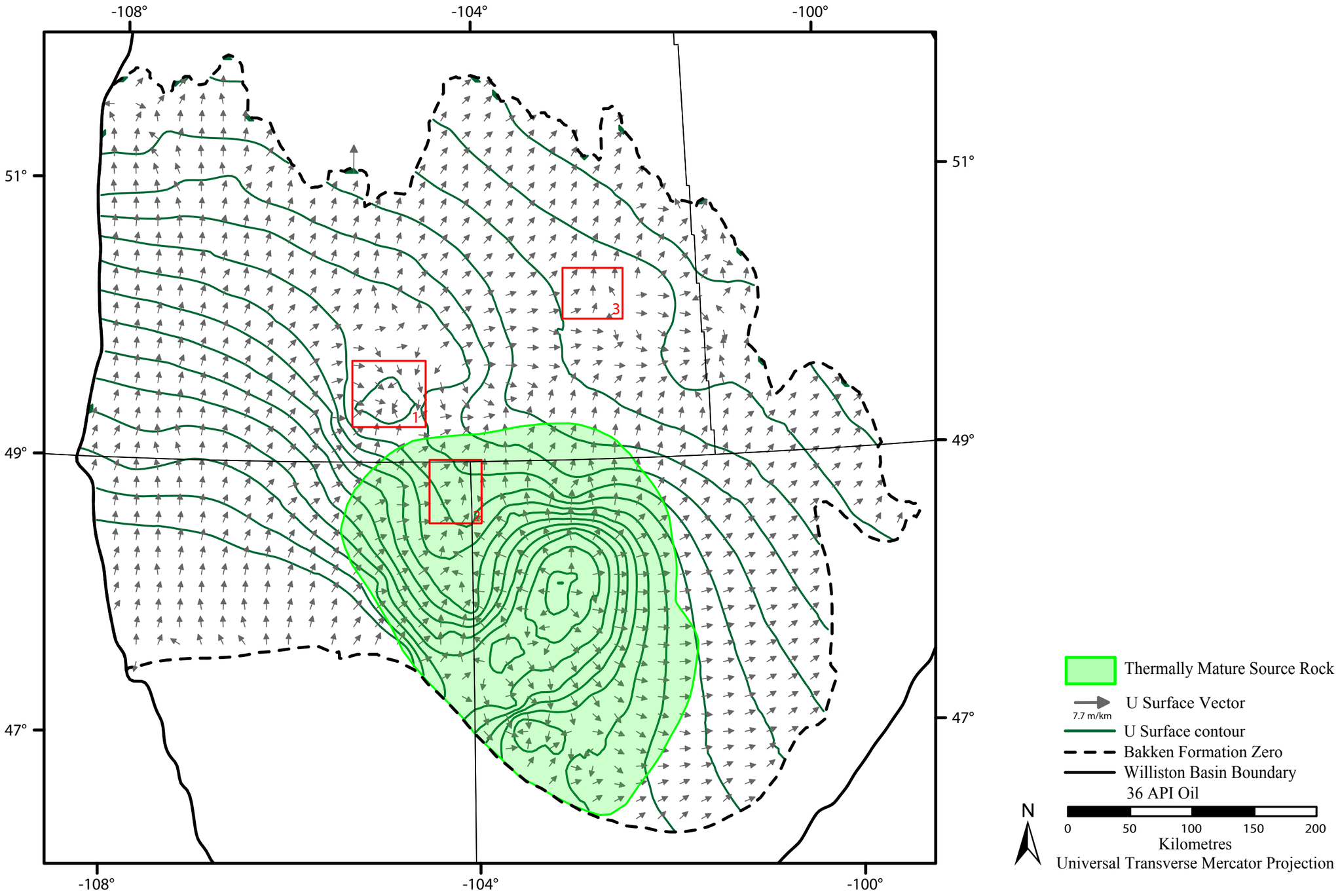

Figure 7.7: UVZ map of the Bakken Formation utilizing 36 API oil. Outlined in red are areas for potential future development.

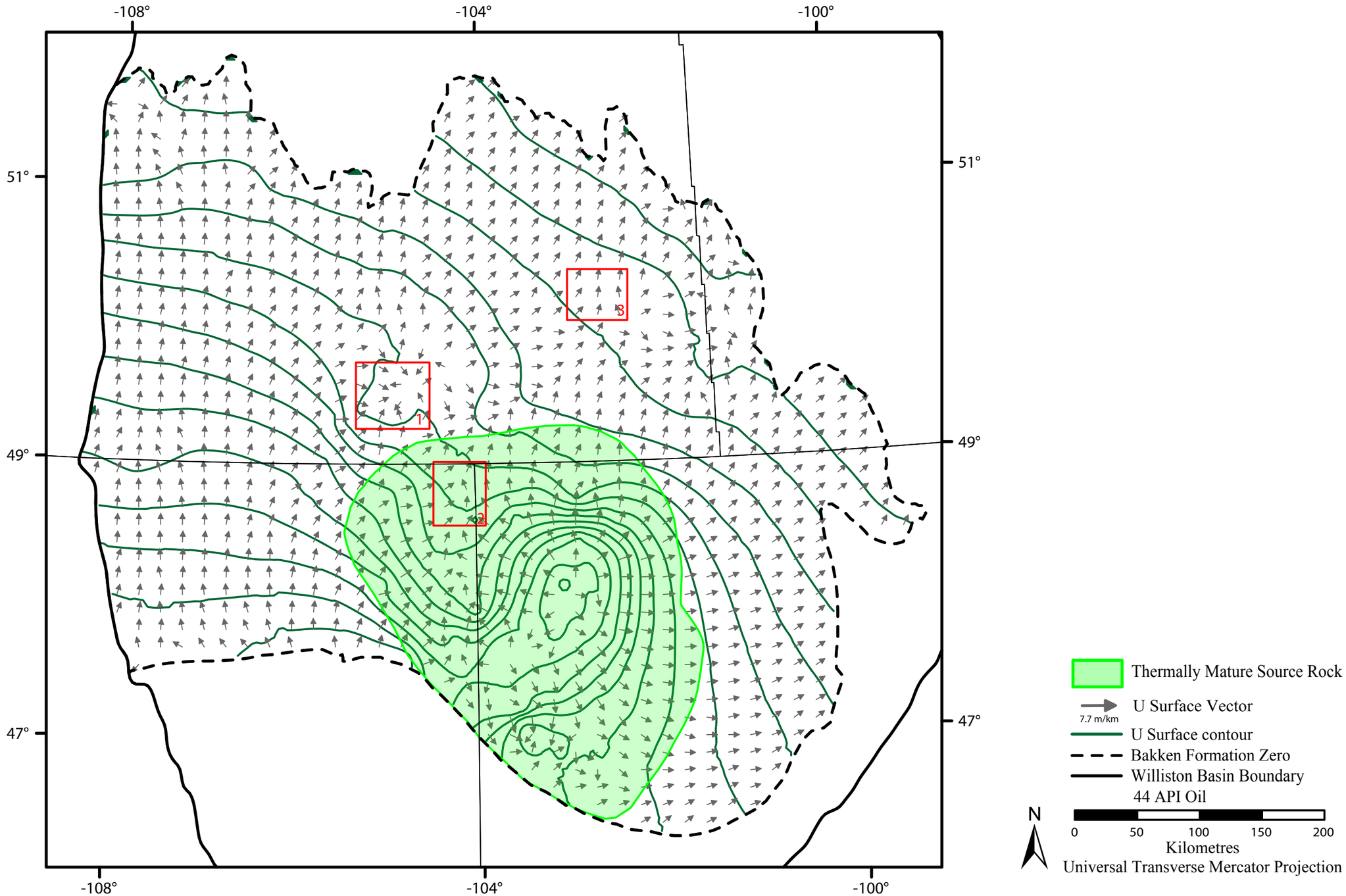

Figure 7.8: UVZ map of the Bakken Formation utilizing 44 API oil. Outlined in red are areas for potential future development.

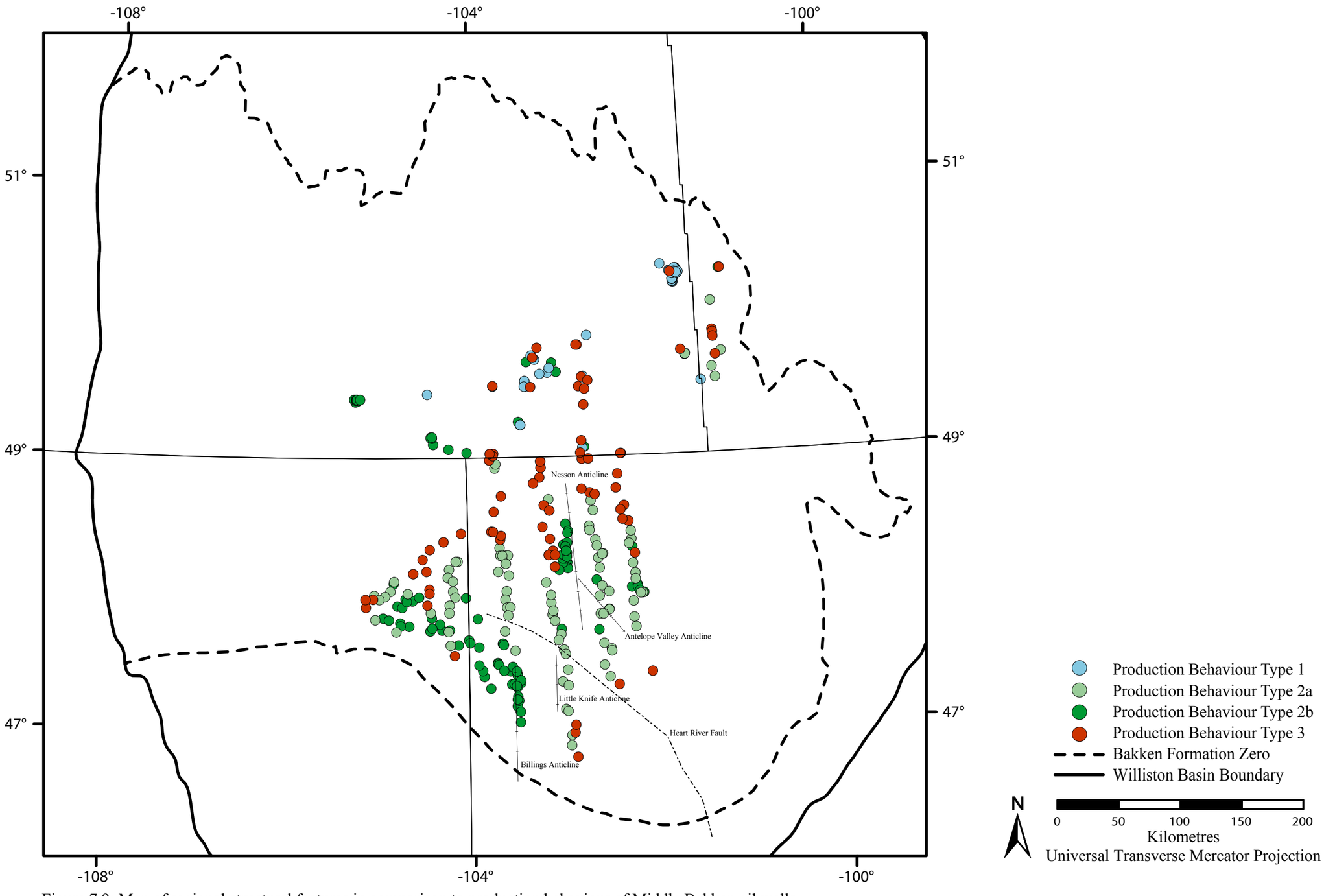

Figure 7.9: Map of regional structural features in comparison to production behaviour of Middle Bakken oil wells.

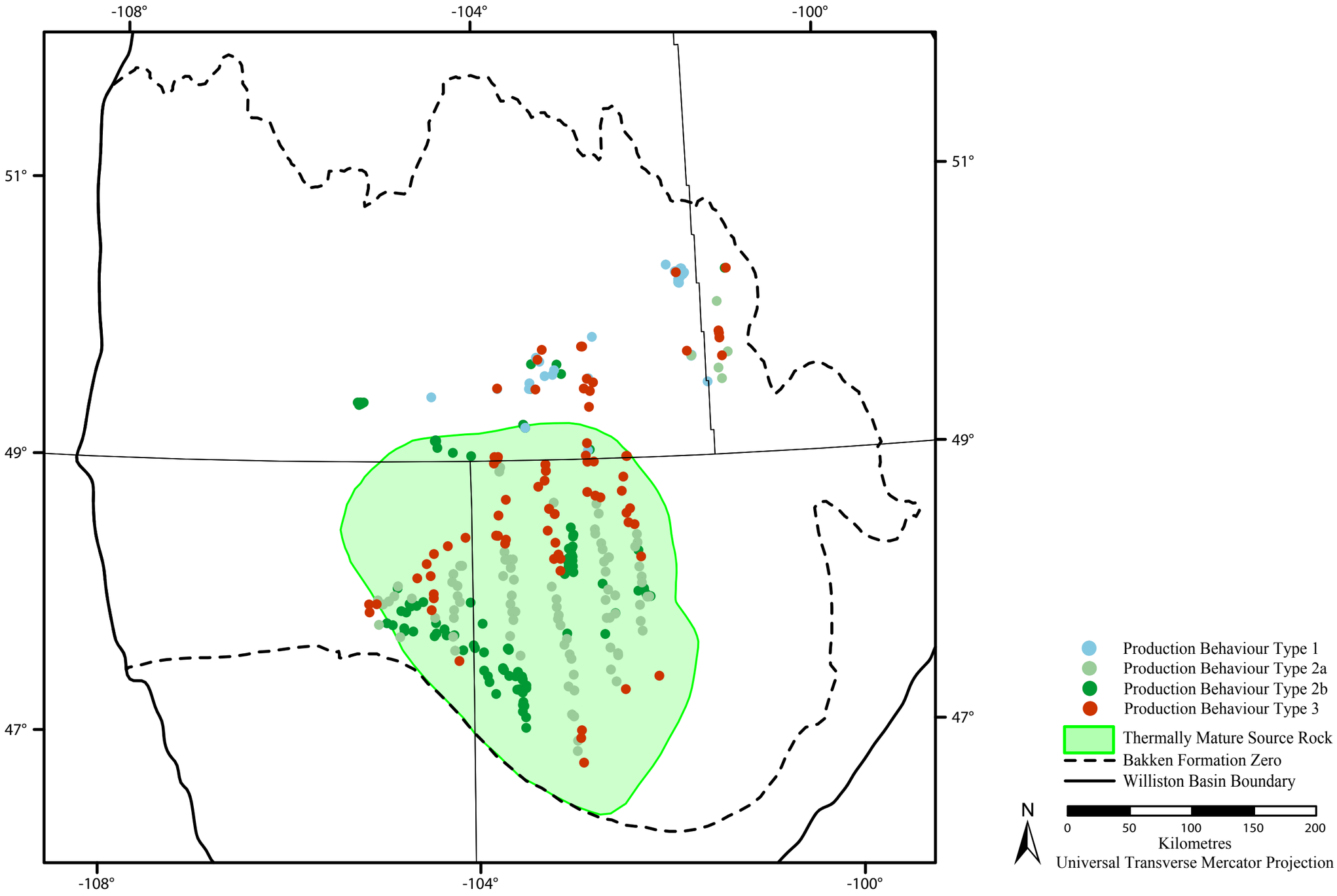

Figure 7.10: Map of thermally mature portion of the Bakken Formation (after Meissner, 1978) and production behaviour of Middle Bakken oil wells.

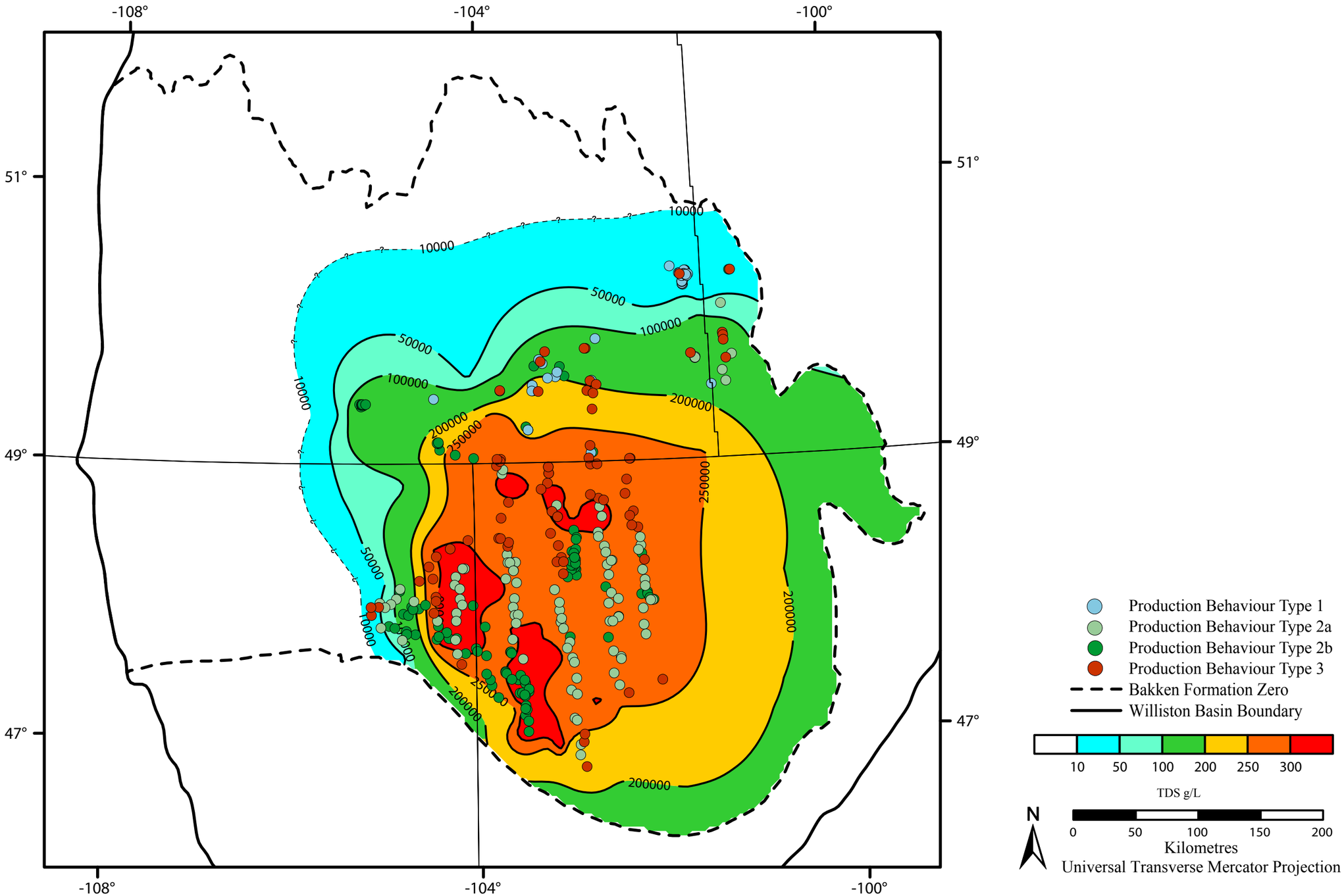

Figure 7.11: Map of total dissolved solids in the Bakken Aquifer and production behaviour of Middle Bakken oil wells.

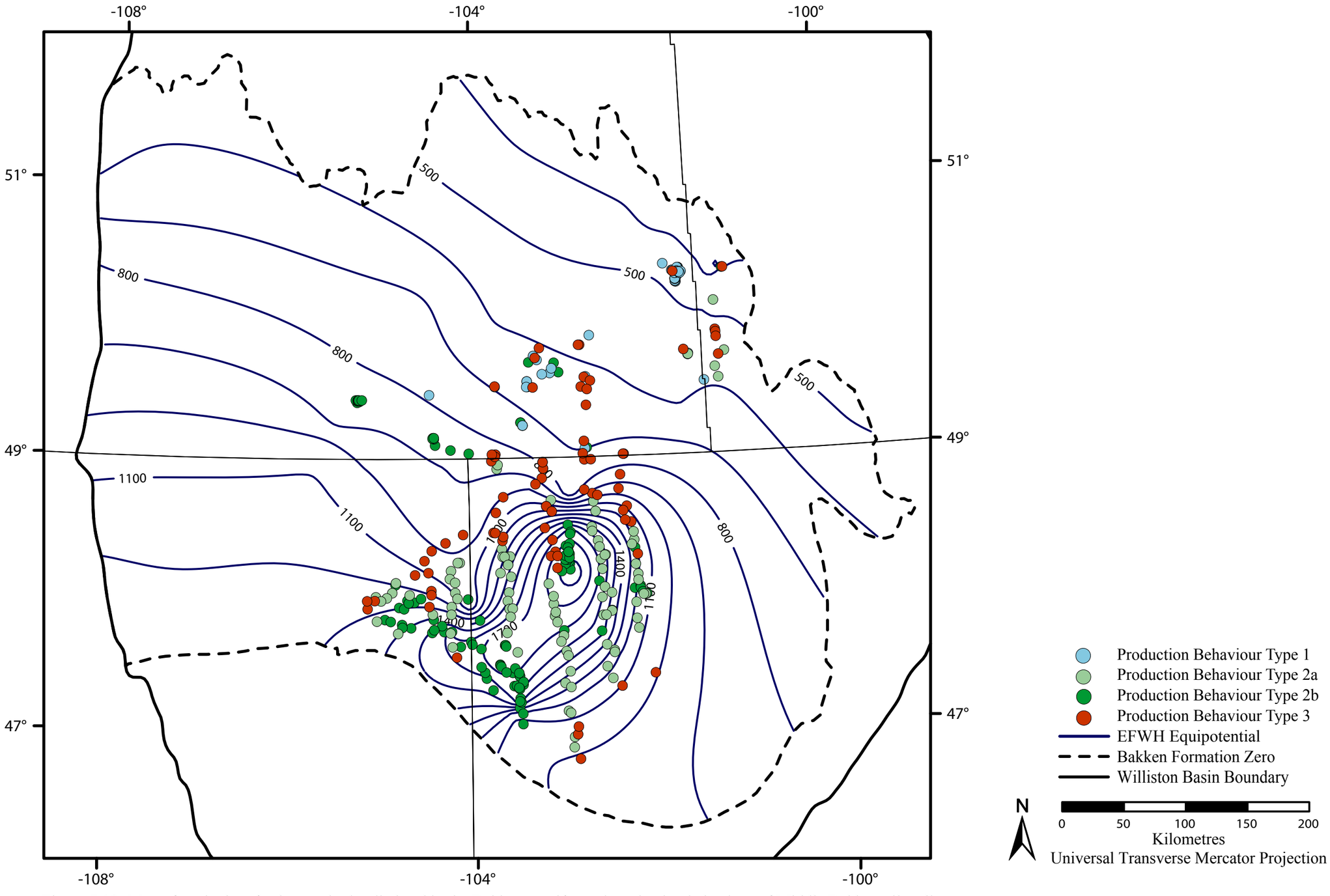

Figure 7.12: Map of equivalent freshwater hydraulic head in the Bakken Aquifer and production behaviour of Middle Bakken oil wells.

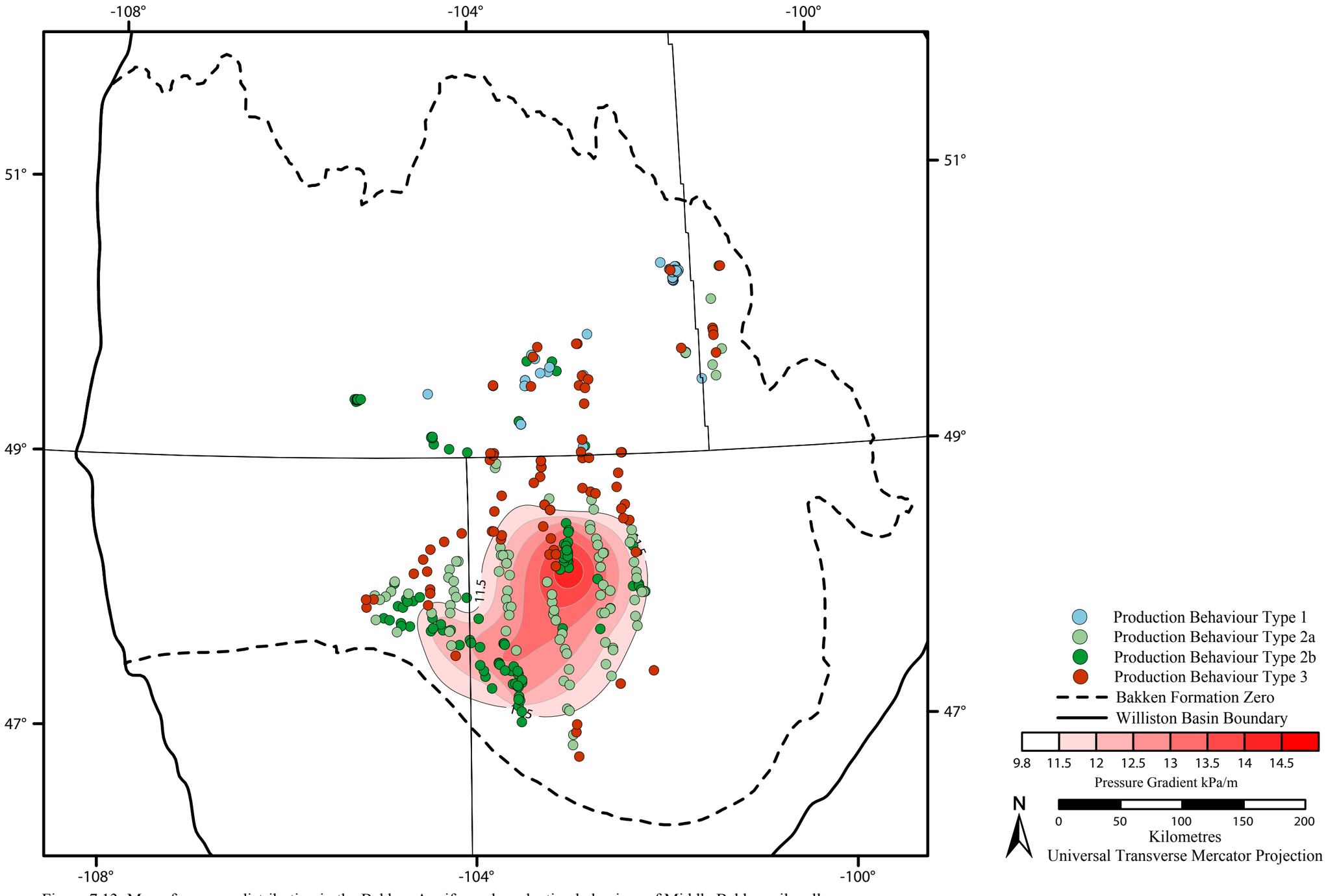

Figure 7.13: Map of pressure distribution in the Bakken Aquifer and production behaviour of Middle Bakken oil wells.

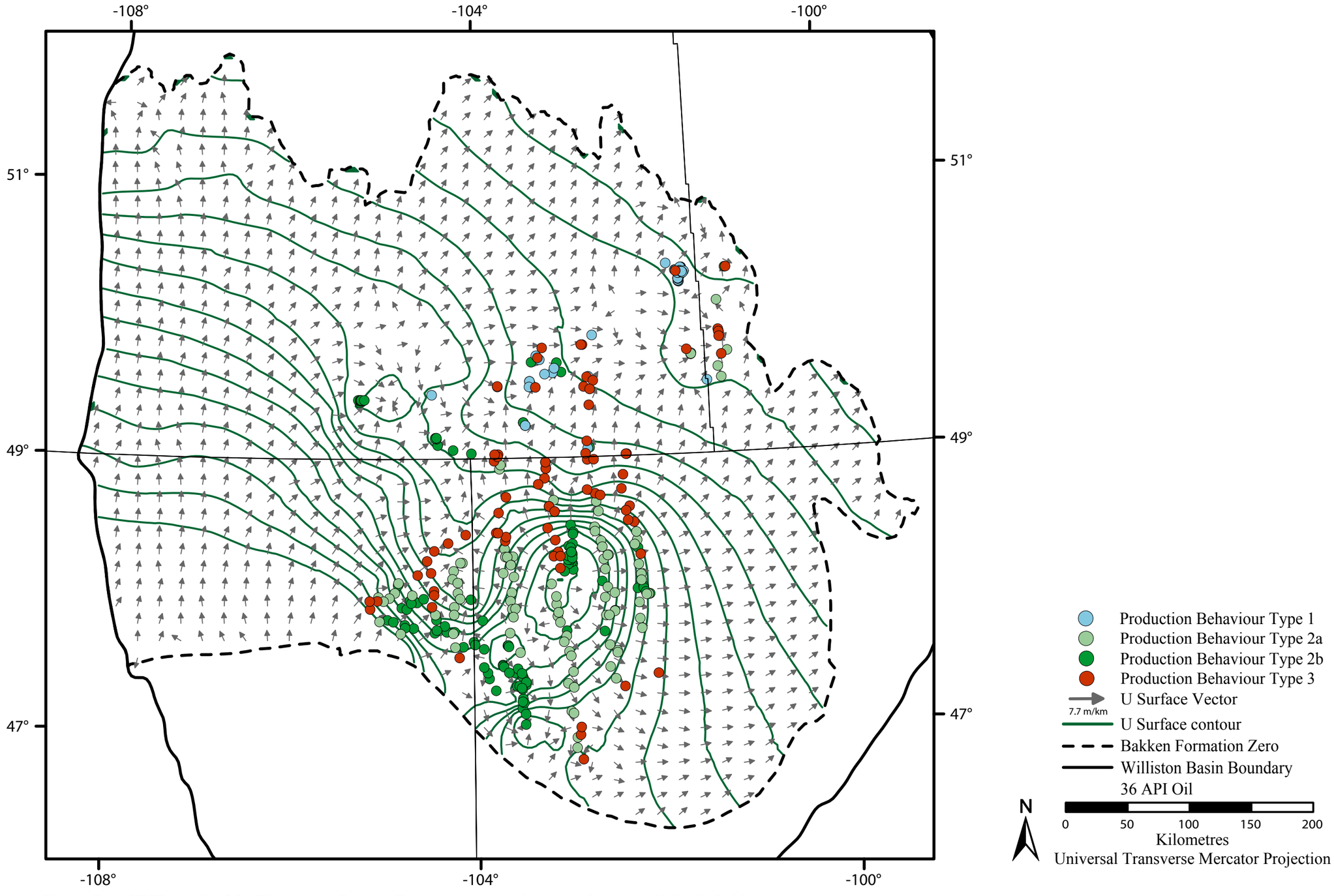

Figure 7.14: UVZ map for 36 API oil in the Bakken Formation and production behaviour of Middle Bakken oil wells.

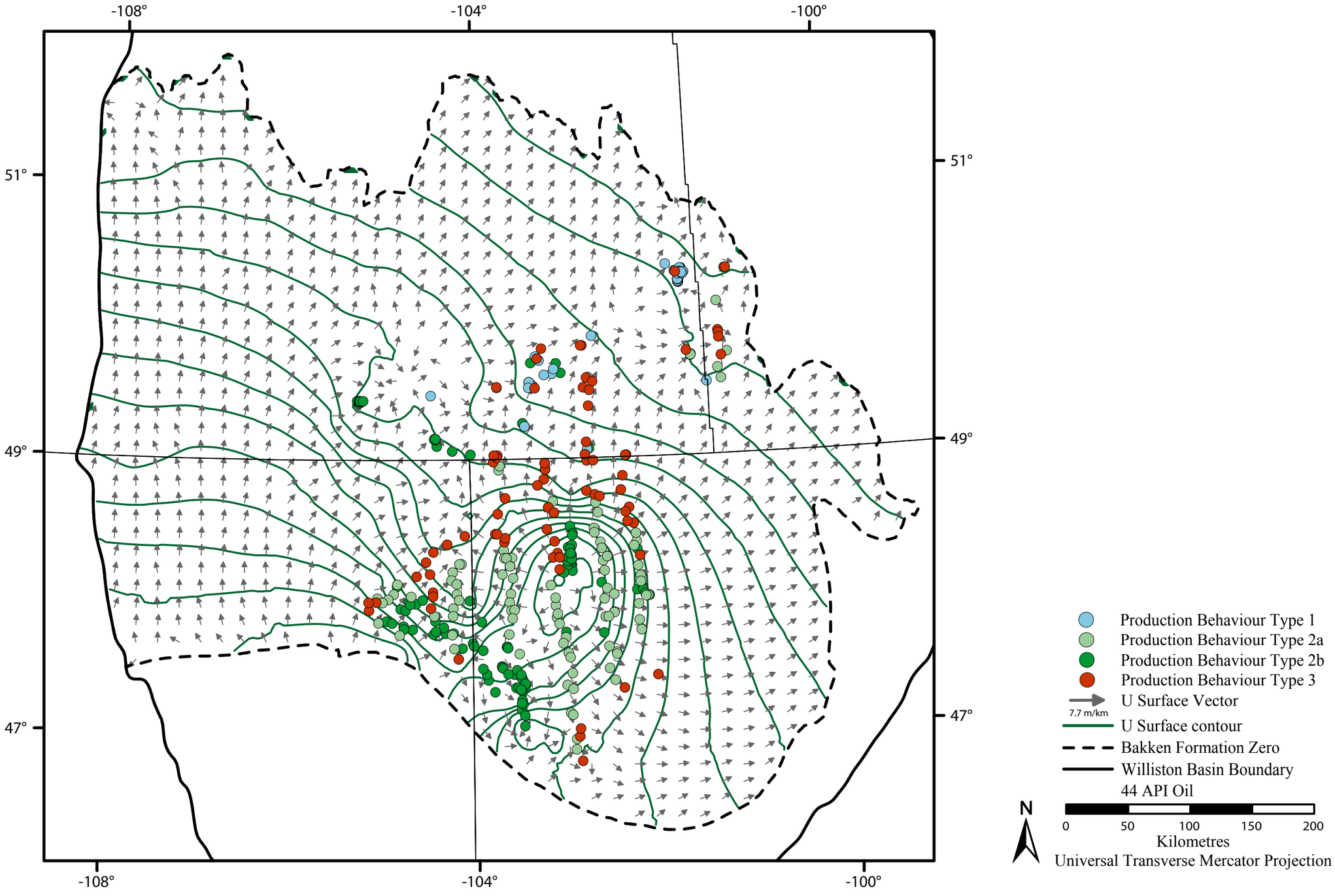

Figure 7.15: UVZ map for 44 API oil in the Bakken Formation and production behaviour of Middle Bakken oil wells.

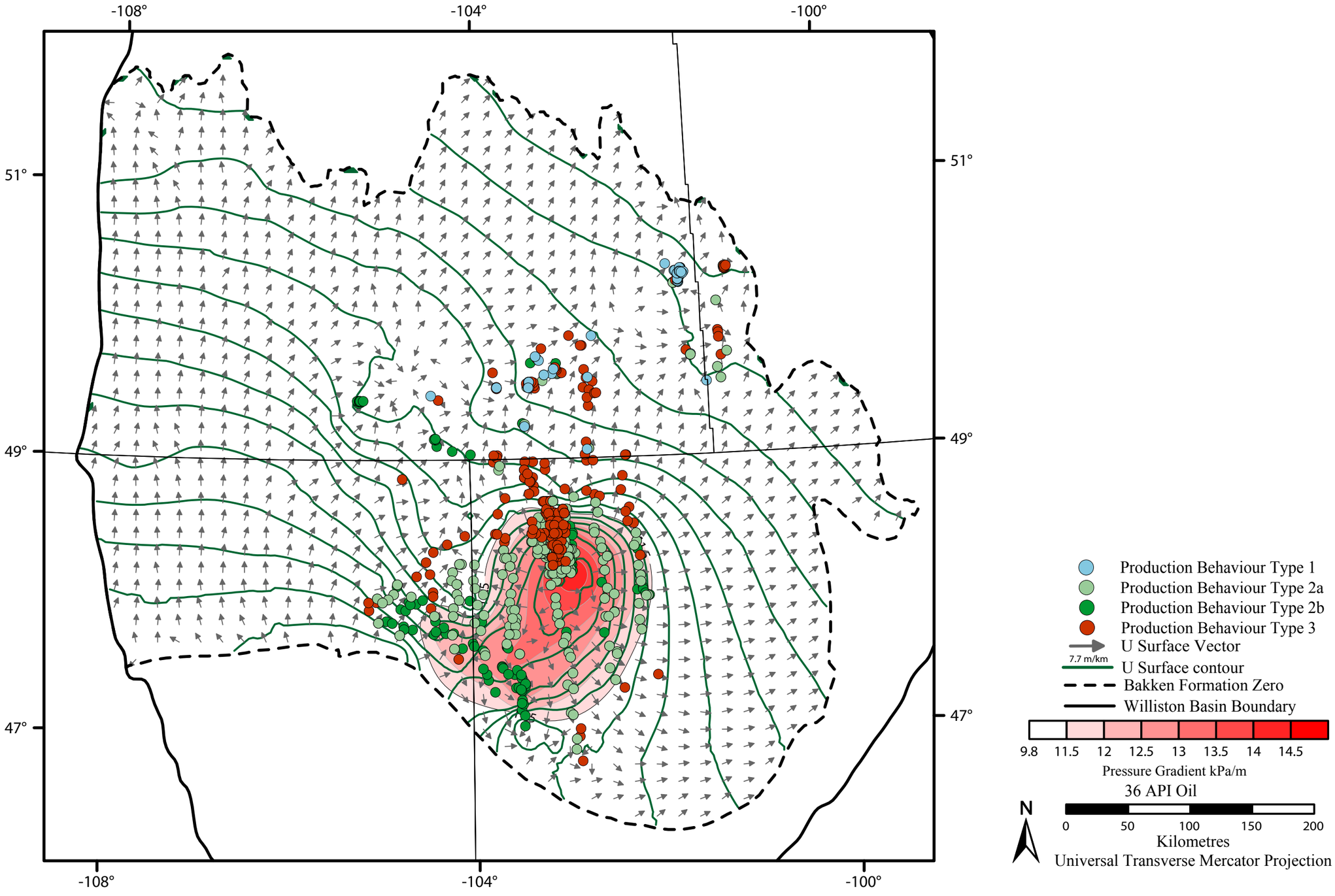

Figure 7.16: Location of a production anomaly in the overpressured portion of the Bakken Formation.

8. Conclusions and Recommendations

8.1. Conclusions

1. Total dissolved solids concentrations in the Bakken Aquifer range between <10,000 to >300,000 mg/L. The highest salinity waters are located in the central portion of the aquifer decreasing radially outward.

2. The Bakken Aquifer is composed of two distinct water types, Na-SO_4 and Na- Cl type waters. Na-Cl formation waters can be further broken up into three separate water types based on the TDS and Ca^{2+} concentrations:

Type 1: (Na-SO_4) waters have <10,000 mg/L TDS and >50% SO_4^{2-}. Type 1 waters are found on the Bakken Aquifer margins.

Type 2a: (Na-Cl) waters have a TDS range between 10,000 and 280,000 mg/L, containing <400 meq/L Ca^{2+}. Type 2a waters are found in Saskatchewan, Manitoba, and northern Montana.

Type 2b (Na-Cl) waters have high TDS ranging between 250,000 and >300,000 mg/L, containing >400 meq/L Ca^{2+}. Type 2b waters are found in the central portion of the Bakken Aquifer in Montana and North Dakota.

Type 2c (Na-Cl) waters have a TDS range between 200,000 and 235,000 mg/L and have >400 meq/L Ca^{2+}. Type 2c formation waters are only found in southern North Dakota.

3. Na-Cl-Br systematics show the presence of three water groups in the Bakken Aquifer.

Group 1 waters largely originated from halite dissolution. These waters are found near the Bakken Formation subcrop edge near the Manitoba Saskatchewan border. These waters are classified as Type 2a Na-Cl formation waters with salinities <50,000 mg/L.

Group 2 waters represent a mixing between paleoseawater and halite dissolution brines. These waters are located near the border between Canadian and the United States. These waters are classified as Type 2a Na-Cl waters with salinities between 100,000 and 250,000 mg/L.

Group 3 waters represent paleoseawaters and do not show evidence of halite dissolution. These waters are located in the central portion of the Bakken Aquifer. Group 3 waters are classified as Type 2b Na-Cl brines and have a TDS >250,000 mg/L.

4. There are three distinct types of fluid flow in the Bakken Aquifer: topography driven groundwater flow, buoyancy driven flow (resulting from density variations within the aquifer) and pressure driven flow (caused by the overpressure resulting from hydrocarbon generation).

5. Hydraulic head values in the Bakken Aquifer range from <400 m to >2000 m. A large closed potentiometric mound is located in North Dakota extending partially into Montana. Tightly spaced contours surround this mound indicating a steep hydraulic head gradient. Contour spacing increases outwards from the mound indicating a lower hydraulic head gradient. Excluding the mound, the highest head values are located in the southwest of the study area approaching 1300 m. Hydraulic head values decrease toward the Saskatchewan Manitoba border. Regional flow is from the southwest to the northeast.

6. A large area with greater than hydrostatic conditions is located in North Dakota partially extending into Montana. The maximum pressure gradient in the

Bakken Aquifer exceeds 14.5 kPa/m. Pressures decrease outwards from the deep center of the basin returning to hydrostatic, and near hydrostatic conditions over the remaining Bakken Aquifer.

7. Density-dependent flow effects are present within the Bakken Aquifer. Significant density effects are present in northeast Montana as well as southeast Saskatchewan. Locally flow can be as much as 170 degrees deviated from the expected flow direction. While there are deviations in the flow within the aquifer, regional flow remains southwest to northeast over the majority of the Bakken Aquifer.

8. Hydrocarbons generated in the thermally mature portion of the Bakken Formation migrate outward and north towards Canada. Water flow in the Bakken Formation has created preferential migration pathways as well as possible hydrodynamic traps.

9. Four distinct production behaviours (Type 1, Type 2a, Type 2b, Type 3) are observed in Middle Bakken oil wells.

Type 1 production wells have a large initial oil production with little initial water production. Within five years, oil production decreases and water becomes the dominant produced fluid. This behaviour continues for the remaining lifecycle of the well.

Type 2a production wells produce large volumes of oil in the initial stages of production and then quickly decrease stabilizing after the first few years. Monthly production slowly declines over a long (20+ year) production cycle. These wells produce oil nearly exclusively; even in advanced stages of reservoir depletion, water production remains negligible.

Type 2b production wells produce more monthly oil than water, or nearly the same amount of oil and water over the entire life cycle of the well. There is no increase in water production even in advanced stages of depletion

Type 3 production wells produce more water than oil month over month for the entire lifecycle of the well. Production volumes are related in that an increase in

one fluid results in an increase in the other. As in Type 2b wells, there is no relative increase in water production in advanced stages of reservoir depletion.

8.2. Recommendations

To further refine the regional flow system and hydrochemistry, it is recommended that additional data be obtained beyond the current data limits. Data could be obtained through a wellhead sampling program or possibly through an industry partnership. With a larger data extent, more could be known about the TDS distribution, and groundwater flow direction near the Bakken Aquifer margins.

To investigate the production anomaly further, a detailed hydrochemical study is recommended. Produced water from these wells could be compared to formation waters from other aquifers in the region thus possibly revealing the source of this water.

References

Aderoju, T. E., and S. L. Bend, 2013, A Rock-Eval Evaluation of the Bakken Formation in Southern Saskatchewan, *in* Summary of Investigations 2013, v.1, Saskatchewan Geological Survey, Saskatchewan Ministry of the Environment, Misc. Report 2013-4.1, Paper A-2, 14p.

Ahern, J. L., and S. R. Mrkvicka, 1984, A Mechanical and Thermal Model for the Evolution of the Williston Basin: Tectonics, v. 3, p. 79-102.

Alkalali, A., 2002, Petroleum Hydrogeology of the Nisku Aquifer in the Western Canadian Sedimentary Basin: M.Sc. Thesis, University of Alberta, Edmonton, Alberta, Canada, 152 p.

Anderson S. B., and W. P. Eastwood, 1968, Natural Gas in North Dakota, *in* Natural Gasses in Rocks of Paleozoic Age: American Association of Petroleum Geologists Memoir No. 80, 50p.

Anna, L. O., 2013, Geological Assessment of Undiscovered Oil and Gas in the Williston Basin Province, Montana, North Dakota, and South Dakota, chapter 3 *of* U.S. Geological Survey Williston Basin Province Assessment Team, Assessment of undiscovered oil and gas resources of the Williston Basin Province of North Dakota, Montana, and South Dakota, 2010 (ver. 1.1, November 2013): U.S. Geological Survey Digital Data Series DDS-69-W, 71p.

Anna, L. O., R. Pollastro, and S. Gaswirth, 2010, Williston Basin Province – Stratigraphic and Structural Framework to a Geologic Assessment of Undiscovered Oil and Gas Resources, chapter *2 of* U. S. Geological Survey Williston Basin Province Assessment Team, Assessment of undiscovered oil and gas resources of the Williston Basin Province of North Dakota, Montana, and South Dakota, 2010 (ver. 1.1, November 2013): U.S. Geological Survey Digital Data Series DDS-69-W, 17p.

Bachu, S., and B. Hitchon, 1996, Regional-Scale Slow of Formation Waters in the Williston Basin: American Association of Petroleum Geologists Bulletin, v. 80, p. 248-264.

Barson, D. B., 1993, The Hydrogeological Characterization of Oil Fields in North Central Alberta for Exploration Purposes: Ph.D. Thesis, University of Alberta, Edmonton, Alberta, Canada, 301 p.

Benn, A. A., and B. J. Rostron, 1998, Regional Hydrochemistry of Cambrian to Devonian Aquifers in the Williston Basin, Canada – USA, *in* J.E. Christopher, C.F. Gilboy, D.F. Paterson and S.L. Bend, *eds.*, Eight International Williston Basin Symposium: Saskatchewan Geological Society Special Publication 13, p. 238-246.

Berg, R. R., W. D. DeMis, and A. R. Mitsdarffer, 1994, Hydrodynamic Effects on Mission Canyon (Mississippian) Oil Accumulations, Billings Nose Area, North Dakota: American Association of Petroleum Geologists Bulletin, v. 78, p. 501-518.

Blondes, M. S., K. D. Gans, E. L. Rowan, J. J. Thordsen, M. E. Reidy, M. A. Engle, Y. K. Kharaka, and B. Thomas, 2016: U. S. Geological Survey National Produced Waters Geochemical Database, ver. 2.2, accessed May 13, 2016.

Bredehoeft, J. D., C. E. Neuzil, and P. C. D. Milly, 1983, Regional Flow in the Dakota Aquifer – A Study on the Role of Confining Layers: U. S. Geological Survey Water Supply Paper 2237, 45p.

Caprenter, A. B., 1978, Origin and Chemical Evolution of Brines in Sedimentary Basins: Society of Petroleum Engineers 53rd Annual Fall Technical Conference and Exhibition, SPE 7504, 8 p.

Chebotarev, I.I., 1955, Metamorphism of Natural Waters in the Crust of Weathering: Geochemica et Cosmochimica Acta, v. 8, p. 22-48, 137-170, 198-212.

Chierici, G. L., 1994, Principles of Petroleum Reservoir Engineering, v. 1: Berlin, New York, Springer-Verlag, 430 p.

Core Laboratories, Stratigraphic Correlation Chart, Calgary Alberta.

Clayton, R. N., I. Friedman, D. L. Graf, T. K. Mayeda, W. F. Meents, and N. F. Shimp, 1966, The Origin of Saline Formation Waters: 1. Isotopic Composition: Journal of Geophysical Research, v. 71, p. 3869-3882.

Cwiak, C. L., N. Avon, C. Kellen, P. C. Mott, O. M. Niday, K. M. Schulz, J. G. Sink, and J. B. Webb Jr, 2015, The New Normal: The Direct and Indirect Impacts of Oil Drilling and Production on the Emergency Management Function in North Dakota: North Dakota State University, 159 p.

Dahlberg, E. C., 1995, Applied Hydrodynamics in Petroleum Exploration (second edition): New York, Springer-Verlag, 295 p.

Davies, P. B., 1987, Modeling Areal, Variable-Density, Groundwater Flow Using Equivalent Freshwater Head- Analysis of Potentially Significant Errors, *in* Proceedings of the NWWA/IGWMC Conference, Solving groundwater problems with models: Dublin, Ohio, National Water Well Association, p. 888–903.

Davis, S. N., 1988, Where are the Rest of the Analyses?: Groundwater, v. 26, p. 2-5.

Dayboll, R., 2010, Review of Methods for use in Determining the Water Line of the Bakken Formation of Southeast Saskatchewan: IPG 601 Project Report, University of Alberta, Edmonton, Alberta, Canada 30 p.

DeMis, W. D. 1995, Effects of Cross-Basinal Hydrodynamic Flow on Oil Accumulations and Oil Migration History of the Bakken Petroleum System; Williston Basin, North America, *in* Hunter, L. D. V., and R. A. Schalla, eds., Seventh International Williston Basin Symposium, Montana Geological Society, Billings, Montana, p. 291-301.

Dow, W. G., 1974, Application of Oil-Correlation and Source Rock Data to Exploration in Williston Basin: American Association of Petroleum Geologists Bulletin, v. 58, p. 1253-1262.

Downey, J. S., 1982, Hydrodynamics of the Williston Basin in the Northern Great Plains, *in* D. G. Jorgensen and D. C. Signor, eds., Geohydrology of the Dakota aquifer: Worthington, Ohio, National Water Well Association, p. 92-98.

Downey, J. S., 1984, Geohydrology of the Madison and Associated Aquifers in Parts of Montana, North Dakota, South Dakota, and Wyoming: U. S. Geological Survey Professional Paper 1273-G, 47 p.

Downey, J. S., 1986, Geohydrology of Bedrock Aquifers in the Northern Great Plains in Parts of Montana, North Dakota, South Dakota, and Wyoming: U. S. Geological Survey Professional Paper 1402-E, 87 p.

Downey, J. S., and G. A. Dinnwiddie, 1988, The Regional Aquifer System Underlying the Northern Great Plains in Parts of Montana, North Dakota, South Dakota, and Wyoming-summary: U.S. Geological Society Professional Paper 1402-A, 63 p.

Downey, J. S., J. F. Busby, and G. A. Dinwiddie, 1987, Regional Aquifers and Petroleum in the Williston Basin Region of the United States, *in* J. A. Peterson, D. M. Kent, S. B. Anderson, R. H. Pilatske, and M. W. Longman, *eds*., Williston Basin: Anatomy of a cratonic oil province: Denver Colorado, Rocky Mountain Association of Geologists, p. 299-312.

Engle, M. A., and E. L. Rowan, 2012, Interpretation of Na-Cl-Br Systematics in Sedimentary Basin Brines: Comparison of Concentration, Element Ratio, and Isometric Log-Ratio Approaches: International Association for Mathematical Geosciences, 45, p. 87-101.

Freeze, R. A., and J. A Cherry, 1979, Groundwater: New Jersey, Prentice-Hall, 604 p.

Gerhard, L. C., S. B. Anderson, J. A. LeFever, and C.G. Carlson, 1982, Geological Development, Origin, and Energy Mineral Resources of Williston Basin:

North Dakota American Association of Petroleum Geologists Bulletin, v. 66, p. 989-1020.

Grasby, S. E., and Z. Chen, 2005, Subglacial Recharge into the Western Canada Sedimentary Basin – Impact of Pleistocene Glaciation on Basin Hydrodynamics: Bulletin of the Geological Society of America, v. 117, p. 500-514.

Gupta, I., A. M. Wilson, and B. J. Rostron, 2011, Cl/Br Compositions as Indicators of the Origin of Brines: Hydrogeological Simulation of the Alberta Basin, Canada: Geological Society of American Bulletin 101, p. 200-212.

Hannon, N., 1987, Subsurface Water Flow Patterns in the Canadian Sector of the Williston Basin, *in* M. W. Longman *ed*., Williston Basin Anatomy of a Cratonic Oil Province, Rocky Mountain Association of Geologists, p. 299-312.

Hanor, J. S., 1994, Origin of Saline Fluids in Sedimentary Basins: Geological Society Special Publication, *in* Parnell, J ed., 1994, Geofluids: Origin, Migration and Evolution of Fluids in Sedimentary Basins, p. 151-174.

Hitchon, B., 1996, Rapid Evaluation of the Hydrochemistry of a Sedimentary Basin Using Only Standard Formation Water Analysis: Example from the Canadian Portion of the Williston Basin: Applied Geochemistry, v. 11, p. 789-795.

Hitchon, B., and M. Burlotte, 1994, Culling Criteria for "Standard" Formation Water Analyses: Applied Geochemistry, v. 9, p. 637-645.

Horner, D. R., 1951, Pressure Build-Up in Wells: Third World Petroleum Congress, Proceedings., Section II. Leiden, Holland, p. 503-521.

Hubbert, M. K., 1940, Theory of Groundwater motion: Journal of Geology, v. 48, p. 785-944.

Hubbert, M. K., 1953, Entrapment of Petroleum Under Hydrodynamic Conditions: American Association of Petroleum Geologists Bulletin, v. 37. p. 1954-2026.

Iampen, H. T., 2003, The Genesis and Evolution of Pre-Mississippian Brines in the Williston Basin, Canada-U.S.A.: M.Sc. Thesis, University of Alberta, Edmonton, Alberta, Canada, 124p.

Iampen, H. T., and B. J. Rostron, 2000, Hydrogeochemistry of Pre-Mississippian Brines, Williston Basin, Canada, USA: Journal of Geochemical Exploration, v. 69-70, p. 29.35.

Jarvie, D. M., 2001, Williston Basin Petroleum Systems: Inferences from Oil Geochemistry and Geology: The Rocky Mountain Geologist, v. 38, p. 19-41.

Jensen, G. K. S., 2007, Fluid Flow and Geochemistry of the Mississippian Aquifers in the Williston Basin, Canada-U.S.A.: M.Sc. Thesis, University of Alberta, Edmonton, Alberta, Canada, 123p.

Jensen, G. K. S., B. J. Rostron, D. Palombi, and A. Melnik, 2015, Saskatchewan Phanerozoic Fluids and Petroleum Systems Project: Bakken Aquifer- Freshwater Hydraulic Heads. Saskatchewan Ministry of the Economy, Saskatchewan Geological Survey, Open File 2015-1, map 13 of 28.

Johnson, M. S., 2011, Discovery of Parshall Field, North Dakota, J. W. Robinson, J. A. LeFever, S. B. Gaswirth, *eds.*, Chapter 16 *of* The Bakken-Three Forks Petroleum System in the Williston Basin: The Rocky Mountain Association of Geologists, p. 418-427.

Kent, D. M., and J. E. Christopher, 1994, Geological History of the Williston Basin and Sweetgrass arch, *in* G.D. Mossop and I. Shetsen, *comps*., Geological atlas of the Western Canada sedimentary basin: Calgary, Canadian Society of Petroleum Geologists and Alberta Research Council, p. 421-429.

Khan, D. K., 2006, Hydrogeological Characterization of the Weyburn CO_2 Project Area and Gradient-Free Inverse Conditioning of Heterogeneous Aquifer Models to Hydraulic Head Data: Ph.D. Thesis, University of Alberta, Edmonton, Alberta, Canada, 238 p.

Kreis, L. K., M. Gent, and L. W. Vigrass, 1991, Subsurface Brines in Southern Saskatchewan, *in* J.E. Christopher and F. Haidl, *eds*., Proceedings of the sixth International Williston Basin Symposium: Saskatchewan Geological Society Special Publication 11, p. 283-292.

Kreis, L. K., A. Costa, and K. Osadetz, 2006, Hydrocarbon Potential of Bakken and Torquay Formations, Southeastern Saskatchewan, *in* Gilboy, C. F., and S. G. Whittaker *eds*., Saskatchewan and Northern Plains Oil and Gas Symposium 2006, Saskatchewan Geological Society Special Publication 19, p. 118-137.

Kuhn, P. P, R. D. Primio, R. Hill, J. R. Lawrence, and B. Horsfield, 2012, Three-Dimensional Modeling Study of the Low-Permeability Petroleum System of the Bakken Formation: American Association of Petroleum Geologists Bulletin, v. 96, p. 1867-1897.

Kume, J., 1960, An Investigation of the Bakken and Englewood Formations (Kinderhookian) of North Dakota and Northwestern South Dakota: M.Sc. Thesis, University of North Dakota, Grand Forks, North Dakota, USA, 86 p.

Kume, J., 1963, The Bakken and Englewood Formations of North Dakota and Northwestern South Dakota: Grand Forks, North Dakota, North Dakota Geological Survey Bulletin 39, 87p.

Laird, W. M., 1956, The Williston Basin – A Backwards Look with a View to the Future: First international Williston Basin Symposium, Bismarck, North Dakota, October 9, 1956, p. 14-22.

Langmuir, D., 1997, Aqueous Environmental Geochemistry: New Jersey, Prentice-Hall, 600 p.

Leenheer, M. L., 1984, Mississippian Bakken and Equivalent Formations as Source Rocks in the Western Canadian Basin: Organic Geochemistry, v. 6, p. 521-532.

LeFever, J. A., 1991, History of Oil Production from the Bakken Formation, North Dakota, *in* W.B. Hansen *ed*., Geology and horizontal drilling of the Bakken Formation: Montana Geological Society 1991 Guidebook, p. 3-17.

LeFever, J. A., 2005, Oil Production from the Bakken Formation: A Short History: North Dakota Geologic Survey Newsletter, v. 32, p. 5-10.

LeFever, J. A., 2008, Structural Contour and Isopach Maps of the Bakken Formation in North Dakota: North Dakota Geological Survey Geological Investigation 59, 5 map series.

LeFever, R. D., 1998, Hydrodynamics of Formation Waters in the North Dakota Williston Basin, *in* J.E. Christopher, C.F. Gilboy, D.F. Paterson and S.L. Bend, *eds*, Eighth International Williston Basin Symposium: Saskatchewan Geological Society Special Publication 13, p. 229-237.

LeFever, J. A., C. D. Martiniuk, E. F. R. Dancsok, and P. A. Mahnic, 1991, Petroleum Potential of the Middle Member, Bakken Formation, Williston Basin, *in* J.E. Christopher and F. Haidl, *eds*., Proceedings of the sixth International Williston Basin Symposium: Saskatchewan Geological Society Special Publication 11, p. 76–94.

Lowenstein, T. K., L. A. Hardie, M. N. Timofeeffm, and R. V. Demicco, 2003, Secular Variations in Seawater Chemistry and the Origin of Calcium Chloride Basinal Brines: Geology, 31, p. 857-860.

Lowenstein, T. K., B. Kendall, and A. D. Anbar, 2014, 8.21- The Geologic History of Seawater *in* Holland H. D., and K. K. Turekian *eds*., Treatise on Geochemistry, 2nd edition. Elsevier, Oxford, p. 562-622.

Lowenstein T. K., and M. N. Timofeeff, 2008, Secular Variations in Seawater Chemistry as a Control on Chemistry of Basinal Brines: Test on the Hypothesis: Geofluids, v. 8, p. 77-92.

Margitai, Z, 2002, Hydrogeological Characterization of the Red River Formation, Williston Basin, Canada-USA: M.Sc. Thesis, University of Alberta, Edmonton, Alberta, Canada, 92p.

Marsh, A., and M. Love, 2014, Upper Devonian-Lower Mississippian Bakken Formation: Isopach map, Saskatchewan Phanerozoic Fluids and Petroleum Systems Project, Saskatchewan Ministry of the Economy, Saskatchewan Geological Survey Open File 2014-1, map 99 of 159.

Martiniuk, C. D., 1988, Regional Geology and Petroleum Potential of the Bakken Formation, Southwestern Manitoba: Manitoba Energy Mines, Petroleum Branch, Petroleum Open-File Report POF 8-88, 34p.

McCaffery, M. A., B. Lazar, and H. D., Holland, 1987, The Evaporation Path of Seawater and the Coprecipitation of Br^- and K^+ with Halite: Journal of Sedimentary Petrology, v. 57 p. 928-937.

Meissner, F. F., 1978, Petroleum Geology of the Bakken Formation Williston Basin, North Dakota and Montana, *in* D. Rehrig, *ed*., 1978 Williston Basin Symposium: Billings, Montana, Montana Geological Society, p. 207-227.

Melnik, A., 2012, Regional Hydrogeology of Southwestern Saskatchewan: M.Sc. Thesis, University of Alberta, Edmonton, Alberta, Canada, 142p.

Millard, M., and M. Dighans, 2014, The Three Forks and Pronghorn in McKenzie County, North Dakota: More Than a Simple 'Basin Centered Oil Accumulation': adapted from oral presentation at AAPG 2014 Annual Convention and Exhibition, American Association of Petroleum Geologists, Article 10600

Munn, M. J., 1909, The Anticlinal and Hydraulic Theories of Oil and Gas Accumulation: Economic Geology, v. 4 p. 509-529.

Murray, G. H. Jr, 1968, Quantitative Fracture Study-Sannish Pool, McKenzie County, North Dakota: American Association of Petroleum Geologists Bulletin, v. 52, p. 57-65.

Nordquist, J. W., 1953, Mississippian Stratigraphy of Northern Montana, *in* J. M. Parker, *ed*., fourth Annual Field Conference Guidebook, Billings, Montana, Billings Geological Society, p. 68-82.

Norford, B. S., F. M. Haidl, R. K. Bezys, M. P. Cecole, H. R. McCabe, and D. F. Peterson, 1994, Middle Ordovician to Lower Devonian Strata of the Western Canada Sedimentary Basin, *In* G.D. Mossop and I. Shetsen, *comps*., Geological atlas of the Western Canada sedimentary basin: Calgary, Canadian Society of Petroleum Geologists and Alberta Research Council, p. 109-128.

Osadetz, K. G., and L. R. Snowdon, 1995, Significant Paleozoic Petroleum Source Rocks in the Canadian Williston Basin: Their Distribution, Richness, Thermal Maturity (Southeastern Saskatchewan and Southwestern Manitoba): Geological Survey of Canada Bulletin, 60 p.

Osadetz, K. G., P. W. Brooks, and L. R. Snowdon, 1992, Oil Families and Their Sources in Canadian Williston Basin (Southeastern Saskatchewan and Southwestern Manitoba): Bulletin of Canadian Petroleum Geology, v. 40, p. 254-273.

Palciauskas, V. V., 1991, Primary Migration of Petroleum, *in* R. K. Merrill, ed., Source and Migration Processes and Evaluation Techniques: American Association of Petroleum Geologists Treatise of Petroleum Geology, Handbook of Petroleum Geology, p. 13-22.

Palombi, D. D., 2008, Regional Hydrogeological Characterization of the Northeastern Margin in the Williston Basin: M.Sc. Thesis, Edmonton, Alberta, Canada, University of Alberta, 196 p.

Palombi, D. D., and B. J. Rostron, 2013, Regional Hydrogeological Characterization of the Northeastern Margin of the Williston Basin: Saskatchewan Ministry of the Economy, Saskatchewan Geological Survey, Open file 2010-45/Manitoba Innovation, Energy and Mines, Manitoba Geological Survey, Open file OF2011-3, 55 sheets.

Peterson, J. A., and L. M. MacCary, 1987, Regional Stratigraphy and General Petroleum Geology of the U.S. Portion of the Williston Basin and Adjacent Areas, *in* J. A. Peterson, D. M. Kent, S. B. Anderson, R. G. Pilatske, and M. W. Longman, *eds*., Williston Basin: Anatomy of a cratonic oil province: Denver, Colorado, Rocky Mountain Association of Geologists, p. 9-44.

Price, L. C., and J. A. LeFever, 1994, Dysfunctionalism in the Williston Basin: The Bakken/mid-Madison Petroleum System: Bulletin of Canadian Petroleum Geology, v. 42, p. 187-218.

Price, L. C., T. Ging, T. Daws, A. Love, M. Pawlewicz, and D. Anders, 1984, Organic metamorphism in the Mississippian–Devonian Bakken shale North Dakota portion of the Williston Basin, *in* J. Woodward, F. F. Meissner, and J. C. Clayton, *eds*., Hydrocarbon source rocks of the greater Rocky Mountain region: Denver, Colorado, Rocky Mountain Association of Geologists, p. 83–134.

Rittenhouse, G., 1967, Bromine in Oil-Field Waters and its use in Determining Possibilities of Origin of These Waters: American Association of Petroleum Geologists, v. 51, p. 2430-2440.

Rostron, B. J., 1994, A New Method for Culling Pressure Data Used in Hydrodynamic Studies: AAPG Annual Meeting Abstracts - American Association of Petroleum Geologists and Society of Economic Paleontologists and Mineralogists, p. 247.

Rostron, B. J., and S. Arkadaksky, 2014, Fingerprinting “Stray” Formation Fluids Associated with Hydrocarbon Exploration and Production: Elements, v. 10, p. 285-290.

Rostron, B. J., and C. Holmden, 2003, Regional Variations in Oxygen Isotopic Compositions in the Yeoman and Duperow Aquifers, Williston Basin (Canada- USA): Journal of Geochemical Exploration, v. 78-79, p. 337-341.

Schmoker, J. W., and T. C. Hester, 1983, Organic Carbon in the Bakken Formation, United States Portion of Williston Basin: American Association of Petroleum Geologists Bulletin, v. 67, p. 2165-2174.

Schmoker, J. W., and T. C. Hester, 1990, Formation Resistivity as an Indicator of Oil Generation- Bakken Formation of North Dakota and Woodford Shale of Oklahoma: Log Analyst, v. 31, p. 1-9.

Shouakar-Stash, O., 2008, Evaluation of Stable Chlorine and Bromine Isotopes in Sedimentary Formation Fluids: Ph.D. Thesis University of Waterloo, Waterloo, Ontario, Canada, 332 p.

Singh, A., D. Palombi, N. Nakevska, G. Jensen, and B. Rostron, 2017, An Efficient Approach for Characterizing Basin-Scale Hydrodynamics: Marine and Petroleum Geology, v. 84, p. 332-340.

Sonnenberg, S. A., and A. Pramudito, 2009, Petroleum Geology of the Giant Elm Coulee Field, Williston Basin: American Association of Petroleum Geologists Bulletin, v. 93, p. 1127-1153.

Sorensen, J. A., S. B. Hawthorne, S. A. Smith, J. R. Braunberger, G. Liu, R. C. L. Klenner, L. S. Botnen, E. N. Stedman, J. A. Harju, and T. E. Doll, 2014, Final report for subtask 1.10 - CO2 storage and enhanced Bakken recovery research program: AAD Document control, U.S. Department of Energy Report, 79 p.

Thom, W. T. Jr, and C. E. Dobbin, 1924, Stratigraphy of Cretaceous-Eocene Transition Beds in Eastern Montana and the Dakotas: Geological Society of America Bulletin, v. 35, p. 23-25.

Tissot, B. P., and D. H Welte, 1978, Petroleum Occurrences and Formation, Berlin, Springer-Verlag, 699 p.

Tóth, J., 1978, Gravity-induced Cross Formational Flow of Formation Fluids, Red Earth Region, Alberta, Canada: Analysis, Patterns, Evolution: Water Resources Research, v. 14, p. 805-843.

Tóth, J., 1980, Cross-Formational Gravity-Flow of Groundwater: A Mechanism of the Transport and Accumulation of Petroleum (The Generalized Hydraulic Theory of Petroleum Migration), *in* W. H. Roberts, III, and R. J. Cordell, *eds*., Problems of Petroleum Migration: Association of American Petroleum Geologists, Studies in Geology 10, p. 121-167.

Tóth, J., 1988, Ground Water and Hydrocarbon Migration, *in* W. Back, J. S. Rosenshein, and P. R. Seaber, *eds*., The Geology of North America-Hydrogeology: Geological Society of America, v. 0-2, p. 485-502.

Tóth, J., and T. F. Corbet, 1986, Post-Paleocene Evolution of Regional Groundwater Flow Systems and Their Relation to Petroleum Accumulations, Taber Area, Southern Alberta, Canada: Bulletin of Canadian Petroleum Geology, v. 34, p. 339-363.

Walter, L. M., A. M., Stueber, and T. J. Huston, 1990, Br-Cl Systematics in Illinois Basin fluids: Constraints on Fluid Origin and Evolution: Geology, v. 18, p. 315-318.

Wardlaw N. C., and W. M. Schwerdtner, 1966, Halite-Anhydrite Seasonal Layers in the Middle Devonian Prairie Evaporite Formation, Saskatchewan, Canada: Geological Society of America Bulletin, v. 77, p. 331-342.

Webster, R. L., 1984, Petroleum Source Rocks and Stratigraphy of the Bakken Formation in North Dakota, *in* J. Woodward, F.F. Meissner, and J.C. Clayton, *eds*., Hydrocarbon source rocks of the greater Rocky Mountain region: Denver, Rocky Mountain Association of Geologists, p.57-81.

Williams, J. A., 1974, Characterization of oil types in Williston Basin: American Association of Petroleum Geologists Bulletin, v. 58, p. 1243–1252.

Zherebtsova, I. K., and N. N. Volkova, 1966, Experimental Study of Behaviour of Trace Elements in the Process of Natural Solar Evaporation of Black Sea Water and Sasyk-Sivash Brine: Geochemistry International 3, p. 656-670.